



Evolutionary & Disruptive Visions Towards Ultra High Capacity Networks

For Crowd and Broadband/Dense Applications

Access, Backhaul and User Equipment

April 2, 2014

Notice and Disclaimer –

The statements and viewpoints expressed in this White Paper are those of the IWPC 5000 X Working Group as of the release date noted on the cover page. Except as expressly stated, they may not reflect the views of individual IWPC members. The IWPC 5000 X Working Group has endeavored to provide information that is current and accurate as of the Release Date, but it does not warrant that all information is complete and error-free. Nor does it undertake to update this white paper based upon new information and developments, though it may elect to do so in its sole discretion and without notice. All information in this white paper is provided on an “AS IS” basis. The IWPC disclaims all express and implied warranties relating to the contents of this white paper.

The IWPC has not investigated or made an independent determination regarding title or non-infringement of any technologies that may be described or reference in this white paper. Persons seeking to implement such technologies are solely responsible for making all assessments relating to title and non-infringement of any technology, standard, or specification referenced in this document and for obtaining appropriate authorization to use such technologies, standards, and specification, including through the payment of any required license fees. IWPC and the IWPC Logo are trademarks of the IWPC.

Table of Contents

Access, Backhaul and User Equipment.....	1
Table of Contents.....	2
Table of Figures.....	5
1 Whitepaper Objectives	6
2 Executive Summary	7
3 Introduction	9
4 Key Incentives for 5G	11
4.1 Massive growth in traffic	11
4.1.1 Use cases that drive future traffic growth	13
4.2 Massive growth in the number of connected devices	14
4.3 Wide range of requirements and characteristics	15
5 Requirements and Challenges for future wireless systems (may be termed as 5G).....	16
5.1 Architecture trends in 3G and 4G	17
5.2 Architecture Requirements and Solutions for future Wireless Systems	17
5.3 Deployment Models in Future Wireless Systems.....	19
5.3.1 Planned Small Cells Deployment	19
5.3.2 Unplanned Small Cells Deployment.....	20
6 Spectrum & Propagation Aspects	21
6.1 New spectrum from 6 GHz to 100 GHz.....	21
6.2 Other uses of the spectrum above 6 GHz.	22
6.3 Propagation in mm-wave bands	23
6.4 Terrestrial propagation and deployment issues for mm-wave systems.....	26
6.5 The interference and power advantage of mm-wave spectrum	28
7 Propagation characteristics of mm-wave bands.....	29
7.1 Frequency dependence of propagation mechanisms	29
7.1.1 Free-space propagation:.....	29
7.1.2 Atmospheric effects:.....	30
7.1.3 Penetration losses:	30
7.1.4 Reflection:.....	31

7.1.1	Diffraction:	32
7.1.2	Scattering:	33
7.1.3	Foliage losses:	33
7.2	<i>Radio channel characterization and modeling</i>	33
7.2.1	Path loss and time dispersion	38
7.3	<i>Challenges with respect to mm-wave outdoor channel modeling</i>	40
7.4	<i>Summary observations of mm-wave prospects</i>	41
8	Overview of Access and Backhaul Technologies for 4G systems	42
8.1	<i>Overview of 4G LTE Access Technology</i>	42
8.1.1	Downlink	43
8.1.2	Uplink	44
8.2	<i>LTE-Advanced Technology</i>	45
8.3	<i>Overview of 4G Backhaul Technology</i>	45
8.3.1	Backhaul Taxonomy	46
9	Access and Backhaul Technologies for 5G systems	46
9.1	<i>General requirements</i>	46
9.2	<i>Future Cellular Architecture: Scenario with radically more spectrum and cell densification</i>	47
9.3	<i>Current mm-wave Standards for Future Cellular Systems</i>	48
9.3.1	802.11ad for Backhaul	50
9.4	<i>Overview of 5G mm-wave Access Technology</i>	51
9.4.1	Waveform Selection	51
9.4.2	Frame Structure	52
9.4.3	Duplexing Scheme	52
9.4.4	Multiple Access	53
9.4.5	Link Budget	53
9.5	<i>Topology Options</i>	55
9.5.1	Topology Gaps	56
10	Enabling Technologies for Base Station and User Equipments for 5G Systems	57
10.1	<i>2D Phased Array Antenna</i>	57
10.2	<i>2D Phased Array Antenna Processing for 3 to 6 GHz Systems</i>	61
10.3	<i>2D Phased Array Antenna Processing for mm-wave Systems</i>	62
10.4	<i>UE Antennas for 3 to 6 GHz</i>	65
10.5	<i>IC Technology for mm-wave Systems</i>	66
10.6	<i>On-chip and In-Package Antennas for mm-wave Systems</i>	67

10.7	<i>User Equipment Power Consumption</i>	68
10.8	<i>Massive MIMO</i>	69
10.9	<i>Device Integration for mm-Wave</i>	69
10.10	<i>Mobility considerations for mm-wave antennas</i>	69
11	Proposed Network Features for Future Cellular Systems (may be termed as 5G systems)	70
11.1	<i>Mobility Management</i>	70
11.1.1	<i>Idle Mobility</i>	71
11.1.1.1	<i>Discovery</i>	71
11.1.1.2	<i>Paging Load Optimization</i>	71
11.1.2	<i>Connected-Mode Mobility</i>	72
11.1.2.1	<i>Selection of Physical Layer Identifier</i>	72
11.1.2.2	<i>Neighbor Discovery</i>	73
11.2	<i>Frequent Handover Mitigation</i>	74
11.3	<i>Transmit Power Management</i>	75
11.4	<i>Radio Resource and Interference Management</i>	77
11.5	<i>Backhaul Management</i>	78
11.6	<i>Power Saving</i>	78
11.7	<i>Centralized versus Distributed RAN</i>	79
12	List of Contributors	80
13	List of acronyms	81
14	References	83

Table of Figures

Figure 3-1. Challenging Scenarios to be addressed in future wireless networks (source: Alcatel-Lucent, used with permission.).....	9
Figure 3-2. Illustrating 3 components to achieve 5000 x capacity relative to a LTE release 8	10
Figure 4-1. Forecasted wireless traffic from Ericsson.....	12
Figure 4-2. Wireless Traffic data and forecasts all normalized to 2011 for ease of comparison.....	13
Figure 6-1: ITU mm-wave mobile frequency allocations.	26
Figure 6-2: Direct comparison of LOS and NLOS propagation as a function of frequency.....	26
Figure 6-3. Attenuation due to rain in the mm-wave spectrum.	27
Figure 6-4. Atmospheric attenuation in the mm-wave spectrum.....	28
Figure 7-1. Block diagram of a 72 GHz E-Band Channel Sounder used to collect Power Delay Profile measurements (52).....	34
Figure 7-2. Photograph of the 72 GHz channel sounder receiver	35
Figure 7-3. Photograph of the 72 GHz channel sounder transmitter	35
Figure 7-4. Small scale fading in the 28 GHz mm-wave channel is quite small, only on the order of 4 dB as the receiver is moved across a very small track (51) (23).....	37
Figure 7-5. Power Delay Profile measured in New York City at 28 GHz in a LOS environment.....	37
Figure 7-6. Scatter plot of 28 GHz path loss at many different NLOS and LOS locations in New York City.....	38
Figure 8.1. LTE system architecture.....	43
Figure 8-2. Taxonomy of Backhaul Solutions.....	46
Figure 9-1. mm-Wave Hot Spot Tiered Architecture (Source Interdigital, used with permission.).....	47
Figure 9-2. PTP, PMP and Mesh topologies (73)	55
Figure 9-3. Industry Coverage of Small Cell Backhaul Solutions	56
Figure 10-1. Notional design of 10x10 element 2D planar phased array.	58
Figure 10-2. Number of antenna elements per row for frequencies of interest – 12” column width.....	60
Figure 10-3. Number of antenna elements per row for frequencies of interest – 18” column width.....	60
Figure 10-4. Simplified block diagram of components supporting each antenna element.	62
Figure 10-5. Simplified block diagram of mm-wave transmitter and receiver.	63
Figure 10-6. Tx RF Beam former with two RF chains.....	64
Figure 10-7. Rx RF Beam former with two RF chains.	64
Figure 11-1: Scenarios for Mobility Management in a Neighborhood Small Cell Network	71
Figure 11-2. Case of PCI Confusion. Small Cell 1 cannot uniquely identify Small Cell 2 and Small Cell 3 from their PCI.....	73
Figure 11-3: Scenarios of frequent handovers in neighborhood small cell deployment	74
Figure 11-4. Pilot pollution regions: shows pilot pollution without power calibration.....	76
Figure 11-5. Pilot pollution regions: shows pilot pollution with power calibration	76
Figure 11-6. Small cell coverage footprints: shows coverage footprints without power calibration	77
Figure 11-7. cell coverage footprints: shows coverage footprints with power calibration.....	77

1 Whitepaper Objectives

This whitepaper is aimed at the technical and contributing members of 5G development organizations including:

- Radio Access Network (RAN) Executives from Operators
- Wireless standards representatives and delegates
- OEMs, device manufacturers and ecosystem planners
- Spectrum Regulators
- ITU and WRC Delegates
- Researchers contributing to the Beyond 2020 and 5G fora.

The aim of this whitepaper is to advance certain understandings and concepts for adoption in wireless systems to be deployed beyond the year 2020, referred to here as “5G.” It is understood that the nomenclature “5G” will be fluid and used by various organizations and that the generational numbering scheme is not formally defined¹. Mindful of this ambiguity, the term “5G” is used here to advocate for specific technologies, architectures, and spectrum that will require changes to the wireless networks which will not be backward compatible with existing wireless systems, hence the increment to the “G” number.

Several organizations of standing are working to define “5G.” The European Commission has co-funded the Mobile and wireless communications Enablers for the Twenty-twenty Information Society (METIS 2020 Project) under the Seventh Framework Program for R&D (FP7) with the objective of laying the technical foundation of “5G.” 5GNow and 5GReEn are also supported by the European Commission under FP7 but with a focus on making a more energy efficient wireless network. China’s Ministry of Industry and Information Technology has established the IMT-2020 (5G) Promotion working Group.

The International Telecommunications Union Radiocommunication Sector (ITU-R) study group 5 has approved work items to estimate the amount of spectrum required beyond 2020 in ITU-R M. [IMT.2020.ESTIMATE] and [IMT.2020.INPUT], the consideration of appropriate technologies to support these trends in ITU-R M. [IMT.FUTURE TECHNOLOGY TRENDS], a study of global market and technology trends in ITU-R M. [IMT.VISION], and a new report on potential IMT at higher frequencies by ITU-R M. [IMT.ABOVE 6 GHz].

¹ The International Telecommunications Union (ITU) specified requirements for IMT-2000. This six Radio Access Technologies (RATs) meeting IMT-2000 requirements were collectively referred to by the industry as 3G systems. Subsequent evolution of these “3G” technologies were informally referred to as 3.5G, 3.75G and 3.9G in anticipation of the ITU requirements for IMT-Advanced which were informally referred to as 4G. However, the use of the term 4G by the industry to refer to technologies pre-dating IMT-Advanced has diluted the meaning of the term 4G. In this context, and prior to any direction from the ITU, it is anticipated the industry use of the term 5G may be even more varied than it was for 4G.

While this whitepaper does not authoritatively prescribe what “5G” standards are or of what they will consist, the paper presents technical details and tradeoffs that should be considered in defining “5G.” It is expected these contributions will empower the networks beyond 2020 with critically needed spectrum, air interface advances, and architectural structure to address the rapidly developing demands and imaginative new applications envisioned for this next decade.

2 Executive Summary

- a. This paper provides a summary of factors that will influence the next generation of cellular systems which can also be termed as 5G systems. Specifically, the following conclusions are drawn. Future wireless networks will likely need to address several critical performance areas which include:
 1. Cost
 2. Traffic density
 3. Latency
 4. Reliability including availability, connection retention, and redundancy of network elements
 5. Multi-operator and heterogeneous networks
 6. Multicast/broadcast requirements
 7. Security
 8. The need to serve a variety of devices
 9. Reduced battery consumption
 10. High density usage
 11. Various traffic patterns
 12. Coverage improvements
- b. The three elements required to achieve the projected capacity demand beyond 2020 are increased spectral efficiency, opportunity to use new spectrum bands including those above 6 GHz and increase in spectral reuse through deploying a much increased number of smaller base stations.
- c. The main requirements for future access technologies are driven by people and machines having gigabit experience with ultra-low latency. To meet these requirements ultra-densification of networks is required. Additional 5G requirements are driven by the contrasting need for low

power wide area (LPWA) technology for low cost and low data rate machine-to-machine applications like cheap sensors and gas, electricity and water meters.

- d. Availability of spectrum > 6GHz is one of the key requirements for meeting the goals of 5G. This paper discusses in detail the spectrum and propagation characteristics with new measurements at bands > 28 GHz. These new measurements suggest that access technologies with inter-site distance (ISD) of 100 to 200 meters can be deployed in 28-100 GHz bands to meet the requirements for next generation wireless technologies.
- e. In general, mm-wave communication links often require solutions that provide methods to mitigate Line of Sight (LOS) blockage. One means to achieve this is to utilize steerable, directional antenna arrays. These arrays steer the beam in a direction that achieves a link by i) access to an alternate base station node that is LOS or ii) access to the main, or alternate, base stations with a suitable low loss reflection.
- f. In this paper, multiple access schemes of next generation wireless access and backhaul technologies are discussed along with various beamforming solutions like baseband, RF and hybrid schemes. It is shown that massive antenna arrays need to be supported to close the link budget at mm-wave bands. However, for baseband beamforming one transceiver behind every antenna element needs to be used which will consume large amounts of power and be cost prohibitive. As such, RF or hybrid beamforming approaches are more attractive in these bands.
- g. The network features for future cellular systems with focus on Self Organizing Network (SON), cell identity management, load balancing, mobility robustness and power saving features are also discussed.
- h. Future 5G networks are expected to be complimentary to and integrated with existing cellular and Wi-Fi networks below 6 GHz, and will not replace them in the foreseeable future.

3 Introduction

Future wireless networks will likely need to address several critical performance areas diagrammed below in Figure 3-1, diagrammed below. These include cost, traffic density latency, reliability, multi-operator and heterogeneous networks, multicast/broadcast requirements, availability, security, the need to serve a variety of devices (machine to machine, sensors, appliance, handheld, tablet, dongle, laptop, vehicular devices and multi-tiered tethered devices), reduced battery consumption, high density usage, various traffic patterns including highly asymmetric and sporadic traffic, including highly correlated traffic bursts, coverage improvements, all with increasing cost constraints.

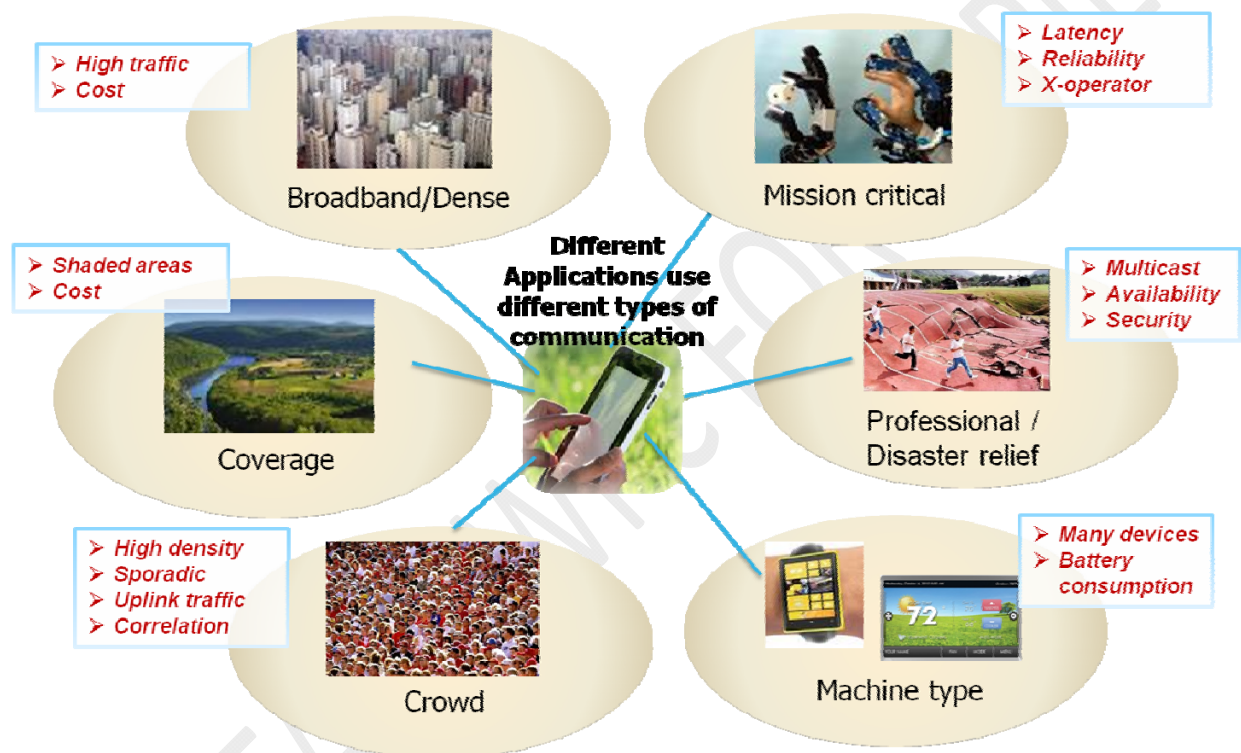


Figure 3-1: Challenging Scenarios to be addressed in future wireless networks (source: Alcatel-Lucent, used with permission.)

In September 2013, the Mobile and wireless communications Enablers for the Twenty-twenty (2020) Information Society (METIS) released a list of 5G "scenarios" and a set of requirements derived from these scenarios. The scenarios are broken down as "amazingly fast," "great service in a crowd," "ubiquitous things communicating," "best experience follows you," and "super real-time and reliable connections." (1)

One performance area, in particular, that is addressed in depth in this whitepaper, is the need to increase overall aggregate wireless capacity.

Wireless data traffic is projected to increase 5000 fold by the year 2030. This 5000-fold increase in traffic demand can be met through increases in performance, spectrum availability and massive densification of small cells as illustrated in Figure 3-2. It may be noted that the numbers in the boxes in the left side of Figure 3-2 are indicative of what might be achieved.

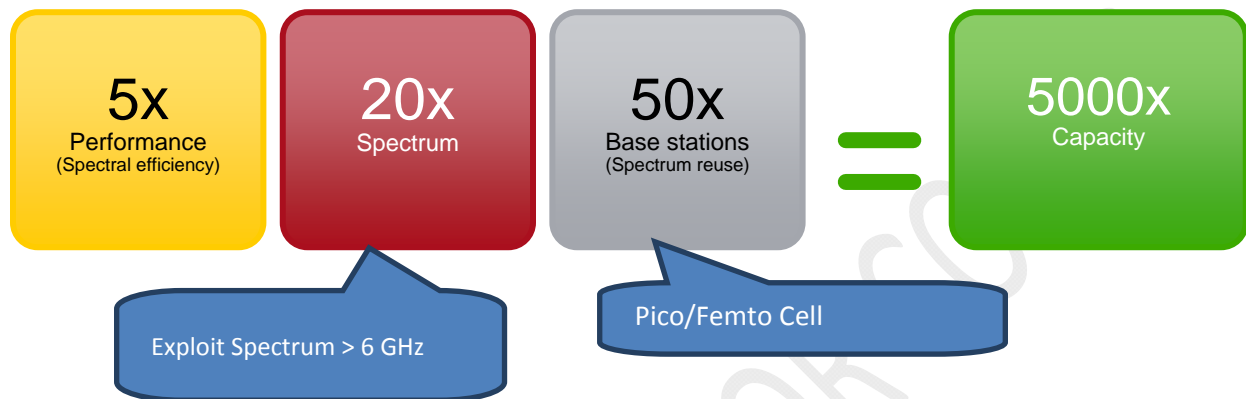


Figure 3-2: Illustrating 3 components to achieve 5000 x capacity relative to a LTE release 8

Recent innovations in cellular air-interface design, through 3GPP LTE, provide spectral efficiency performance that is very close to the Shannon limit. Spectral efficiency can be improved through techniques such as Coordinated Multi-Point (CoMP), Massive MIMO, Interference management and cancellation schemes etc. These techniques are especially useful for bands below 10 GHz while in bands above 30 GHz the potential availability of large amounts of spectrum could be exploited enabling the possibility of much larger transmission bandwidth (~ 1GHz). Also, at these higher frequencies, where the wavelength and antenna elements are smaller, large arrays are feasible for beamforming and low order MIMO to achieve system capacity and throughput gains.

To meet the growing traffic demand, the system capacity per square meter must be increased by either adding more network nodes (densification) or making additional spectrum available. To that end, the industry is already pursuing more dense networks by means of heterogeneous deployments consisting of low-power nodes (small cells such as metro-cells, microcells, picocells and femtocells) deployed under an overlaid high efficiency macro layer. Future cellular systems (e.g. may be termed as 5G) will need to use massive small cell densification to meet the massive capacity demands (e.g. 5000x capacity). Acquiring additional spectrum is one major focus for future wireless systems both below and above 6 GHz. Currently in 3GPP LTE Rel-12, efforts are being made to further enhance and optimize the performance of local area networks targeted towards carrier frequencies below 6 GHz. However, the available spectrum below 6 GHz is limited and there are practical limits due to propagation for how small these cells can shrink. Therefore, the cellular industry should, in a longer time perspective, consider new frequency bands in the 30-100 GHz range to meet this demand. If one third of that

spectrum could be made available longer term for mobile broadband that would amount to 23 GHz around 50 times the typical deployed cellular spectrum in most regions today below 6 GHz.

Like 4G systems, future wireless systems will evolve both in the licensed (e.g. 3GPP) and unlicensed bands (e.g. 802.11-ad). In other words, technologies developed in both licensed and unlicensed bands will continue to contribute to wireless usage, both as complementary air interfaces and in sharing spectrum with each other and with other wireless systems including RADAR and broadcast services among others. Finally, it needs to be emphasized that 5G will not replace 4G but will complement 4G LTE systems - for example in local area scenarios.

4 Key Incentives for 5G

4.1 Massive growth in traffic

Wireless data traffic has grown at an astonishing rate. AT&T, for example, reports 30,000% growth from 2007 through 2012. (2) This corresponds to a compound annual growth rate (CAGR) of $\sqrt[6]{301} - 1 = 2.59 - 1$ or 159%, which averages more than doubling per year over more than 6 years. However, this is down slightly from the tripling per year seen in the years immediately following the introduction of the iPhone in 2007. (3)

CISCO's VNI statistics show that the total wireless data traffic in TB/month nearly doubled for both North American and global wireless traffic growth with an average CAGR of 77% forecasted from 2012 through 2017 globally and 56% for North America (which had a larger base of traffic in 2012). (4) This explains CISCO's forecast, "Global mobile data traffic will increase 13-fold between 2012 and 2017."

Ericsson regularly publishes their understanding of current traffic and forecasts, and reported that global wireless traffic "almost doubled between Q2 2012 and Q2 2013." (5) Their August 2013 forecasts are shown in Figure 4-1 and show a total global growth of 47X from 2010 to 2018 (12.1X from 2012 to 2017) or 340X from 2010's traffic to a further extrapolation to 2030. (6)

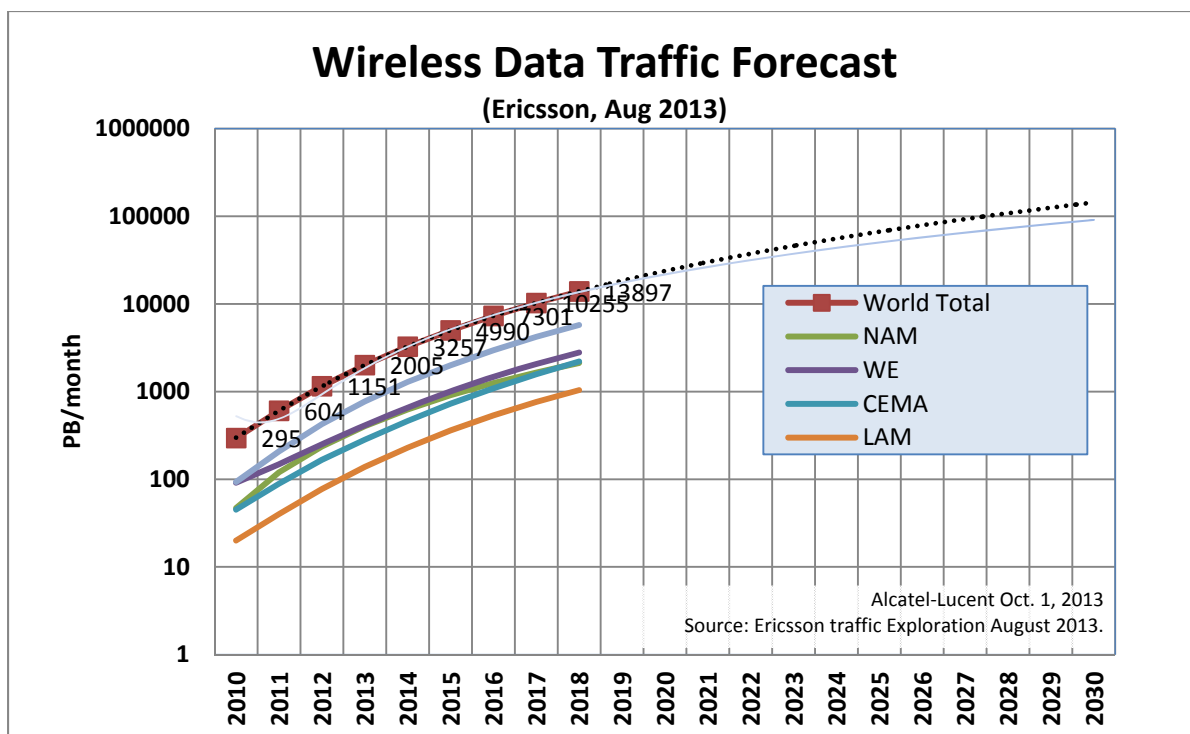


Figure 4-1 : Forecasted wireless traffic from Ericsson

Notably, even as the percentage growth has fallen below 100% recently, this decline is due to the large cumulative base in the denominator; the absolute increase in traffic is seen to continue to climb to record breaking levels year after year. That is to say, the growth while substantial is not exponential.

Alcatel-Lucent Bell Labs has evaluated alternative growth possibilities including evolutionary growth “stories” using “Crossing the Chasm” methodologies. (7) These forecasts and many other historical and forecasted data all normalized to 2011 are shown below in Figure 4-2. This includes a 100% CAGR reference line and the total Ericsson traffic data given earlier. The Cisco VNI forecasts have moderated since reports published in 2010.

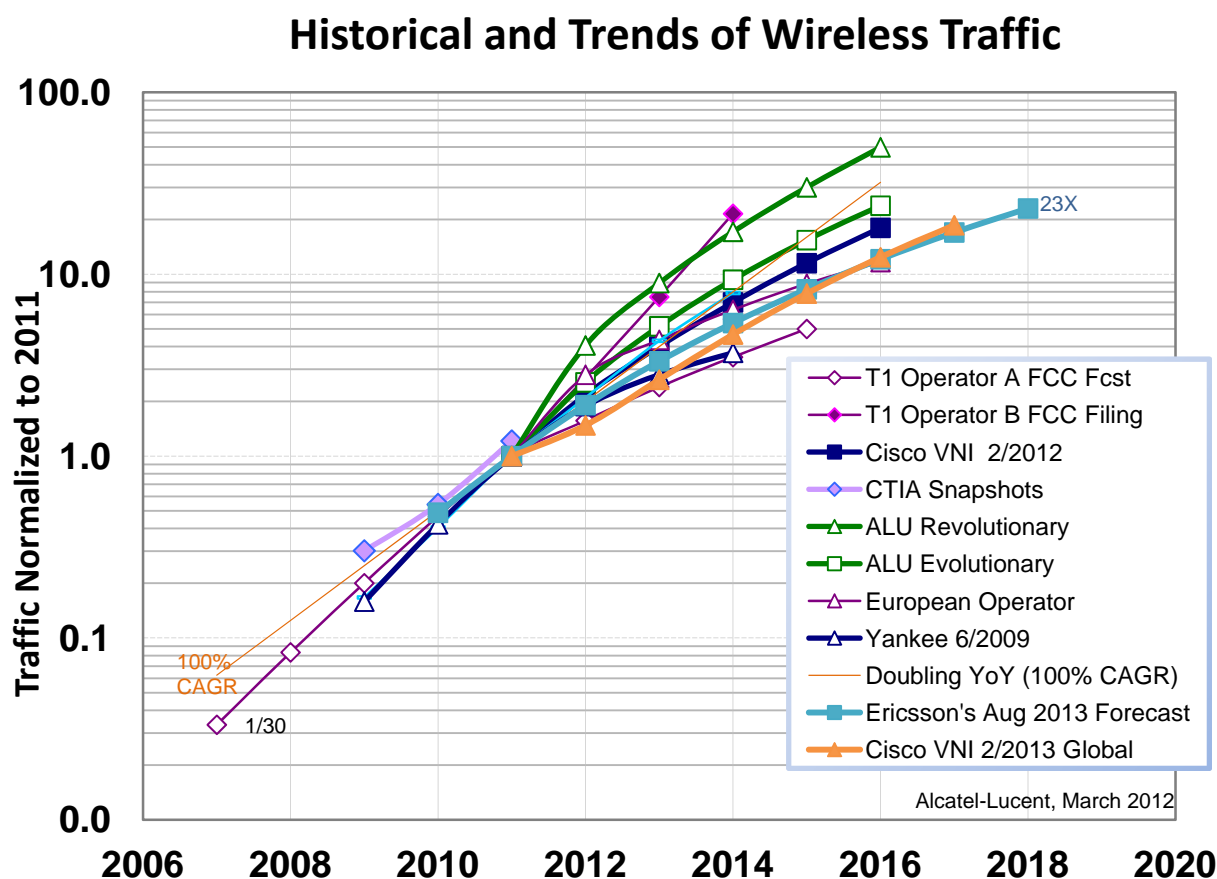


Figure 4-2 : Wireless Traffic data and forecasts all normalized to 2011 for ease of comparison.

For many years, forecasts of wireless subscriber penetration, subscriber data usage and Minutes of Use (MOU) notoriously underestimated the actual demands placed upon earlier wireless systems, and the same was true for the first decade of this century concerning mobile broadband traffic. And while forecasts have been moderating lately, forecasts are, as the expression goes, “extremely difficult, particularly about the future.” As new applications and use cases arise, the historical trends may, yet again, not hold true for the future and traffic may surge with the next generation and demand 100 or perhaps 1000 times more traffic. Traffic growth may also be fueled by emerging applications and new use cases associated with “communicating machines” as elaborated below. In all these cases however, traffic consumption will ultimately be moderated by the achievable cost of delivery.

4.1.1 Use cases that drive future traffic growth

Video is the KEY driving force

From a consumer devices point of view, application usage and over the top (OTT) services have drastically changed the experience, habits and thereby the consumption of viewing. The mobility aspect and the freedom given to control one's viewing experience have pushed for a distinctive increase of video consumption over the last years. It is expected by 2017 that more than 50% of the mobile cloud traffic is expected to be video traffic. The evolution of improved video quality and on-demand, seamless video streaming and sharing will set even higher requirements on future connectivity and system capacity.

Cloud intelligence and big data analytics

The role of devices in future systems could be seen from the perspective on where the intelligence and processing capabilities lie. The devices in a 5G scenario could, as one extreme, act as pure windows to the cloud with basic connectivity functions, while all the intelligence processing is in the cloud. The other extreme is devices that are powerful and intelligent and uses the classic cloud only as a complement. Combining the intelligence, computation capacities and storage with the avalanche of all devices on the market, new distributed cloud can be created and utilized.

Consumer devices are the key for big data analytics since they can collect and/or enable the collection of user data (especially behavioral). The user may not see a direct benefit of the data collected however this data is vital for the businesses that will rely on big data for their services.

Seamless mobility

From the consumer device point of view, the full access to use cases anywhere and anytime will put further requirements on wireless link reliability and availability. The user wants the optimal experience of seamlessness, without the knowledge upon which RAT the connectivity is established, as far as the pricing is acceptable for the service that is utilized.

4.2 Massive growth in the number of connected devices

There are currently on the order of 7 billion connected devices worldwide, most of which are mobile phones, smart phones, tablets, and laptops with wireless connectivity. In the future, these currently dominating human-centric devices are expected to be surpassed tenfold and more by new machine types of devices such as surveillance cameras, smart-home/grid devices, connected sensors etc. Just as the many tens of billions of microprocessors embedded in the world's infrastructure have become nearly uncountable, a future with several 100 billion connected devices may be expected. To handle such an enormous number of devices will, in itself, be a formidable challenge for future wireless access networks.

4.3 Wide range of requirements and characteristics

Future mobile-communication systems will also have to cope with a much wider range of applications and use cases, with a correspondingly much wider range of requirements and characteristics, compared to today. Mobile broadband services, including web browsing, video streaming and different forms of data sharing (e.g.: your hard disk in the cloud, real time backup services, etc.), will remain key applications and will continue to drive demand for higher data rates. Future demands for data rates exceeding peak rates of 10 Gbit/s in specific scenarios and general availability of data rates at least in the order of 100 Mbit/s can be anticipated.

In addition, the large-scale introduction of communicating machines will go hand in hand with the emergence of many new applications and use cases with characteristics and requirements that will not only differ significantly from the currently dominating mobile-broadband applications, but which will also vary significantly between applications.

- Some applications, such as augmented reality, may require data plane latency in the order of 1 ms or less, while, for other application the latency requirements may be very relaxed
- Applications related to the control of critical infrastructure, (e.g. the electrical grid or industrial control) may require extremely high reliability in terms of availability or some “guaranteed” maximum latency. In other cases (E.g. certain types of sensors such as temperature or moisture sensors in the home) the reliability and latency requirements may be much less critical.
- Some applications may be associated with major volumes of information to be conveyed while other applications, such as cargo tracking in the shipping industry, may be associated with very small data payloads.
- In some cases (e.g. battery-powered sensor networks) low device cost and/or energy consumption is extremely important while for other applications, this may be less of an issue.

To summarize, future wireless networks should be able to:

- Handle hugely more aggregate traffic than 2013’s networks (e.g. 5000x)
- Handle 100+ billion devices
- Provide end-user-experienced data rates of at least 10 Gbps in specific scenarios
- Provide generally available end-user-experienced data rates of at least 100 Mbps
- Provide the possibility for latency of 1 ms or less for some scenarios
- Provide the possibility for extreme reliability/availability for specific services and applications
- Provide the possibility for very low device cost and power consumption for specific applications

- Enable new business models
- Wireless backhaul should be included as an integrated part of future wireless-access technologies to handle situations where wired (fiber) backhaul is not suitable.
- Different means for self-organization, self-configuration, etc. should be an integral part of future wireless technologies.
- It is desirable that the overall network energy consumption should be minimized compared to the wireless access networks of today: 5000x capacity cannot mean 5000x energy consumption.
- Must be able to support very long life sensors or M2M nodes with battery lifetimes of at least 10 years.
- An increasingly diverse set of networks operating with different air interface generations, in licensed and unlicensed bands, and possibly sharing spectrum with other radio systems may be required.

It is desirable that these requirements should be fulfilled in an affordable and sustainable way. Thus, future wireless-access networks should allow for low CapEx and OpEx.

5 Requirements and Challenges for future wireless systems (may be termed as 5G)

It is predicted that 5G networks will include new local area radio access technology which will co-exist with 4G-LTE systems. Table 5-1 lists some characteristics for such radio access:

Access/Backhaul		
5G local area access KPI's	Values	Comment
Peak Data Rate	>10 Gbps	100x that of currently deployed 4G
Bandwidth	0.5-2GHz	Utilize large bandwidths for spectrum > 10 GHz
Minimum data rate	>100 Mbps	When needed
Duplexing	TDD	
Latency	~ 1msec	Tactile Internet Latency
Backhaul	>10 Gbps	Including wireless self backhauling
Machine to Machine		
Battery Life	➤ 15 years	Low utilization Sensors
Coverage	20dB + LB	Coverage for e.g. basements
Cost	Low	Much lower than current GPRS device

Table 5-1: Radio Requirements for 5G Local Area Technology

5.1 Architecture trends in 3G and 4G

In order to meet the traffic volume and latency requirements for projected mobile data traffic, several broad trends have been emerging in both 3G and 4G networks.

- 1st Trend: A flattening of the network to reduce the number of operator nodes the traffic must traverse before reaching its destination in order to minimize latency. Since each node that the traffic passes through incurs a processing cost and management cost, reducing the number of nodes is a clear direction to prepare networks for large traffic volumes. Direct Tunneling in UMTS and the flat RAN architecture in LTE are manifestations of this trend.
- 2nd Trend: A related trend is to allow traffic to “break out” to the internet as soon as possible. This also reduces the number of nodes traffic traverses before reaching its destination, and contributes to latency reduction. Breakout of traffic in the Visited Operator network is one of the first examples of break-out related enhancements, and provides significant latency and transport cost reductions in cases of roaming. More recently, Local IP Access (LIPA) and Selective IP Traffic Offload (SIPTO) were introduced in 3GPP to move the break-out function closer to the radio nodes. In fact, with LIPA, the traffic traverses exactly one operator node, which is the cell itself.
- 3rd Trend: The rapid improvement in Content Delivery Networks. These improvements serve both wireless and wire-line traffic, and focus on bringing the content closer to the end user in a transparent manner. Bringing the content closer reduces the latency and also reduces the transport cost of moving content across the internet.
- 4th Trend: The adoption of architectural solutions that allow closer interworking of different radio technologies, in particular licensed band technologies and unlicensed or shared spectrum technologies. Given that the challenge of traffic increase is foreseen to be met by an appropriate combination of several technologies, providing a seamless user experience across technologies is becoming increasingly important. Work in this area has been occurring in both 3GPP and the Wi-Fi Alliance. Although improved interworking does not by itself directly reduce latency (as the first three trends do) improved interworking contributes to improved load balancing across technologies which indirectly reduces latency by balancing the queue sizes across technologies.

5.2 Architecture Requirements and Solutions for future Wireless Systems

Architecture solutions as listed in Table 5-2 for 5G are expected to continue the trends from 3G and 4G.

Flat RAN has already been successfully deployed in LTE and should be considered a requirement for future wireless systems (e.g. 5G) in order to maintain latency and scalability advantages. Solutions that make the network more flat should be considered, e.g. moving some of the Mobility Management Entity (MME) functions to the periphery of the RAN architecture. This may mean, as well, the movement of node B functions closer to the physical core network (fronthauling or cloud RAN) to take advantage of pooling and virtualization opportunities.

Local IP Access (LIPA) is beginning to see deployment in 4G and should play a greater role in 5G. Moving towards LIPA decouples the core network from the traffic growth that is expected in 5G, and is potentially a significant cost saver in the core network. One disadvantage of LIPA is the lack of mobility support, so addressing this will be a key challenge for 5G. A possible way of improving mobility support is to make applications and consumer devices more robust to IP address change.

Content Delivery Networks (CDNs) are a key part to designing a scalable internet for service delivery to users. By placing commonly used content in servers close to the ISP point of presence, significant reductions in transport cost can be attained. This trend of moving the content closer to the user will continue in the future including migration of some CDN functions to radio nodes such as the eNB.

The interworking of different technologies, in particular LTE and WLAN, is another key requirement for 5G. Solutions have to work whether the LTE and WLAN nodes are collocated or non-collocated, and whether the nodes are operator or user deployed. As the network becomes more focused on small cells, it is likely that WLAN and LTE are in the same node, and particular focus should be placed on that case.

Requirement	Solution Candidate and Challenge
Flat Network	Moving some MME functions to the RAN or RAN functions to the core
Local Breakout	Good mobility support with local breakout to hotspot
Inter-RAT interworking	Allow tighter integration between radio nodes of different technologies
CDN	Move some of the CDN function to a local radio node (eNB)

Table 5-2: Architectural Requirements for 5G with Solution Candidates and Challenges

5.3 Deployment Models in Future Wireless Systems

5.3.1 Planned Small Cells Deployment

The advent of smart phones has served as a catalyst for the significant increase in mobile broadband data traffic on cellular networks. The mobile data demand continues to grow prodigiously (70-100% annually) (8). In the not so distant future, there will be a need to support vastly more mobile data traffic (e.g. 5000x) compared to traffic carried by today's cellular networks due to increased smart phone and tablet usage as well as an increase in data consumed per user. This data demand needs to be met at a low cost to the operator as well as the end user to sustain and further fuel wireless data growth. Addressing this massive data demand in a cost-effective manner presents formidable technical challenges and requires innovative solutions. Today's cellular technology standards are already designed to exploit very high radio link spectral efficiencies (e.g., LTE Rel. 10 has peak downlink spectral efficiency of 30 bps/Hz), but operation at such efficiencies due to achievable SINR is impractical and so radio link level enhancements at PHY/MAC layers alone will not solve the capacity problem. Several alternative approaches are needed including:

- Increased spectral reuse (~50x) through network densification, i.e., deploying more base stations and repeaters/relays, each with a small coverage footprint, in geographical areas with high data demand,
- Additional spectrum (~20x), and
- Improvement in system efficiency (~5x) (e.g., more efficient use of existing spectrum, optimal use of multiple technologies concurrently).

This section focusses on network densification.

Network densification boosts system capacity through increased spectrum re-use by cell-splitting. In addition, it brings base stations closer to users, thereby reducing path losses and serving fewer users per base station which provides additional improvement in capacity as well as reduced battery consumption. However, network densification by deploying more traditional macro-base stations is unviable due to difficulty in finding suitable installation sites as well as high costs of installing/maintaining macro-base stations. Rather, network densification (small cells) is achieved through deploying base stations having a small form factor with increased flexibility for rapid deployment, and low transmit power.

Offloading users from macro to small cells not only increases overall capacity but significantly enhances experience of both macro and small cell users. Splitting traffic into macro cells and small cells increases the share of available data pipes for all users and thus boosts users' data rates. Further, technological

advances in the last several years have dramatically reduced the cost of small cells compared to traditional macro cells.

Considering these benefits, 3GPP made small cells an integral part of LTE in Rel. 10 (LTE Advanced) by developing the concept of HetNets, i.e., heterogeneous networks consisting of a mix of macro cells and small cells (comprising picocells, femtocells, metrocells). LTE Rel. 12, studied small cells as one of the key areas for LTE evolution (9), (10), (11).

Several major operators worldwide are either in the process of or planning to deploy HetNet to densify their networks in the next few years. Such HetNet deployments consist of a few to tens of small cells deployed by an operator to meet high data demand in specific areas (e.g., malls, downtown areas, event venues). These traditional HetNet deployments can meet near-term mobile data demand, but it is questionable to whether the same deployment model can scale to meet the projected massive data demand of the future (e.g. 5000x).

Even though the small cell equipment costs have been dramatically reduced, there are significant hurdles for scalability of such an operator-deployed network densification when deploying millions of such cells. Traditionally, operators have had to perform RF planning to find the optimal locations to place cell-sites and then send technicians to install them. This situation is changing with the gradual introduction of SON in 4G, and the adoption and further development of SON will need to be integral to 5G systems.

Also, a suitable grade of backhaul needs to be provisioned if it is not already available.

Not only do the above require a lot of effort from the operator but the site rent, utilities, and backhaul are all recurring costs that contribute to high OpEx. The traditional deployment approach then incurs high cost that is not scalable as the number of small cells increase into the millions.

5.3.2 Unplanned Small Cells Deployment

One approach that can provide scalability is to move to more of an unplanned deployment where cells can be installed with minimal supervision and/or RF provisioning (reducing installation costs) and utilize commercially available backhauls (reducing cost of high QoS backhaul enjoyed in current macro/pico deployment).

While solving scalability to a great extent, this approach, if not properly implemented, could have serious impacts on users' experiences and expected QoS that includes:

- non provisioned backhaul may lead to poor performance compared to what the user can get on macro sites deeming the small cell not useful for a class of users
- With high density, random selection of pilot signatures (PN in C2K, PSC in UMTS and PCI in LTE) can lead to ambiguity during mobility and consequently call drops

The unplanned nature of deployment can cause highly interference-contaminated areas due to many small cells within a close range to the user, i.e. areas with very limited link quality. Conversely, it may cause areas of limited coverage.

However, if the carrier frequency is dramatically increased from today's 1-2 GHz range, the wavelength will proportionally decrease, thereby allowing physically small, high-gain, adaptive antennas that provide real-time beam forming at both mobile devices and infrastructure equipment. When combined with cooperation techniques across the array of infrastructure equipment in a particular coverage or capacity zone, low cost base stations and relays with real-time beam forming will be able to optimize connectivity between UEs and the infrastructure, as well as backhaul connectivity between the infrastructure equipment (12), (13).

6 Spectrum & Propagation Aspects

6.1 New spectrum from 6 GHz to 100 GHz

New techniques applied to existing cellular spectrum can and will provide needed capacity increases, but these increases will not be enough to meet anticipated demand. CoMP techniques, which are not trivial in complexity, are expected to provide up to ~2x improvements. Massive MIMO gains and its cost and complexity are difficult to predict, but it should not be expected that massive MIMO will save us from the bandwidth crunch either.

New spectrum, and a lot of it, will ultimately need to be part of the solution to meet anticipated data capacity.

Simply put, there is the potential to have access to much larger amounts of spectrum at millimeter wave frequencies. The frequencies above 6GHz in Table 6-1 are potential mobile allocations in the ITU Radio Regulations (14). This means that any of those frequency bands could, in theory, be used for 5G without having to add a Mobile allocation in ITU.

Frequency Designation	ITU-R*		US (Non Federal)	
	Frequency Range (GHz)	Available Spectrum (GHz)	Frequency Range (GHz)	Available Spectrum (GHz)
6GHz	5.925-8.500	2.575	6.425-7.125	0.35
10GHz	10.5-13.25	2.63	12.70-13.25	0.35
14GHz	14.4-15.35	0.95		
17GHz	17.7-17.81	0.11		
18GHz	18.1-19.7	1.6		
21GHz	21.2-23.6	2.4	21.2-23.6	2.4
25GHz	25.25-25.5	0.25		
28GHz	27.0-29.5	2.5	27.5-29.5	2

31GHz	31.0-31.3	0.3	31.0-31.3	0.3
36/38/40GHz	36-47	11	36.0-42.5 45.5-47.0	8
50GHz	47.2-52.6	5.4	42.7-52.6	5.4
55GHz	55.78-57.0	1.22	55.78-57.0	1.22
60GHz	57-64	7	57-64	7
65GHz	64-71	7	64-71	7
70GHz	71-76	5	71-76	5
80GHz	81-86	5	81-86	5
90GHz	92-94	2	92-94	2
90GHz	94.1-95.0	0.9	94.1-95.0	0.9
95GHz	95-100	5	95-100	5
Total Available		62.835GHz		52.12GHz

* Where ITU-R Regions 1, 2 and 3 differ, Region 2 (Americas)

Table 6-1 ITU mm-wave mobile frequency allocations

As can be seen from Table 6-1, the spectrum above 6 GHz represents a large bandwidth opportunity. For instance, the 60GHz unlicensed band provides more spectrum than all of the sub-6GHz bands combined. Similarly, the 71-76 GHz and 81-86 GHz bands are available worldwide typically via either a “lightly licensing” or traditional point-to-point licensing regime, where each band boasts 5GHz of bandwidth making them suitable for high data-rate wireless communications. Other frequencies may become available, such as the 10 GHz, 28 GHz and 38 GHz bands.

With industry support and representation at regulatory bodies, some of this bandwidth could potentially be repurposed for 5G system deployment.

Having access to such large blocks of spectrum also enables early deployments to leverage bandwidth against spectral efficiency, i.e., high data rates can be achieved more easily and at lower power with a large bandwidth thus enabling lower cost radios for early deployments.

With massive bandwidth allocations, and through the use of high gain adaptive antennas at mm-wave frequencies, cellular networks will revert from today's interference-limited regime to a noise-limited regime, thereby allowing new technologies to provide more dramatic capacity improvements over time as mm-wave networks evolve (15).

6.2 Other uses of the spectrum above 6 GHz.

It is also to be noted that current applications above 6 GHz include radio astronomy, wireless backhaul, inter-satellite links, RADAR, radiolocation, amateur radio and space research. Possible coexistence with these applications would need to be studied. The wireless industry is already experienced with adjacent channel coexistence issues that have existed in the lower bands from the earliest days of radio. However, channel sharing strategies are being explored only recently. Various database approaches to

Spectrum Authorization Systems (SAS) and Licensed Shared Access (LSA) are emerging as important ways for multiple services to share frequency bands based upon time and geography.

6.3 Propagation in mm-wave bands

Propagation losses at millimeter wave frequencies have historically been thought to be too large for practical communication in large networks that involve links of more than a few tens of meters. The dependency of the free-space path loss can be clearly seen in the well-known Friis equation for free space propagation loss (16).

$$\begin{aligned} P_r &= \left(\frac{P_t}{4\pi r^2} \right) \left(\frac{\lambda^2}{4\pi} \right) = P_t \left(\frac{\lambda}{4\pi r} \right)^2 \\ P_r &= P_t \left(\frac{c/f}{4\pi r} \right)^2 = P_t \left(\frac{c}{4\pi r f} \right)^2 \end{aligned} \quad (1)$$

The first term in the top of Equation (1), $\left(\frac{P_t}{4\pi r^2} \right)$ is the transmit power density on a sphere of radius r . The second term is the “capture area” or aperture of the receive antenna for a half wave dipole of dimension $\lambda/2$, the factor of π in the denominator is a correction for the dipole characteristic. This states that the receive power is equal to the transmit power density at the receiver, times the effective capture area of the receive antenna. This is also expressed in terms of frequency in the second line of Equation (1). This shows that just by moving from a 2 GHz carrier to a 60 GHz carrier (an emerging unlicensed millimeter wave band), the path loss $PL = P_t/P_r$ (without considering atmospheric absorption) increases by nearly 30 dB in free space, yet the wavelength λ , given by $\lambda = c/f$, shrinks from one sixth of a meter at 2 GHz to a miniscule 5 millimeters at 60 GHz. The loss at 60 GHz is even greater than 30 dB in practice, since oxygen absorption causes an additional 20 dB/km of loss on top of the theoretical free space propagation loss (17). The 30 dB increase in free space loss sounds disastrous for millimeter waves at first, but this is not the case, since propagation must also consider the impact of the transmit and receive antennas used in a communications link.

Fortunately, the gain of a receiver antenna can completely mitigate the increase in path loss with frequency given in Equation (1). For a given physical size or aperture, an antenna has greater gain as the wavelength shrinks, such that path loss is not frequency dependent as long as receiver antennas with the same physical size are used in comparing different frequencies. This is illustrated in Figure 6-1 for three cases of antenna combinations. On the left is the case representative of Equation (1) in which both transmit and receive antennas are omnidirectional. The middle shows an omnidirectional antenna paired with a horn antenna of fixed aperture (fixed in terms of square meters not square wavelengths).

The third case shows two directional antennas of fixed aperture of the sort common in fixed point-to-point microwave links. But this can also apply to antenna arrays of constant aperture size as well.

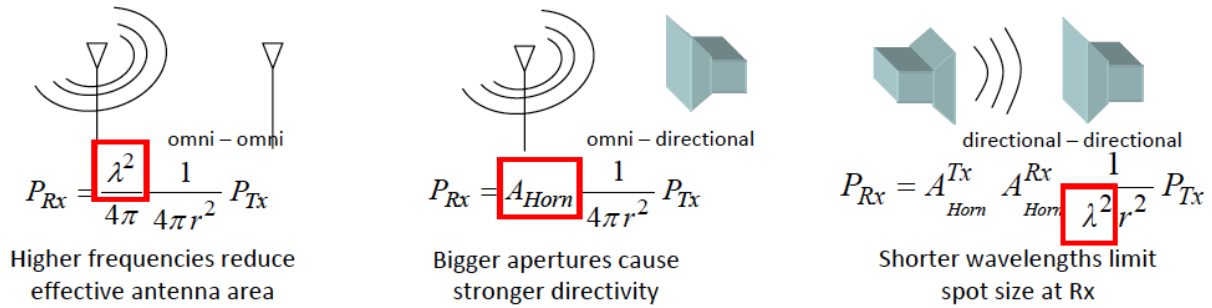


Figure 6-1. Comparison of propagation loss equations for different antenna combinations. (Source: Alcatel-Lucent, used with permission.)

To illustrate the fact that path loss is not frequency dependent in free space when a constant physical size is assumed at the receiving antenna, regardless of frequency, consider the power flux density (measured in W/m^2) of the plane wave at the receive antenna at distance d from the transmit antenna (18):

$$\rho = \frac{P_T}{4\pi r^2} \text{ W/m}^2 \quad (2)$$

Equation (2) shows that the received power density is not a function of frequency, but is only a function of the transmitter power and path distance. The reason for the larger path loss at higher frequencies in Equation (1) is because the antenna gain at the receiver is implicitly assumed to be the same for all frequencies, which further implies the receiver antenna size shrinks at higher frequencies in order to maintain a physical size that is proportional to the operating wavelength. However, instead of shrinking antennas in proportion to the wavelength, if it is assumed the same physical size (aperture) receiver antenna is used at any frequency, the fixed physical dimension of the receiver antenna can be used to implement high gain phased array antennas at mm-wave frequencies instead of the low gain antennas in current wireless systems.

With the assumption that the receiver antenna size (and not the gain) remains constant at any frequency, the expression for free-space path loss in Equation (1) becomes Equation (3) as illustrated in the right of Figure 6-1.

$$PL = G_T G_R (4\pi d)^2 \quad (3)$$

where Equation (3) assumes the physical area of the mm-wave phased array at the receiver is the same physical area as lower frequency antennas, and G_T and G_R are transmitter and receiver gains respectively.

It is noted that Equation (3), as in Equation (2), is independent of operating frequency, since the assumption of identical physical sized antennas at any frequency causes the path loss to decrease (e.g. the channel gain to increase) by a factor of λ^2 as the frequency increases, since the gain of the receiving antenna implicitly increases with increasing frequency.

The result in Equation (3) can be implemented at mm-wave frequencies using a phased array antenna that has an area comprised of a number of smaller individual antenna elements that are proportional to λ^2 in area such that a fixed physical antenna area will have more elements in a phased array as the frequency increases, thus providing greater gain at higher frequencies.

The high gains achievable by phased array antennas can more than make up for the perceived propagation loss at mm-wave frequencies from Equation (1), while adding the benefit of flexible, steerable beams that can adapt to changing interference and propagation conditions in real time.

The assumption that the antenna gain increases with frequency is equivalent to saying that the directionality of antennas increases with frequency. From this arises an important challenge for mobile access – how to aim the antennas at each other? There are in addition, hands, heads and other nearby obstructions that deform the antenna patterns at the UE that threatens to make high gain antennas in the handset unusable for access. It becomes a bit like making one's way through a thicket at night with a laser pointer when a broad beamed flashlight is needed. Significant innovation will be needed to enable frequencies currently limited to fixed point backhaul to be usable for mobile access.

As the antenna gain increases so does the directivity, therefore more care must be taken to aim the transmit and receive antennas at each other. The scattering environment surrounding a non-line-of-sight (NLOS) communication link increases the angle-of-arrival spread such that the incoming (or, through reciprocity, the outgoing) radio energy is spread over angle space beyond the beamwidth of the antenna located in the clutter. For example, consulting a number of publications, including the 3GPP standard channel model recommendations, the following angle spread parameters are chosen for the case of an urban macro cell placed above the clutter and the remote Customer Premises Equipment (CPE) placed below clutter. These angle spread parameters shown in Table 6-2 were reported for street level remote terminals and are judged conservative when the remote CPE is placed well above street level, perhaps near roof top:

Base azimuthal Angle Spread at rooftop	Base Elevation Angle Spread at rooftop	Remote Azimuthal Spread in clutter	Remote Elevation Spread In clutter
8°	8°	50°	18°
Source: (19)	Source: (20) but source is unclear, the number is judged conservative, much higher than that reported in reference (21)	Source: (19)	(20)

Table 6-2 – Angle Spread Parameters

As a result, the antenna gain can work against the system and reduce the amount of radio energy coupled between the transmitter and receiver. A simple analysis of this using the 3GPP Spatial Channel Model (SCM) results in the following calculation of received SNR for a point-to-point link with antennas pointed at each other. Assuming a 30 dBm transmit power, 9 dB noise figure, a 10 MHz bandwidth, a 10 dB shadow margin only in the clutter, 10 dB of Rayleigh fading margin, free space propagation loss for Line-Of-Sight (LOS) and the 3GPP urban macrocell model for NLOS (22), it is possible to calculate the SNR for a point-to-point link as shown in Figure 6-1. The LOS curve is as described in Equation (3), however; the NLOS case is shown as substantially degraded.

SNR vs frequency for 30x30mm antennas for both above-rooftop BTS and a 10m high node. 1W, 500m, 10MHz, 15mm/hr rain

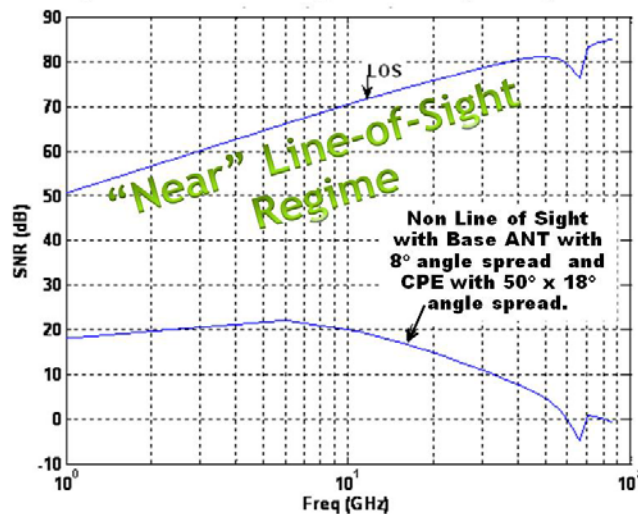


Figure 6-1: Direct comparison of LOS and NLOS propagation as a function of frequency.

For LOS, free space spreading loss as well as absorption due to atmospheric gases and precipitation is included. For NLOS, the 3GPP propagation loss as well as the absorption and gain degradation due to scattering are included, in addition to shadow and Rayleigh margins. (Source: Private Alcatel-Lucent correspondence D.Chizhik, March 20, 2013, used with permission.)

6.4 Terrestrial propagation and deployment issues for mm-wave systems

Propagation of millimeter wave signals through realistic terrestrial environments face unique challenges. Two often-cited loss mechanisms are losses due to rainfall and losses due to atmospheric gasses. These both significantly impact signals at frequencies greater than 6GHz. As shown in Figure 6-2, for a heavy rainfall (~25mm/hr.), the additional loss is about 6-10 dB/km in the 28-60GHz range, and in extreme downpour conditions (~75mm/hr.), the additional loss can be in the 15-25 dB/km range (23).

Molecular oxygen absorption for 60 GHz is particularly high ($\sim 13\text{dB/km}$, depending on altitude) but falls off rapidly away from the resonance frequency, to well below 1dB/km just a few GHz away from the oxygen resonance. While these absorptions are considered high for multi-km links, cell densification has already reduced the required link distance to be substantially smaller in urban areas, and the densification process will continue to shrink cell sizes. For a link distance of $\sim 200\text{m}$, even the loss for a 60 GHz link in heavy rain is less than 3dB .

Figure 6-2 and Figure 6-3 illustrate the impact of rainfall and oxygen absorption throughout the mm-wave spectrum.

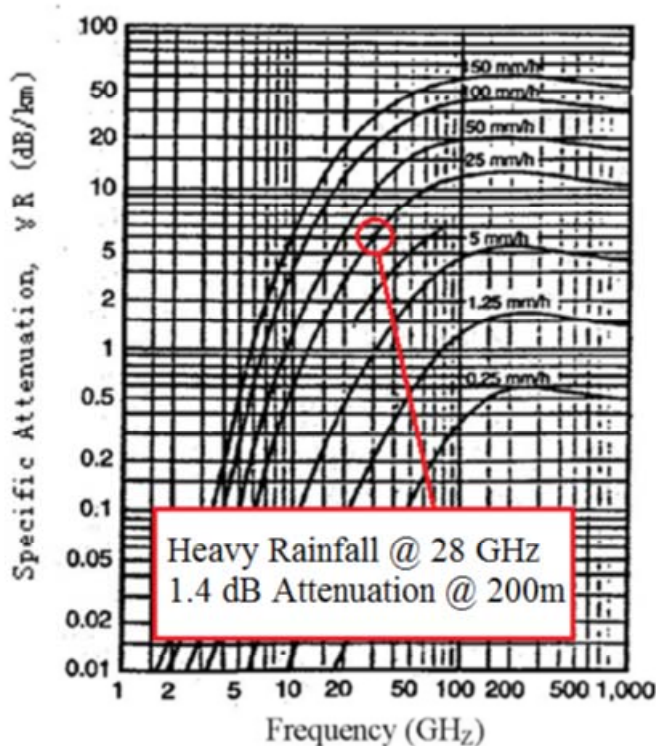


Figure 6-2. Attenuation due to rain in the mm-wave spectrum.

Figure 6-3 shows that for heavy rainfall (25 mm/hr.), a 200m link at 28 GHz is attenuated by 1.4 dB , or 7 dB/km (24).

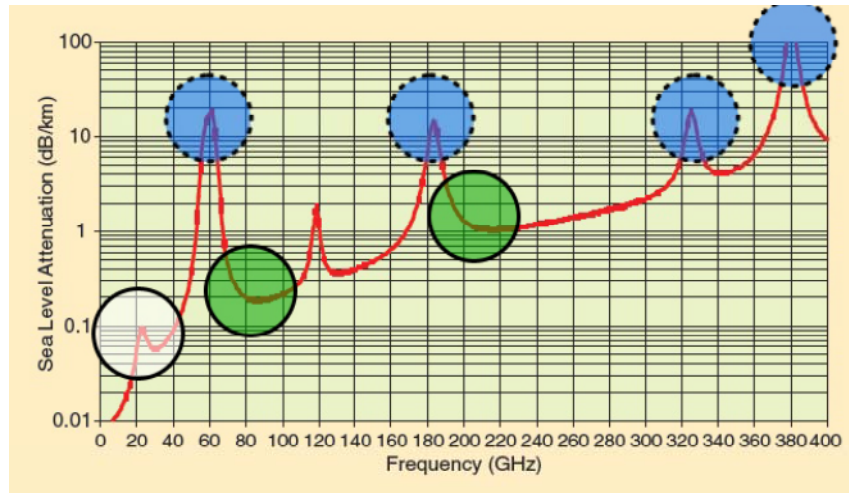


Figure 6-3. Atmospheric attenuation in the mm-wave spectrum.

In Figure 6-4 the white circles shows that attenuation is less than 0.1 dB/km at frequencies below 50 GHz, and the blue circles show the atmospheric absorption resonances at 60, 180, 330 and 380 GHz. Also note that at 100 GHz and 200 GHz, atmospheric absorption is at or below 1 dB/km (25).

A more serious issue than free-space loss for mm-wave carriers is their limited penetration through materials and limited diffraction. In the urban environment, coverage for large cells could be particularly challenging, but again, since cell densification is included as one of the contributors to achieving the massive capacity goal (e.g. 5000x), millimeter wave base stations will by necessity, be placed close enough to enable high capacity.

Providing good coverage for the access link between the base station and mobile is not the only coverage issue. Backhaul must also be provided to all the base stations. Bringing fiber to all these nodes will be a cost prohibitive option in many cases. Again, the high density of millimeter wave nodes helps to provide a low-cost solution. The millimeter wave nodes can be mounted on common street fixtures (lamp posts) along streets in good coverage of each other to form a mesh in the millimeter wave coverage, so that the mm-wave bands could additionally provide backhaul connectivity (12) (13). To further keep deployment costs down, electrically steerable antennas can be employed for automated mesh formation for backhaul. Another area for further cost optimization is the joint access and backhaul approach, where mm-wave spectrum can be used both for access and backhaul links (12).

6.5 The interference and power advantage of mm-wave spectrum

The limited propagation of millimeter waves can also prove beneficial. The natural limits discussed reduce the overall interference temperature in the millimeter wave environment and make the system noise limited rather than interference limited.

As previously mentioned, high gain antennas that are physically no bigger than today's antennas will be used to overcome the perceived propagation loss at mm wave frequencies. This also implies that the

antennas have very narrow beamwidth. The narrow beams and high gain antennas provide further advantage in interference mitigation. The transmit energy is focused in a narrow direction towards the intended receiver, and thereby does not interfere with most of the coverage area. At the receiver, additional spatial filtering is performed with another high gain steerable antenna, and any residual interference arriving outside of the receiver's beamwidth is further reduced by the spatial discrimination of the high gain antenna.

The directional beams of both the transmitter and receiver work in tandem leading to a system that is primarily noise (or power) limited rather than interference limited – effectively eliminating the traditional interference limited cell-edge problem.

While this concept is not new, the ability to integrate small, high gain antennas in UE equipment has only recently been available with the interest in 60 GHz WiGig and WirelessHD (17) (26).

Another benefit from high gain antennas is better energy efficiency. At the transmitter, a much higher Effective Isotropic Radiated Power (EIRP) is achieved for a given total radiated power budget. At the receiver, the high gain adds directly to performance (or reduced TX power requirement).

Technological developments are still needed, e.g. to make very efficient high gain antennas and mm-wave RF power amplifiers in integrated form factors. Work is rapidly advancing in this field, and new theories have recently been developed to allow engineers to more effectively design mm-wave components (17) (27).

7 Propagation characteristics of mm-wave bands

7.1 Frequency dependence of propagation mechanisms

In general, radio wave propagation is affected by diverse physical mechanisms that more or less corrupt the original transmitted signal arriving at the receiver. Propagation mechanisms include free-space propagation, object penetration, reflection, scattering, diffraction as well as absorption caused by atmospheric gases, fog and precipitation. To what extent each mechanism contributes to the overall signal attenuation and distortion depends greatly on the propagation scenario (e.g. link distance, indoor/outdoor, LOS/NLOS) and the radio frequency of operation.

7.1.1 Free-space propagation:

Free-space propagation conditions can be assumed if the first Fresnel zone is substantially free of obstacles. According to the well-known Friis equation (28) (29), the free-space path loss increase with the square of link distance and carrier frequency, as shown in Equation (1). If either the distance or the frequency is doubled, the propagation path loss increases by 6 dB (20 dB increase per decade). As a result, a transmitted signal at 60 GHz undergoes an almost 36 dB higher attenuation on the same way to the receiver compared to a signal at 1 GHz, even before the atmospheric absorption due to Oxygen as shown in Figure 6-3

7.1.2 Atmospheric effects:

Atmospheric effects mainly involve oxygen and water vapor absorption as well as fog and precipitation. They scale exponentially with the link distance (30). Confining to distances below 1 km, attenuation caused by atmospheric gases can be neglected up to 50 GHz, as shown in Figure 6-3. However, above 50 GHz, it becomes important to take into account the oxygen absorption peak of approx. 15 dB/km at 60 GHz and the water vapor resonance peak at 183 GHz (approx. 29 dB for rel. humidity of 44% under standard conditions). Neither fog nor rain is relevant for frequencies below 5 GHz. At frequencies above 80 GHz, dense fog related to a visibility of less than 70 m has a visible impact (≥ 3 dB/km) and becomes severe above 200 GHz (≥ 10 dB/km). Drizzle and steady rain are not a substantial issue for distances up to 1 km (3.0–4.4 dB/km above 70 GHz). However, as shown in Figure 6-3, heavy rain yields values up to 10-15 dB/km, and for downpours, attenuations up to 40 dB/km can be experienced. Also, hail storms, while rare, can greatly attenuate links, causing as much as 35 dB of attenuation on a 670 m path (31).

In summary, atmospheric effects, especially under bad weather conditions are relevant for mm-wave links over distances above 100 m and a crucial issue for longer distances of 1 km.

7.1.3 Penetration losses:

Electromagnetic waves are attenuated when they propagate through objects. It is well known that the transmission coefficient for dielectric materials is a function of the wavelength (32) (33), although recent works shows that at mm-wave frequencies, most outdoor building materials, such as tinted glass and brick, are high loss, but indoor materials are relatively easy to penetrate (34).

At frequencies up to several GHz, it is possible to achieve coverage inside buildings from a base station outside, though the signals can be attenuated by several dB up to around 20 dB (35) (36).

The attenuation depends on the building materials and the building type, especially on the type of windows and the percentage of the windowed area. The reason for that is that glass can provide a relatively low loss path even to millimeter waves on the one hand (37) (38). On the other hand, losses due to glass with metallic tints and coating can be as high as 30 dB, even in the lower GHz range (39). The attenuation caused by concrete or brick walls becomes very high in the mm-wave band, on the order of 30-40 dB as shown in Figure 7-1 and Figure 7-2, which means that solid walls and buildings are practically impenetrable (32) (38) (34).

However, recent work at 28 and 72 GHz demonstrate that once inside of a building, propagation between rooms is relatively easy to accomplish, as shown in Table 7-1 and Table 7-2 of penetration measurements (34) (40).

Environment	Location	Material	Thickness (cm)	Received Power - Free Space (dBm)	Received Power - Material (dBm)	Penetration Loss (dB)
Outdoor	ORH	Tinted Glass	3.8	-34.9	-75.0	40.1
	WWH	Brick	185.4	-34.7	-63.1	28.3
Indoor	MTC	Clear Glass	<1.3	-35.0	-38.9	3.9
	WWH	Tinted Glass	<1.3	-34.7	-59.2	24.5
		Clear Glass	<1.3	-34.7	-38.3	3.6
		Wall	38.1	-34.0	-40.9	6.8

Table 7-1. Comparison of penetration losses for different environments at 28 GHz.

Thicknesses of different common building materials are listed. Both of the horn antennas have 24.5 dBi gains with 10 degree half-power beamwidth. (34)

RX ID	TX-RX Separation (m)	# of Partitions				Received Power for Free Space (dBm)	Received Power for Test Material (dBm)	Penetration Loss (dB)
		Cubicle Wall	Metal Cabinet	Dry Wall	Wood Door			
1	6.8	1	0	0	0	-34.1	-39.4	5.3
2	8.0	1	1	0	0	-35.6	-52.8	17.2
3	10.1	2	2	0	0	-37.6	-61.4	23.8
4	11.5	1	2	1	1	-38.7	-75.5	36.8
5	8.6	0	2	0	0	-36.2	-50.3	14.1
6	8.1	0	2	0	0	-35.7	-45.4	9.7
7	8.8	1	2	0	0	-36.4	-63.0	26.6
8	14.0	0	2	1	1	-40.4	-55.6	15.2
9	13.0	1	3	0	0	-39.7	-53.0	13.3
10	15.2	1	2	1	0	-41.1	-60.4	19.3
11	15.2	1	2	1	0	-41.1	-59.0	17.9

Table 7-2. Penetration losses at different receiver locations

At 73.5 GHz. numbers and types of obstructions are listed. Both of the transmit and receive antennas have 20 dBi gain with 15 degree half-power beamwidth. The RX ID numbers correspond to the locations. (40)

7.1.4 Reflection:

Reflection is the main reason for multipath propagation and occurs if the wave arrives at a surface of an object, which is large compared to the wavelength (41). A specular reflection takes place if the surface is flat and plane. The reflected amount of energy depends on the material properties, the incident angle and the polarization of the wave. It is given by the Fresnel reflection coefficients (42) (43). It is worth mentioning that the coefficients, themselves, are not frequency-dependent, as long as the frequency dependence of material properties is neglected. The main reason for frequency dependence is related to surface roughness. If the surface is rough, the reflection is diffuse, spreading the energy in all directions rather than reflecting it in a single direction. The Rayleigh criterion, which is a function of the surface irregularities (quantified by their standard deviation σ), wavelength and incidence angle, can be

used to determine whether a specular or a diffuse reflection can be expected (42). For normal incidence a surface is definitely rough if σ is in the order of the wavelength, and the results in (38) indicate that roughness has distinct influence if σ is in the order of tenth of the wavelength. The losses can be taken into account by introducing scattering reduction factors in order to modify the reflection coefficients (43) (38).

For indoor scenarios typical materials can be considered as smooth for frequencies up to 30 GHz. In the mm-wave band moderate losses can occur due to surface roughness.

With respect to outdoor propagation, the roughness of materials is typically higher as frequency is increased, so one would expect there to be moderately more attenuation of reflections than in the lower GHz region.

Surprisingly, however, recent measurements in New York City and Austin, Texas at 28, 38, 60 and 72 GHz show that typical outdoor environments have very strong reflected or scattered signals, thereby providing a rich multipath environment for a wide range of scenarios (44) (45) (12) (46). This means that signal processing techniques will be able to exploit the large number of multipath components, as well as different angles of arrivals, to create multi Gbps links at mm-wave frequencies.

Table 7-3 illustrates recent measured outdoor reflection coefficients at 28 GHz in Brooklyn, NY, illustrating the strong reflective environment of typical urban channels (34).

Environment	Location	Material	Angle (°)	Reflection Coefficient ($ \Gamma_{ } $)
Outdoor	ORH	Tinted Glass	10	0.896
		Concrete	10	0.815
			45	0.623
Indoor	MTC	Clear Glass	10	0.740
		Drywall	10	0.704
			45	0.628

Table 7-3. Comparison of reflectivity for different materials at 28 GHz.

Concrete and drywall measurements were conducted with 10 degree and 45 degree incident angles, while tinted and clear glass reflectivity were measured at 10 degrees. Both of the horn antennas have 24.5 dBi gain with 10 degree half-power beamwidth. (34)

7.1.1 Diffraction:

When a radio wave encounters sharp irregularities like edges and corners of a dense object with large dimensions relative to the wavelength, diffraction occurs – an apparent bending of the wave around the edge/corner (42). At frequencies up to several GHz the diffracted field around objects and building edges can significantly contribute to the total received power and it is important to consider diffraction for outdoor propagation. However, as frequency increases to above 10 GHz, diffracted energy rapidly

decreases. In the mm-wave bands, diffraction effects are only relevant if the size of the obstacle is quite small (in the order of tens of cm for typical propagation scenarios), and normally diffraction can be neglected. This reduces the coverage areas because of the sharper shadows from obstructions.

7.1.2 Scattering:

Scattering is related to interactions of the electromagnetic wave with objects having dimensions in the order of the wavelength or smaller than the wavelength. Depending on the shape of the object, the incoming wave is spread out into many directions, and it is very difficult to accurately compute the effects in a deterministic manner. This also applies to cases with a large number of obstacles, where a deterministic description is not meaningful, e.g. the foliage of trees – even if the leaves might be much larger than the wavelength. In these cases only the overall effects, e.g. foliage losses for the direct propagation path, are taken into account. Measurements in 28, 38, 60 and 72 GHz shows that there are strong scattering components found from both outdoor and indoor measurements, thus scattering will be a viable propagation mechanism for creating sufficient coverage in the densest urban NLOS environments.

7.1.3 Foliage losses:

Foliage in the path of a radio link causes signal attenuating, scattering, depolarization and beam broadening. Numerous factors influence the attenuation through vegetation: path length through foliage, vegetation type, density and seasonal conditions, wetness, wind speed and frequency. The attenuation rate is high for short vegetation depths and reduces for large depths (47) (48).

Losses as well as their variance tend to increase with frequency. For trees in leaf, a substantial increase in loss between 9.6 and 28.8 GHz was observed, whereas the growth rate seems to be much smaller between 28.8 and 57.6 GHz. However, the measurement results do not present a fully consistent picture. The attenuation caused by a single tree at mm-wave frequencies can vary between 9 and 22 dB (48) (49) (50) (47), and more work is needed to understand the impact of foliage, when it is wet and dry, and the impact that foliage has from both an attenuation standpoint, as well as from a scattering standpoint (to be used as a viable reflector to increase coverage).

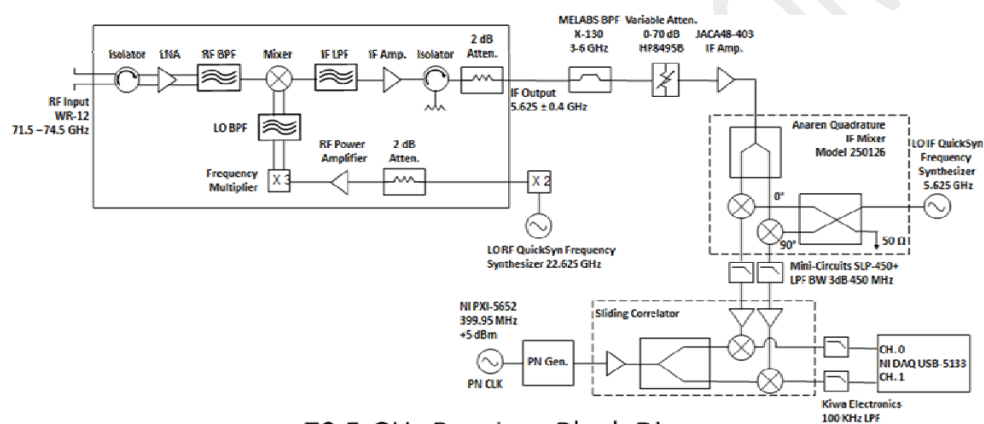
The ability for mm-wave devices to steer away from heavy shadowing created by foliage, in order to exploit other propagation paths at different angles (such as reflections or scattering from buildings) will be important.

7.2 Radio channel characterization and modeling

Accurate channel characterization and modeling is indispensable in order to predict the system performance and thus for system design as well as for network deployment. The most important characteristics of a channel are given by the path loss (as this impacts coverage, link-budget design, and co-channel interference) and temporal dispersion caused by multipath propagation (as this impacts the timing, equalization or cyclic prefix timing, packet sizes, frame sizes, and other air interface design parameters). The multipath time dispersion is commonly characterized by the root-mean-square (RMS)

delay spread. With high gain directional mm-wave antennas, important consideration will also need to be given to spatial channel models, such as the angle of arrival (AOA) and angle of departure (AOD) of multipath, as well as the beamwidths used to capture signals (51). Typically, a channel sounder is used to collect power delay profiles (PDPs) of typical mobile channel scenarios. A block diagram of a typical channel sounder, used to generate a 400 Megachip per second spread spectrum signal (e.g. 800 MHz RF bandwidth), is shown in Figure 7-1 with photographs in Figure 7-2 and Figure 7-3.

72 GHz Channel Sounder Hardware



73.5 GHz Receiver Block Diagram

63

Figure 7-1. Block diagram of a 72 GHz E-Band Channel Sounder used to collect Power Delay Profile measurements (52).



Figure 7-2. Photograph of the 72 GHz channel sounder receiver



Figure 7-3. Photograph of the 72 GHz channel sounder transmitter

A video of the channel sounder in operation may be viewed at:

<http://nyuwireless.com/ThePulse/04/The-Latest-on-NYU-WIRELESS'-72-GHz-Measurement-Campaign.php>

By using a channel sounder to collect experimental propagation data in the field, it becomes possible to collect a vast number of PDPs, from which statistical channel models may be created. The statistical channel model may then be used by manufacturers and standards bodies to support the development

and evolution of modems and new air interface approaches for future mm-wave systems. **Error! Reference source not found.** illustrating the important parameters needed to develop mm-wave channel models (51).

Terminology	Definition	Statistics
Cluster	Group of multipath components within a PDP traveling closely in propagation time delay at a specified lobe or direction in space	<ol style="list-style-type: none"> 1. Cluster time duration 2. Internal RMS delay spread 3. Multipath amplitude distribution 4. Inter-arrival distributions of multipath within cluster 5. Number of multipath components within the cluster 6. Number of clusters in a PDP for a specified lobe or direction in space
Void	Time interval between two consecutive clusters	<ol style="list-style-type: none"> 1. Void duration 2. Number of voids in a PDP
Path	The strongest multipath component within a cluster	<ol style="list-style-type: none"> 1. Excess time delay 2. Amplitude
Sub-path	Individual multipath component	<ol style="list-style-type: none"> 1. Excess time delay 2. Amplitude

Table 7 4. Summary of temporal channel model statistics and definitions (48).

As an example of the type of typical channel responses possible in urban environments using mm-wave communications at 28 GHz, Figure 7.4 , Figure 7.5 and Figure 7.6 illustrate a rich multipath environment with many possible angles of arrival, many multipath components, and rich diversity from which to extract viable signals in outdoor cellular scenarios (12) (23) (44) (53).

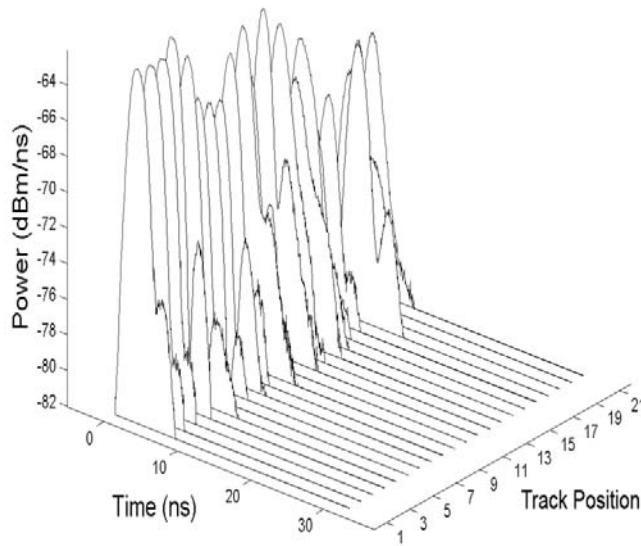


Figure 7-4. Small scale fading in the 28 GHz mm-wave channel is quite small, only on the order of 4 dB as the receiver is moved across a very small track (51) (23)

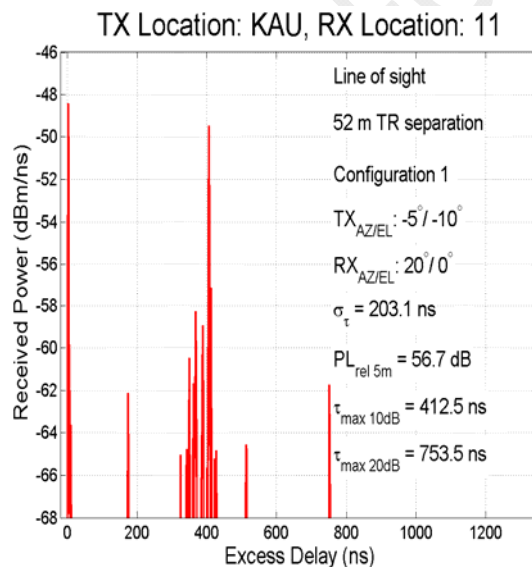


Figure 7-5. Power Delay Profile measured in New York City at 28 GHz in a LOS environment.

At this particular antenna orientation at both the TX and RX, it can readily be seen that there are many observable multipath components, and reflections from many buildings, inducing large propagation multipath excess delays of about 800 ns.

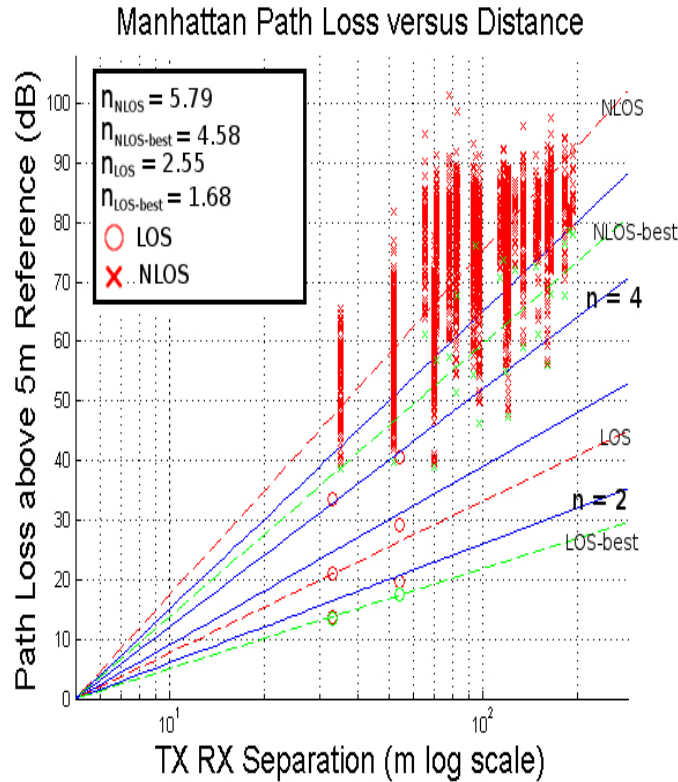


Figure 7-6. Scatter plot of 28 GHz path loss at many different NLOS and LOS locations in New York City.

Note that when arbitrary antenna pointing angles are used, the path loss exponent is worse than today's low GHz channels, but when the best pointing angles are used at both the TX and RX, the path loss behaves very similarly to today's low GHz cellular systems, with path loss exponents of 2.0 and 4.58.

Recent work (54) shows that by combining beams from different angles, it becomes possible to drive the path loss exponent shown in Figure 7.5 to well below 4.0. The use of spatial path combining, MIMO, and other techniques promise to improve links for mm-wave technologies.

7.2.1 Path loss and time dispersion

Frequently used path loss models indicate that the mean path loss increases exponentially with distance: $PL \propto (d/d_0)^n$, where n is the path loss exponent, indicating how fast path loss increases with distance. d_0 is the reference distance and d is the TX-RX distance (55) (42) (18). For small distances and under LOS conditions, n is usually close to two, which corresponds to free-space propagation, as clearly seen in Equations (1), (2) and (3). Beyond a certain distance, defined by the Fresnel zone break point, the ground reflection can lead to steady losses and n rises to four (55). For NLOS scenarios, similar path loss exponents can arise.

Channel measurements at 0.9 and 1.9 GHz in urban areas for microcell deployment (56) (55) reveal that the path loss exponents vary between 2.1 and 3.8 including LOS as well as NLOS scenarios. The standard

deviation of the actual path loss around the mean is between $\sigma = 7.7$ dB and $\sigma = 10$ dB. The RMS delay spread was found to be a strong function of antenna height [FBR+94], and the maximum values varied between 732 and 1860 ns. Confirmed by (56), the delay spread seems to be typically less than 2 μ s for microcellular sites in the lower GHz range.

With respect to mm-wave propagation considerable work has been carried out since the 1990s, mainly related to 60 GHz indoor propagation, but also to outdoor channels (57) (58) (59) (60). As mobile data rates are continuously increasing, mm-wave outdoor propagation for access links has become a current research topic (53) (61) (45) (62) (12) (44).

The most important finding of previous studies is that multipath propagation is an issue for outdoor scenarios as is it for indoor propagation. Though it might be difficult to penetrate buildings, cars and also smaller objects like trash cans or signs are potential reflectors, and recent measurements show that even humans are highly reflective at mm-wave frequencies (45). Due to reflections from these objects and the ground, as well as tunnel walls, measurements in environments like airport fields, urban streets, city tunnels, parking lots and parking garages show that the received signal is constituted by the sum of several rays (57). More recent measurements in New York City and Austin, Texas in outdoor environments show that there is rich multipath, and many angles of arrival are possible for propagation at most locations. While perhaps not surprising, (12) shows that there is greater loss in deep urban canyons when compared to light urban environments, yet in all cases, the propagation distance for modest powered (13 dBm) mm-wave systems with reasonable gain antennas (15 to 25 dB steerable antennas at TX and RX) permitted coverage distances of up to 200m in virtually all NLOS environments, with path loss exponents not far different from today's cellular systems (53) Dominant contributions to the received power result from specular reflections, either induced by smooth surfaces or small incidence angles with respect to the surface. The ground reflection can have an important impact and result in typical two-ray propagation fading (63) (64). However, as the wavelength is very small at mm-wave bands, the break point distance easily exceeds the targeted transmission distance even for small antenna heights. This means that the fourth order power law for LOS propagation is not expected to apply. Measurement results consistently confirm that the path loss exponent is very close to two for LOS propagation (53) (62) (61) (60). Some variation towards smaller or larger values in the range between $n = 1.9$ – 2.5 can be observed due to strong multipath or partially obstructed LOS conditions, respectively. Trees primarily cause losses when they obstruct relevant propagation paths. Related diffuse scattering is negligible and cannot be exploited (57).

In the mm-wave band, shadowing effects are considerably more severe and losses due to trees, rooftops and human bodies. In the past, it was commonly thought that only LOS conditions could possibly yield sufficient signal strength for radio transmission. However, the presence of specular reflections with significant power motivates the use of mm-waves for cellular applications even under obstructed LOS (OLOS) or NLOS conditions – at least for small cell sizes below 200 m in radius. Assuming that highly directional steerable antennas can be utilized, a receiver might be able to establish a link by pointing to one of the available reflection sources in relation to a rooftop-mounted transmitter (45) (61) (62) (44)

(12). Exploitable NLOS paths were found to be 10 to 40 dB weaker compared to LOS, and NLOS path loss exponents are in the range 3.2–4.2 in connection with $\sigma = 8.4\text{--}13.4$ dB. It can be concluded that these results are quite similar to the path loss behavior at lower frequencies, but keeping in mind that the results are related to much smaller cell sizes and to applying high-gain steerable antennas.

Time dispersion under LOS conditions was found to be very small in most of the cases, but expectably is highly dependent on the environment as well as on the antennas. According to [SC97] city streets and tunnels do not present a severe multipath situation and RMS delay spread values are typically lower than 20 ns. However, the street width has large effect (58). Stronger dispersion can occur on city squares, and especially in parking garages because of the large dimensions and the relatively smooth surfaces (57). In accordance to these declarations, very low RMS delay spreads (up to 1.4 ns) were observed for the peer-to-peer and cellular scenario in (53) (45) (38 and 60 GHz), where 25 dBi antennas were used at both sides. Values to be considered for point-to-point links with higher antenna gains are even lower ($\tau_{\text{rms}} < 0.21$ ns with 45 dBi antennas according to E-band specifications stated in (65)). When also (partially) obstructed LOS conditions are taken into account, the delay spread increases and can take values up to 16 ns (62).

The conditions change when NLOS scenarios are considered. Though average RMS delay spreads are still in the moderate range 7–24 ns, maximum values up to 133 ns can be observed (62) (53). It was further found that the RMS delay spread is a strong function of the off-bore sight pointing angles and TX-RX separation, respectively excess path loss (62) (53) (45).

In summary, the RMS delay spread of mm-wave outdoor channels seems to be of the same order as for indoor and in-cabin propagation, where values between 10–100 ns have been found (57) (66) (67) and it stays one order below the spread occurring at classical cellular frequencies. Again, it should be noted these results must be seen in relation to transmission distances below 200 m and high-gain steerable antennas considered for the mm-wave outdoor links.

7.3 Challenges with respect to mm-wave outdoor channel modeling

A channel model is intended to include all relevant propagation aspects and to comprehensively describe the channel behavior on a detailed level. In principle, it can either be of deterministic or statistical nature (57). There are well established models for cellular scenarios in the classical frequency band (68), whereas comprehensive mm-wave outdoor channel modeling is still at the beginning.

With regard to high-gain LOS point-to-point links, modeling in good approximation is equivalent to predicting the path loss between two aligned antennas. In the lower GHz region, atmospheric effects can be neglected for short links. However, for mm-wave links, effects such as oxygen and water vapor absorption as well as fog and rain attenuation have to be taken into account. Comprehensive path loss models like (30) can be applied for this task.

Things become more complex when multipath propagation is an issue, which is the case if obstacles are close to the LOS path, antenna gains are lower, or if even NLOS links are considered. Ray tracing (RT)

has already been shown to be an appropriate tool to predict mm-wave outdoor propagation (57). Though RT relates to deterministic modeling, in the mm-wave range it has usually been more intended to roughly reproduce the channel characteristics on a site-specific basis rather than to predict the channel impulse response with very high accuracy. Results indicate that models based on a highly simplified geometry can deliver good results and reflections of third order or higher as well as diffraction may be neglected as long modeling of the path loss is focused. Geometric models besides RT are useful to cover special scenarios like propagation in street canyons with lower computational complexity (69) (65).

In order to achieve meaningful predictions for rich multipath environments and for OLOS and NLOS scenarios, the requirements on model accuracy rise significantly. It is absolutely crucial to involve appropriate material parameters and thoroughly consider surface roughness: it may decide between a good and an infeasible link. As the materials highly depend on the building type and their effective roughness is a strong function of the incidence angle, results will be extremely dependent on the propagation scenario. This dependence can expect to be stronger than for lower frequencies – a trend, which seems to be confirmed by the measurement results (53) (61) (45) (62). They reveal vast variations of the received power and the RMS delay spread even within the same measurement site.

Generic statistical models will not be sufficient in order to assess the performance of system approaches. Instead, site-specific models related to real-world reference scenarios and fine classification of sites, also with regard to involved building materials, are required. Further channel measurement campaigns as well as site-related characterization of building materials are highly needed to cover typical propagation scenarios and to derive highly-accurate RT models. The latter provide full access to angular information, which is of great importance for the development of appropriate beam steering algorithms, and can be also be used as basis for precise site-specific statistical models.

7.4 Summary observations of mm-wave prospects

There are significant challenges with using the mm-wave spectrum for access. In general, mm-wave communication links often require solutions that provide methods to mitigate LOS blockage. One means to achieve this is to utilize steerable, directional antenna arrays. These arrays steer the beam in a direction that achieves a link via i) access an alternate base station node this is LOS or ii) access the main, or alternate, base stations with a suitable low loss reflection. Areas that have been identified for further study to optimize the mm-wave solution for access are as follows:

- a. Base station node placement
- b. User device antenna configuration
- c. Detailed channel modeling
- d. Antenna control for supporting steered beam solutions
- e. Low cost mm-wave IC design

8 Overview of Access and Backhaul Technologies for 4G systems

8.1 Overview of 4G LTE Access Technology

Long-Term Evolution (LTE) is the 4G access technology for cellular service. It supports both frequency division duplex (FDD) and time division duplex (TDD) modes using a common subframe structure of size 1ms. Having such a short subframe length allows for latency to be minimized, thus ensuring a good user experience. Currently, Rel-11 LTE supports many advanced features such as scalable deployment bandwidth from 1.4 MHz up to 20MHz, carrier aggregation up to 100 MHz, heterogeneous network, large number of transmit and receive antennas, spatial multiplexing (both for single-user and multi-user MIMO), beamforming, frequency selection scheduling, inter-cell interference coordination, coordinated multi-point transmission and reception, dynamic TDD, and single frequency network. In Rel-12, many additional features are being considered for inclusion such as D2D and M2M communication, small cell enhancements including dual connectivity, MIMO enhancements, joint TDD-FDD operation, centralized RAN, and enhanced LTE-WiFi coordination.

The maximum LTE downlink and uplink data rates for Rel-11 are shown in Table 8-1. Note that these data rates are for FDD. To obtain the corresponding rates for TDD, appropriate scaling based on DL:UL configuration must be applied. From the table, it can be seen that without carrier aggregation, peak data rate of 600 Mbps can be achieved on the downlink. With carrier aggregation of 5 downlink 20MHz carriers (100 MHz bandwidth total), peak downlink data rate of 3 Gbps can be achieved in LTE.

LTE Rel-11 (FDD)	Configuration	Peak Data Rate
Downlink	2Tx-2Rx, 20 MHz	150 Mbps
	4Tx-4Rx, 20 MHz	300 Mbps
	8Tx-8Rx, 20 MHz	600 Mbps
	8Tx-8Rx, 5x20 MHz	3 Gbps
Uplink	1Tx-2Rx, 20 MHz	75 Mbps
	2Tx-2Rx, 20 MHz	150 Mbps
	4Tx-4Rx, 20 MHz	300 Mbps

Table 8-1 Peak LTE Rel-11 data rates.

The LTE system architecture was designed based on the Internet Protocol to efficiently support packet-based transmission. A simplified illustration of the LTE system architecture is shown in Figure 8.1. In the LTE system architecture, the service provisioning is divided into two parts - the Evolved Packet Core (EPC) used to manage core network functionalities and the Evolved Universal Terrestrial Radio Access

Network (E-UTRAN) used to manage radio access functionalities. The core network's main responsibilities include mobility management, policy management, and security. It consists of the Mobility Management Entity (MME), the Serving Gateway (S-GW) and the Packet Data Network Gateway (P-GW). The E-UTRAN, consisting of only eNBs, is responsible for management of radio access and provides user and control plane support to the User Equipments (UEs). Some of these connection management functions include handover, service establishment, resource control, etc.

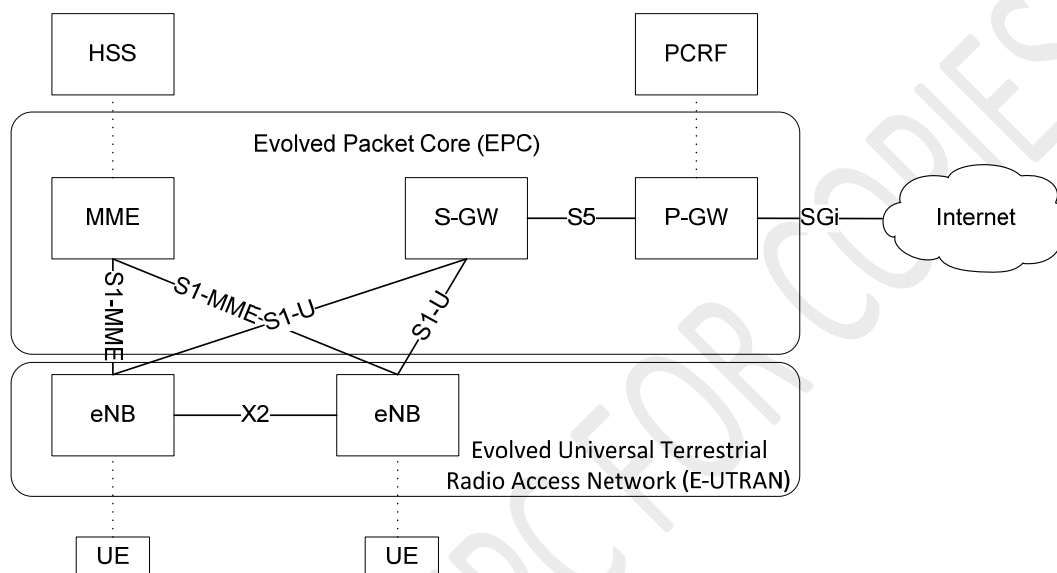


Figure 8.1. LTE system architecture.

The following protocols are used in user plane transmission - Packet Data Convergence Protocol (PDCP), Radio Link Control (RLC), Medium Access Control (MAC), and Physical layer (PHY). The PDCP is responsible for header compression and decompression, security functions such as ciphering and deciphering, and transfer of user protocol data units to the RLC. The RLC sub layer will perform segmentation and reassembly, Hybrid Automatic Request (HARQ) error correction, and delivery of the user protocol data units to the MAC via appropriate logical channels. The MAC is responsible for mapping between logical and transport channels, scheduling of data, HARQ, priority handling, and multiplexing/de-multiplexing of MAC service data units. At the PHY, the transport channels are mapped into physical channels for transmission over the air interface. The PHY is responsible for Cyclic Redundancy Check (CRC) insertion, channel coding, HARQ processing, scrambling, modulation, link adaptation, power control, and resource mapping.

8.1.1 Downlink

The LTE downlink air-interface uses Orthogonal Frequency Division Multiple Access (OFDMA) multiple access technique which can provide high spectral efficiency, orthogonality among intra-cell users, and support for frequency domain techniques such as frequency selective scheduling, single frequency

network and soft fractional frequency reuse. The following downlink physical layer channels are supported -

- Physical Downlink Shared Channel (PDSCH) carries unicast data traffic and common messages such as paging, System Information Blocks, and random access response.
- Physical Broadcast Channel (PBCH) carries the Master Information Block required for system access.
- Physical Multicast Channel (PMCH) carries multicast and broadcast data traffic.
- Physical Control Format Indicator Channel (PCFICH) carries indication of the size of the control portion for each subframe.
- Physical Downlink Control Channel (PDCCH) carries scheduling and power control information for both downlink and uplink.
- Physical Hybrid ARQ Indicator Channel (PHICH) carries HARQ-ACK information corresponding to uplink transmission.

In addition to the channels, physical-layer signals are also supported. They include –

- Primary and Secondary synchronization signals used for cell acquisition, detection of frame timing, and handover purposes.
- Cell-specific reference signal used for demodulation of downlink channels, for estimating channel quality, and also for handoff measurements.
- UE-specific dedicated reference signals used for demodulation of downlink channels.

8.1.2 Uplink

The LTE uplink air-interface uses Single-Carrier Frequency Division Multiple Access (SC-FDMA) transmission scheme. SC-FDMA can provide similar advantages to OFDM such as orthogonality among users and robustness to multipath. However, it has much lower peak-to-average power ratio and sensitivity to the UE amplifier's "cubic metric". This allows for maintaining a low power amplifier back-off or de-rating requirement which translates into higher coverage in the uplink. The following downlink physical layer channels are supported -

- Physical Uplink Shared Channel (PUSCH) carries data traffic and is assigned to users via the uplink scheduling assignment.
- Physical Uplink Control Channel (PUCCH) carries three types of control signalling – ACK/NACK for downlink transmission, scheduling request indicator and feedback of downlink channel information including channel quality indicator, precoding matrix indicator, and rank indicator.
- Physical Random Access Channel (PRACH) carries the random access channel used to request initial access, initiate handoff procedure, and transition from idle to connected state.

In addition to the channels, physical-layer signals are also supported. They include –

- Demodulation reference signal used for demodulation of data and control information.

- Sounding reference signal used for sounding of the uplink channel response.

8.2 LTE-Advanced Technology

In addition to features introduced in the first LTE release, advanced features are continuously being added into LTE. As of Rel-11, the following advanced features are supported -

Carrier aggregation to enable the system to support aggregated bandwidth of up to 100 MHz: This allows LTE-A target peak target data rates of 3 Gbps in the downlink and can also be used by operators to aggregate non-adjacent frequency bands. In addition to the individual increased peak data rates, carrier aggregation also allows advanced features such as multi-carrier scheduling, load balancing, quality-of-service differentiation, interference coordination, and heterogeneous deployment to be used to further increase the spectral efficiency of the system. Carrier Aggregation is also enabling operators to use unpaired spectrum such as the lower 700 MHz D and E blocks (band 29) for downlink only operation. This supplemental downlink addresses the fact that there tends to be much more downlink than uplink traffic, and makes use of previously “stranded” spectrum.

Heterogeneous network and small cell support to provide network densification: Heterogeneous networks consist of a traditional macro-cell based network augmented with various types of low power network nodes that address the capacity and coverage challenges resulting from the growth of data services. To efficiently support small cells, various intercell interference co-ordination techniques have been developed.

Coordinated multi-point transmission (CoMP) to enable cooperation among eNBs to determine the scheduling, transmission parameters and transmit antenna weights for a particular UE: This cooperation will depend on a high capacity backhaul link between eNBs. Closed loop beamforming or precoding based transmissions will be supported in CoMP. Similar to multi-point transmission, multi-point reception is also supported. In this case, transmission from the UE is received at multiple points and combined to provide gain.

Multi-antenna transmission at the UE where up to four power amplifiers and RF transmitter chains will be supported: This allows for MIMO transmission by the UE to increase peak data rate for stronger SINR's.

8.3 Overview of 4G Backhaul Technology

The backhaul for small cells is currently seen as a major challenge for 4G small cell deployments. As the number of cell sites multiply to keep with capacity demand, so can the cost of the operator's backhaul network. While fiber is widely used for macro-cell backhaul, many operators are suggesting that the high cost of fiber installation and leasing fees will kill the small cell business case. Instead, operators are estimating that 80% of the small cells will be connected with wireless backhaul (70). This leads to the technological challenge of finding wireless solutions that provide enough spectrum in a cost effective manner, and that can sustain the expected continued growth in capacity.

8.3.1 Backhaul Taxonomy

Wired solutions such as fiber may make up only a minority of small-cell backhaul links since wired solutions can be expensive both to install and to lease. Availability of these solutions, however, is crucial in small-cell deployments as this provides locations for traffic aggregation points in the wireless backhaul system.

Figure 8-2 shows a taxonomy of existing small cell backhaul solutions. The wireless backhaul options can generally be broken into line-of-sight (LOS), where a direct path through the air is required between the transmitter and receiver, and non-line-of-sight (NLOS), where diffraction, transmission and reflections are sufficient for signal propagation from transmitter to receiver.

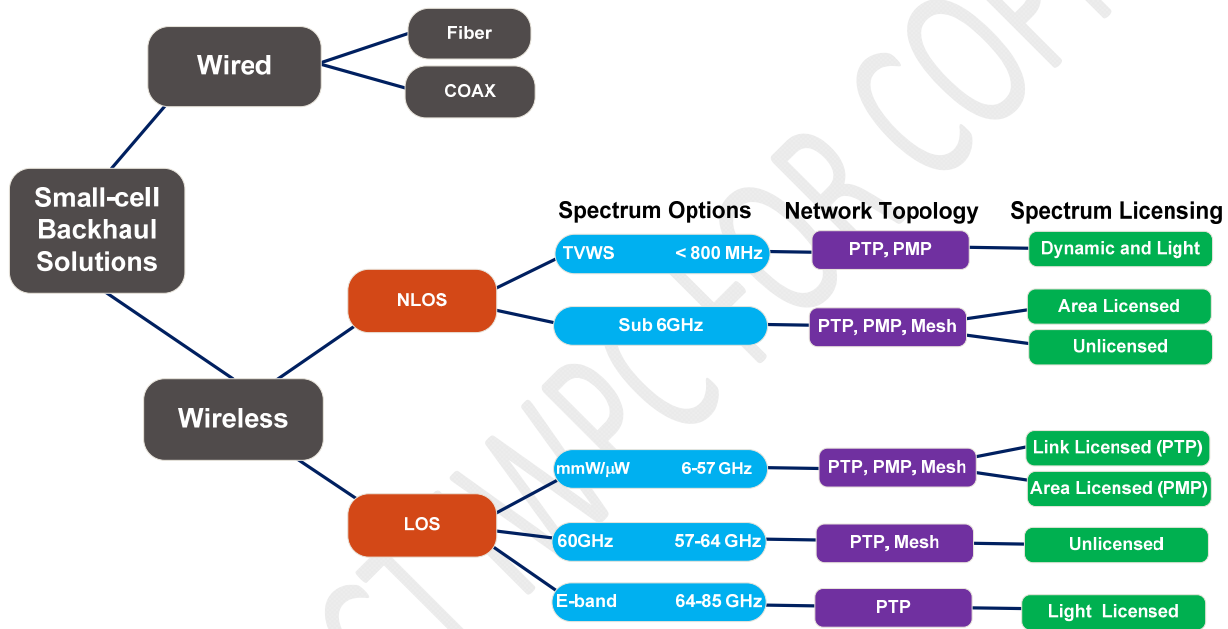


Figure 8-2 Taxonomy of Backhaul Solutions

9 Access and Backhaul Technologies for 5G systems

9.1 General requirements

The projected massive traffic demand (e.g. 5000x) in the next decade calls for bandwidth scalable as well as low cost backhaul. The scalability is obviously to carry the increased demand in traffic parallel to what needs to happen on the access link. The low cost is important to support scalable small cell deployment parallel to relaxing RF planned deployment and site acquisition on the access link. Without a parallel development in backhaul to that of access the former becomes the bottleneck and the mission of meeting this huge data demand is not accomplished. Based on the predicted RAN capacity it is assumed that the backhaul links would require a capacity of be greater than 10Gbps. The huge access

capacity (e.g. 5000x) will be partially achieved using small cell topology, thus distances might be as short as 200m and extending to about a km.

9.2 Future Cellular Architecture: Scenario with radically more spectrum and cell densification

Under a scenario where radically more spectrum is needed and the densification of cells continues, an architecture of mm-wave small cells is envisioned. Figure 9-1 shows options for a forward looking system architecture where a mm-wave base station (mB) supports both access and backhaul connections. The mB integrates other small cell access technologies such as LTE or 802.11. The left side of the diagram shows an 802.11 hotspot deployment, while the right side shows a cellular architecture. These two approaches may be combined with proper mobility and interconnection approaches. LTE, using the eNB shown in the Figure 9-1, provides a macro-cellular overlay while mm-wave and other hotspot technologies provide the ultra-high capacity small cells. The mm-wave backhaul interconnects the mBs, eventually reaching a mm-wave base station aggregation point (mBA), for a connection to the core network.

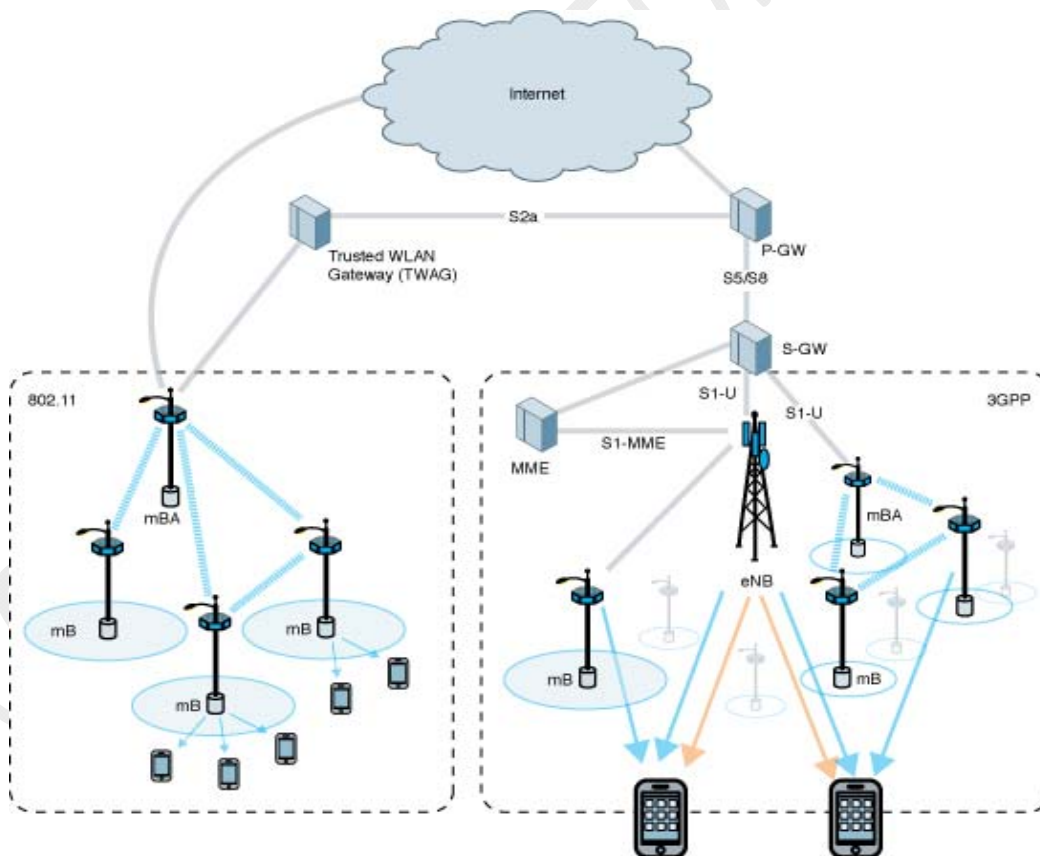


Figure 9-1 mm-Wave Hot Spot Tiered Architecture (Source Interdigital, used with permission.)

9.3 Current mm-wave Standards for Future Cellular Systems

802.11ad is one of the latest amendments from the popular 802.11 WiFi technologies. It is a 60GHz PHY/MAC specification driven primarily by WiGig, now absorbed in WFA. Other 60 GHz standards exist, but 802.11ad is probably the most capable of them. Table 9-1 gives a list 60 GHz standards.

The use cases collected by the 802.11ad community can be found in IEEE 802.11 -07/2988r3 and updated in IEEE 802.11 -09/0583r0. A summary is provided in Table 9-2. The use cases are primarily for short range links with limited support for mobility. There are several use cases that call for longer distance links (e.g., the backhaul cases), but use cases used to agree on performance were decidedly for short range applications.

Receiver performance and simulation assumptions (IEEE 802.11-10/0431r3) agreed upon by 120 members, measured performance in only short range indoor channels corresponding to an enterprise conference room and home living room. The detailed channel models are described in IEEE 802.11-09/0334r8. It seems clear that participating companies intend to target short range indoor application despite the list of use cases.

While the 802.11ad specification clearly supports directional antennas, the node discovery mechanisms do not exploit the high gain antenna at both transmit side and receiver side. During the discovery process, one antenna is configured in a so-called quasi-omni mode, which is the widest beam possible from the antenna array. When high gain antennas are used, such as those that would be needed for a small cell deployment, the sacrificed gain can be very large and limit long range discovery.

Due to directional nature of transmissions and limited diffraction, mm-wave communication for backhaul should target mostly LOS paths. Moreover, due to limited penetration at these frequencies, link failures due to obstructions are highly likely. To overcome the link blockage problem, the mesh architecture with redundant paths to the destination offers a promising solution. Moreover, replacing a long link by a series of shorter hops also naturally minimizes path loss problem discussed above. However, end-to-end latency could limit the number of allowed hops.

The one-hop relaying function included in the 802.11ad standard with support for both amplify-and-forward/full-duplex as well as decode-and-forward/half-duplex modes, falls short as a solution for a multi-hop mesh described above. This is because the standard only supports relaying for two nodes that belong to the same cell to talk to each other via a third node, bypassing the access point (AP). Therefore, this is not truly a range-extension solution, which requires chaining together of multiple such single hops over large distances.

As discussed above, the 802.11ad standard is mainly designed for high bandwidth applications involving high-definition video. However, mm-wave technology deployed for 5G access networks is expected to support an aggregation of sessions, together representing high data rate, but with relatively smaller bandwidth per session. These sessions may be more delay-sensitive such as video chat. Since even the lowest 802.11ad data rate corresponds to several hundred Mbps, a large protocol overhead is involved

in serving users with a few Mbps throughput requirement. This would also be the case for TCP sessions during slow-start and TCP feedback in the reverse direction. For example the preamble and header durations become non-trivial compared to the payload. A new air interface would preferably support small packet transfers more efficiently while still utilizing the full system bandwidth, at least in the access link.

	802.11ad/WiGig	802.15.3c	WirelessHD	ECMA-387
Range (m)	>10	10	10	10
Data rates (Gbps)	6.8	5.8	7.1/28.5 (x4)	6.4
Mesh	Possible with enhancements	Possible with enhancements	No?	No
Mobility	Possible with enhancements	No	No	No
Channel access	Contention free period + Contention period	Contention free period + Contention period	Contention free period + Contention period	Contention free (contention-based in discovery channel)
Antenna	Fixed + BF	Fixed + BF	BF	Fixed + BF
Relaying	AF + DF (1 hop)	No	No	AF + DF (1 hop)
Architecture	Infrastructure + Ad-hoc (centralized MAC)	Ad-hoc (Centralized MAC)	Ad-hoc (Centralized MAC)	Ad-hoc (distributed MAC)

Table 9-1 Table of Air Interface Standards at 60GHz

Category	#	Usage Model
1. Wireless Display	1a	Desktop Storage & Display
	1b	Projection to TV or Projector in Conf Rom
	1c	In room Gaming
	1d	Streaming from Camcorder to Display
	1e	Broadcast TV Field Pick Up
	1f	Medical Imaging Surgical Procedure Support
2. Distribution of HDTV	2a	Lightly compressed video streaming around home
	2b	Compr. video streaming in a room / t.o. home
	2c	Intra Large Vehicle (e.g. airplane) Applications
	2d	Wireless Networking for Small Office
	2e	Remote medical assistance
3. Rapid Upload / Download	3a	Rapid Sync-n-Go file transfer
	3b	Picture by Picture viewing
	3c	Airplane docking
	3d	Movie Content Download to car
	3e	Police / Surveillance Car Upload
4. Backhaul	4a	Multi-Media Mesh backhaul
	4b	Point to Point backhaul
5. Outdoor Campus / Auditorium	5a	Video demos / telepresence in Auditorium
	5b	Public Safety Mesh
6. Manufacturing Floor	6a	Manufacturing floor automation

Table 9-2 802.11AD use cases

9.3.1 802.11ad for Backhaul

While the 802.11ad speciation clearly supports directional antennas, the node discovery mechanisms do not exploit the high gain antenna at both transmit side and receiver side. During the discovery process, one antenna is configured in a so-called quasi-omni mode, which is the widest beam possible from the antenna array. When high gain antennas are used, such as those that would be needed for a small cell deployment, the sacrificed gain can be very large and limit long range discovery.

Due to directional nature of transmissions and limited diffraction, mm-wave communication for backhaul should target mostly LOS paths. Moreover, due to limited penetration at these frequencies, link failures due to obstructions are highly likely. To overcome the link blockage problem, the mesh architecture with redundant paths to the destination offers a promising solution. Moreover, replacing a long link by a series of shorter hops also naturally minimizes path loss problem discussed above. However, end-to-end latency could limit the number of allowed hops.

The one-hop relaying function included in the 802.11ad standard with support for both amplify-and-forward/full-duplex as well as decode-and-forward/half-duplex modes, falls short as a solution for a multi-hop mesh described above. This is because the standard only supports relaying for two nodes that belong to the same cell to talk to each other via a third node, bypassing the access point (AP). Therefore, this is not truly a range-extension solution, which requires chaining together of multiple such single hops over large distances.

9.4 Overview of 5G mm-wave Access Technology

As discussed above, the 802.11ad standard is mainly designed for high bandwidth applications involving high-definition video. However, mm-wave technology deployed for 5G access networks is expected to support greater than 10 Gbps of peak rate and more than 100 Mbps of cell edge rate for new high data rate applications with less than 1 ms latency. A new air interface needs to be designed to suit the propagation conditions at mm-wave bands and to satisfy the 5G requirements as shown in Table 5-2.

This section describes key technology components for consideration for evolving mm-wave access links for 5G. Additionally a sample link budget is provided.

9.4.1 Waveform Selection

The mm-wave access link waveform can be selected among single carrier solutions such as Cyclic Prefixed Single Carrier (CP-SC) and its variants or multi-carrier solutions such as OFDM, SC-OFDM and MC-CDMA. The Peak to Average Power Ratio (PAPR) performance, sensitivity to transmitter non-linearity and other RF impairments, performance with different receiver types, system overhead, resource channelization, multiple access scheme and implementation complexity of each candidate ought to be taken into account with the help of simulations based on accurate mm-wave channel and antenna modeling.

A single carrier solution can have similar performance, efficiency and low signal processing complexity as an OFDM solution, yet has better PAPR performance and is less sensitive to RF impairments such as phase noise and power amplifier nonlinearities. Because of the high directivity of the mm-wave transmission, the mm-wave channel is relatively flat and the equalization of a single carrier solution may be simpler than what is required for a highly frequency-selective channel. The PAPR performance is very desirable in mm-wave frequency band because it enables reuse of low cost PAs.

A variant of CP-SC modulation, called null CP-SC (NCP-SC) (71), offers some additional benefits over regular CP-SC. In NCP-SC the regular CP is replaced by null symbols where null symbols are appended at the end of a group of symbols. At the receiver an FFT is applied to the group of data symbols plus the null symbols (a symbol block for NCP-SC is the group of data symbols plus the null symbols) to enable frequency-domain equalization. Note that the null symbols in one block of symbols are the null prefix for the block of symbols. The first additional advantage of NCP-SC over a regular CP method (OFDM included) is that the null portion enables a built-in guard period for switching of RF beams without destroying the CP property. The second advantage is that since the NCP-SC symbol block includes the group of data symbols plus the null symbols (i.e., the CP), the CP size can be dynamically changed (e.g., per-user) without changing the over-all numerology (e.g., the number of symbol blocks per frame). Finally, the NCP gives a portion of signal without desired signal energy for easy estimation of noise and/or interference. Another variant similar to NC-SC is called zero tailed OFDM (ZT-OFDM) described in (72). ZT-OFDM modulation allows the cyclic prefix (CP) adapt to the propagation environment of the channel. Both NCP-SC and ZT-OFDM have low PAPR compared to OFDM and have the same BLER performance as an OFDM signal.

A single-carrier-based air interface design may lack the ability to schedule resources dynamically in the frequency domain and thus is less flexible in resource channelization. However the narrow beams of mm-wave antennas greatly reduce the number of UEs in the same beam that could benefit from frequency domain scheduling.

An OFDM-based solution may benefit from the existing 4G LTE IP blocks and system implementation, which may enable functional block sharing between 4G and 5G mm-wave implementations, e.g. clock distribution and FFT block in the same network node.

Note the SC and OFDM systems can potentially coexist for mutual benefit and cost reduction, because of the similarities in their basic frequency domain signal processing functions.

9.4.2 Frame Structure

An mm-wave frame structure with a short TTI can enable a significantly reduced end-to-end delay envisioned for the 5G system. The main PHY contributors to the end-to-end delay are the fixed timing constraint of the frame structure, HARQ time line and PHY control signaling. A much shortened TTI length may be applied in mm-wave frame structure compared to the 1-ms LTE TTI. Since the channel bandwidth for a mm-wave carrier is also likely to be substantially larger than LTE carriers, and because frequency domain resources scheduling may be limited in the mm-wave systems, the smaller TTI also helps create a finer granularity of radio resource allocations/grants.

A frame structure of a SC-CP or OFDM system may employ a CP. In that case, channel delay spread and coherent time can drive the CP and symbol length. A choice of these frame structure parameters including symbol length, CP length, slot duration, sub-frame duration, etc. should strive for a balance among identified use cases and deployment scenarios.

9.4.3 Duplexing Scheme

Both FDD and TDD may be considered for the mm-wave access link and a comparison between main features of the two duplex schemes are listed in Table 9-3.

Duplex	End-to-end Latency Contribution	Spectrum Requirement	Device HW Complexity	Flexibility to DL/UL Traffic	Network Synchronization
FDD	Fixed	Paired (require duplex distance guard spectrum between DL and UL allocation)	High (require duplex filter)	Fixed	Not required
TDD	Variable (may be high depending on DL/UL configuration)	Unpaired	Low	DL/UL configuration dynamically adapted to traffic variation	May be Required

Table 9-3 FDD vs. TDD Duplex Scheme

The synchronization of 4G TDD network may not be critical to the mm-wave TDD network due to the narrow beam transmission. The directivity of the transmission may remove potential interferences due to the timing offset between cells. This can be considered as a form of SDD that is realized by the mm-wave narrow beams. This SDD may be applied in combination with the FDD or TDD schemes. Also note that the TDD DL/UL configuration may not need to be coordinated across the network when highly directional beams are used.

9.4.4 Multiple Access

The mm-wave access link multiple access may depend on the antenna array capability. With the assumption that each eNB antenna can form a single beam at a time, it can be further considered how radio resources may be partitioned (or even reused) with a Transmission Time Interval (TTI). If a beam is wide enough that a substantial number of UE may be covered by the beam, then it is possible to consider FDMA within the TTI.

FDMA and TDMA may be applied for multiple UEs that are scheduled in one eNB downlink or uplink antenna beam. In FDMA the devices can be assigned with different frequency resource allocation and operate simultaneously – likely implying OFDMA. TDMA can also be considered wherein the devices can be assigned with all frequency resource allocated in the eNB antenna beam, but operate only in a fraction of the TTI (e.g., certain slots within a subframe). The beams could potentially also be refined for the exact AoA/AoD used by the eNB and UE in each such slot. If there is only one UE operating the beam at a time, the frequency domain scheduling capability of OFDM goes unused and reduces the motivation for OFDM, thus making SC waveforms worth consideration.

If more advanced antenna are considered, SDMA is another option and can be combined with FDMA. SDMA offers the advantage that multiple links from a single antenna may operate simultaneously and on the same frequency given that spatially separated UEs can be paired. The ability to pair UEs can be enhanced with interference mitigation receivers or MU-MIMO techniques to remove interferences.

Combining SDMA and FDMA permits paring of UEs even in the case that there are not spatially separable and do not employ interference mitigation techniques. When such UEs are not separable, they simply given different frequency resources and each has an eNB beam adapted to it. The cost of course is that the radio resources are not reused.

9.4.5 Link Budget

An example link budget for a mm-wave downlink is given in Table 9-4.

The mm-wave eNB is assumed to have a large antenna array, e.g. a ~100 element PAA could provide ~25dBi gain, with an area of about <10cm² at 60GHz. If the same area constraint is kept, lower frequency PAAs will have a smaller number of elements and thus lower gain. With this assumption, the total antenna gain spans from 18 dBi at low mm-wave frequencies (28 GHz) to 26 dB at high mm-wave frequencies (72 GHz). A reasonably large bandwidth of 500 MHz is selected for comparison purpose. An additional loss of 20 dB is added to the NLOS case to account for the blocking of the LOS path. Actual

number may vary depending on geometry, frequency and other factors and this number can be updated when more measurement data becomes available.

All EIRP values are below the regulation limits. At 60 GHz the maximum transmit power in European countries is 10 mW which puts it at something of a disadvantage relative to other bands, but this could possibly be made up with antenna gain. Furthermore, the O₂ resonance at 60GHz causes further attenuation not experienced by the other bands. Depending on the distance another 1-2dB may need to be made up for with the antenna gain. The realization of such large antenna array may be more expensive, but a higher maximum transmit power would allow a small array design, albeit with larger power PAs. Note that the U.S. FCC regulation sets the power limit at 27 dBm and as a result can be used to achieve a higher EIRP.

mm-wave Downlink Link Budget				
Frequency (GHz)	28	38	60	72
Bandwidth (MHz)	500	500	500	500
Tx Power (dBm)	35	35	10	25
Tx Antenna Gain (dBi)	18	21	25	26
EIRP (dBm)	53	56	35	51
Inter Site Distance (m)	200	200	200	200
Cell Radius (m)	100	100	100	100
Rain Absorption (dB)	1	1	1	1
Oxygen Absorption (dB)	0.00	0.00	1.30	0.00
Additional Loss (dB)	20.00	20.00	20.00	20.00
LOS Path Loss (dB)	102.39	105.05	110.31	110.60
NLOS Path Loss (dB)	122.39	125.05	130.31	130.60
Rx Antenna Gain (dBi)	9.00	12	16	17
Received LOS Signal Power (dBm)	-40.39	-37.74	-60.07	-42.19
Received NLOS Signal Power (dBm)	-60.39	-57.74	-80.07	-62.19
Receiver Noise Figure (dB)	7.00	7.00	7.00	7.00
Implementation Loss (dB)	5.00	5.00	5.00	5.00
Receiver Thermal Noise (dBm)	-80.01	-80.01	-80.01	-80.01
Maximum Usable Received LOS SNR (dB)	27.00	27.00	14.94	25.00
Maximum Usable Received NLOS SNR (dB)	14.62	22.27	-0.06	17.82
LOS Theoretical Capacity (Mbps)	4486	4486	2504	4155
NLOS Theoretical Capacity (Mbps)	2452	3703	495	2972

Table 9-4. mm-wave Access Downlink Link Budget

The link budget in Table 9-4 demonstrates that at a distance of 100 meters the mm-wave links are able to provide very high capacity. The cell radius of 100 m is higher than what is considered in the current LTE R12 small cell deployment. For a mm-wave deployment with a cell radius blow 100 meters, the NLOS capacity will be further improved, although the LOS cases may not be able to make use extra SNR

due to radio impairments. Overall the link budget shows a satisfactory performance for the envisioned 5G system capacity.

9.5 Topology Options

The connectivity between the small cells and the aggregation point could be based on point-to-point, point-to-multipoint, or mesh topologies compared to backhaul transport network, where tree and branch architectures are typically used, as shown in Figure 9-2. The “last mile” connectivity is of particular importance as the industry focuses on future cellular small cell connectivity. In point-to-point (PTP) technologies, there is a dedicated RF channel per link between the hub or aggregation point and the end-point. Also the hub or aggregation point has a dedicated radio and antenna for each PTP link. In point-to-multipoint (PMP) technologies, the RF channel is shared across all PMP links. Also the hub or aggregation point has a shared radio antenna that is used for all PMP links at the aggregation point. As a further option, instead of connecting every single small cell to the macro site chain, tree or mesh topologies can be used between the small cell sites to provide the required connectivity.

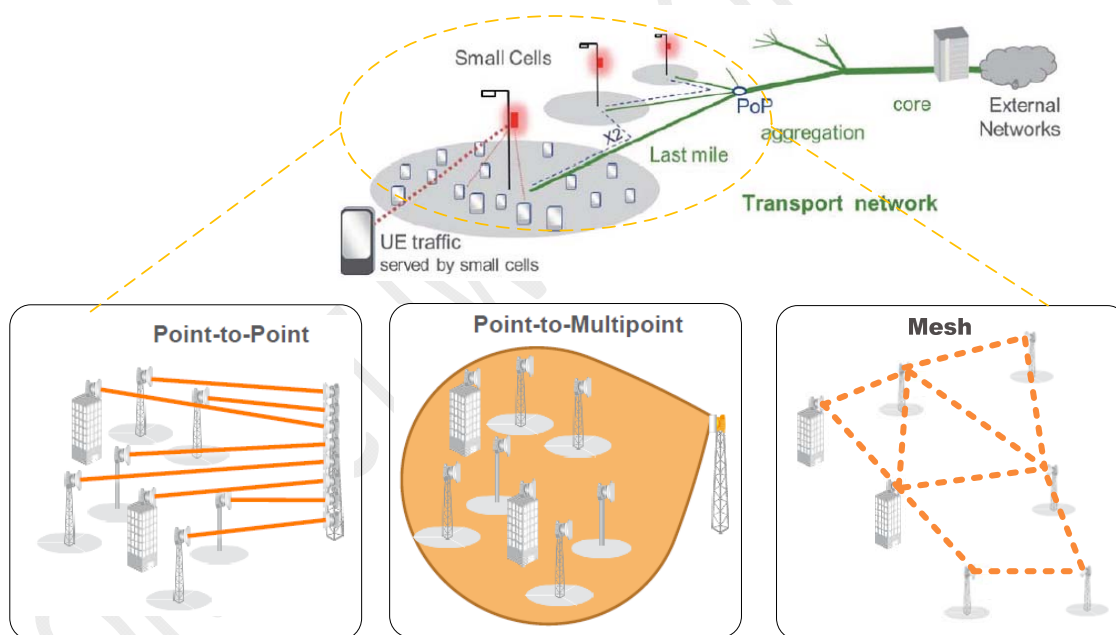


Figure 9-2 PTP, PMP and Mesh topologies (73)

One idea is to use already existing residential backhaul if cells are provided to subscribers for indoor and potentially outdoor coverage. In this case, the end user can utilize the existing backhaul for that purpose. This approach is already done now with 2G and 3G femtocells. In 3GPP, the standards support closed subscriber groups (CSG) and addresses the interoperation with other nodes like pico cells and macro cells. However, it is also possible that these residential nodes are made open access to provide coverage for outdoor users increasing the density of small cells and hence cell split gains. The owner

can be incentivized probably through reduction in bills, being able to access other residential small cells in other neighborhoods than his/her, operators subsidizing his/her backhaul, etc. In addition the user's traffic can have a higher priority over others or can be guaranteed a minimum bandwidth. This approach adds a challenge to the wireless community in terms of dealing with backhauls with dynamic quality (i.e. in terms of the bandwidth available to small cells versus that available to local resident such as WiFi devices).

A second idea is to utilize wireless backhaul (which is already happening on the microwave and mm-wave band). This can extend though to backhauling over WAN (a.k.a. relaying) with proper interference management between the access and backhaul links. It can be on mm-wave bands where huge bandwidth is available, but in a harsh propagation environment that may only enable LOS links. In general, full flexibility is needed in terms of supporting various frequency bands, LOS or non-LOS, point-to-point and point-to-multipoint.

9.5.1 Topology Gaps

The small-cell backhaul market is evolving quickly, and its players are finding their position within the small-cell ecosystem. Figure 9-3 illustrates the approximate industry coverage of small cell backhaul solutions, categorized by spectrum band. Currently there are few mesh or PMP solutions available in the mm-wave frequencies.

	PTP	PMP	Mesh
Sub 6 GHz Licensed	✓✓	✓	
Sub 6 GHz Unlicensed	✓		✓
Microwave < 40GHz	✓✓✓		✓
60GHz	✓✓✓		
E-band	✓✓		

✓ Few Companies

✓✓ Several Companies

✓✓✓ Many Companies

Industry Need

Figure 9-3 Industry Coverage of Small Cell Backhaul Solutions

10 Enabling Technologies for Base Station and User Equipments for 5G Systems

In this section the base station and user equipment (UE) antenna technology required to support 5G systems is described. Although the emphasis in this paper is primarily on millimeter wave (mm-wave) technology, the potential use of technology that operates in the 3-6 GHz region is discussed, i.e. lower microwave frequencies, since the latter could provide an intermediate step between 4G and 5G. This is not to preclude operation between 6 and 10 GHz, but that the 3-6 GHz region is a natural extension beyond the operating frequencies of current cellular systems, which range from 700 MHz to 2.6 GHz.

The antenna envisioned for both the base station and UE at mm-wave frequencies is a “large” 2D planar phased array, where by virtue of the shorter wavelengths, practical implementations are realizable at both ends of the links. The antenna envisioned for the base station at 3-6 GHz is also a 2D planar phased array, but the UE antenna is expected to be similar to what is used today for 4G, i.e. individual antennas where the total number is typically limited to one, two, or four. The resultant system configuration at mm-wave frequencies will be capable of supporting lower order MIMO with beam forming at both ends of the link, while operation at 3-6 GHz region will be capable of supporting higher order, Multi-User (MU) MIMO on both the DL and UL, with the distinct possibility of just a single antenna at the UE when operated in a Time Division Duplex (TDD) mode (74).

In what follows, the large 2D planar phased array is first discussed, where the number of antenna elements that can be supported at various frequencies of interest for a given form factor is compared. The signal processing associated with these 2D arrays is then discussed, which turns out to be different for the two frequency ranges of interest. That is to say, that operation in the 3-6 GHz region allows for the use, in the limit, of a dedicated RF chain per antenna element, and thus, the ability to implement fully digital (baseband) beam forming/precoding on the downlink. In contrast, the high cost and power consumption of mixed signal and RF chains at mm-wave frequencies requires a hybrid approach, where processing is split between baseband and RF. Fortunately, this hybrid approach, which uses a combination of baseband precoding/combining and analog/RF beam steering, has been shown to offer performance approaching that of an unconstrained digital solution (75). A discussion on UE antennas that support operation in the 3-6 GHz region concludes this section.

10.1 2D Phased Array Antenna

The base station antenna envisioned for 5G for both frequency regions of interest is a “large” 2D planar phased array, where large refers to the number of antenna elements, which will depend upon the allowable form factor and specific frequency of operation. In addition, a 2D array is also envisioned as the UE antenna for operation at mm-wave frequencies, where the much shorter wavelengths support implementations that are compatible with device form factors. Because of the limit on the number of RF chains, the mm-wave arrays will employ active analog phase control to support beam steering in addition to baseband precoding. The arrays intended for 3-6 GHz can also be operated in this hybrid fashion, but have the additional flexibility to support a fully digital/baseband beamforming/precoding

solution because each antenna element has a dedicated RF chain. The antenna processing associated with these two approaches will be discussed in more detail in the next two sections.

A square array configuration with $b\lambda$ separation between elements for a notional 10x10 element design is shown in Figure 10-1. A typical value for b is 0.5, but as pointed out in (74) and (76), mutual coupling between adjacent elements will decrease the achievable capacity. This loss due to coupling can be minimized by increasing b to a value between 1 and 2 (74) (76). The separation between elements and the number of elements in the horizontal and vertical direction are very important parameters since they directly affect the width and height of the antenna. Existing macrocell base station antennas were driven to a vertical column implementation to support a vertical beamwidth that is typically much narrower than the horizontal beamwidth. Thus, the limiting dimension of a 2D array if placed on a conventional tower top will typically be the width since any increase in this dimension will affect the wind loading. For other applications, e.g. small cells, space may be even more of a constraint.



Figure 10-1. Notional design of 10x10 element 2D planar phased array.

For example, a typical, dual-polarized base station antenna used in the deployment of LTE that serves both low (<1 GHz) and high frequency (>1.5 GHz) bands has a height that can range from about 4' to 8' and a width of about 12". Assuming that 12 inches sets the allowable width for the 2D array, Figure 10-2 shows the maximum number of elements per row that can be supported for b values equal to 0.5, 1, and 2, for several frequencies of potential interest for 5G in the United States (3.7 GHz, 28 GHz, 38 GHz, and 60 GHz). If the width is allowed to grow to 18", then the number of elements per row increases by about 50% (values were rounded down to integers) as shown in Figure 10-3. From Figure 10-3 it can be observed that in order to support the somewhat arbitrary 10x10 design, operation at 3.7

GHz will require an increase of the allowable width to 18", with an element separation slightly greater 0.5λ. Conversely, Figure 10-2 shows that operation at 28, 38, and 60 GHz can support 14, 19, and 30 elements per row, respectively for the 12" width with a separation of 2λ, thus staying within current design boundaries and minimizing coupling losses. Note most theoretical performance analysis of microwave and mm-wave phased arrays typically assume 0.5λ spacing, and it may be that some implementations are able to operate closer to that limit. For example, a prototype phased array developed by Samsung at 27.925 GHz used an inter-element spacing of about 0.7λ for an 8x8 design, where the 2D dimensions were 66 x 66 mm. (77).

Thus, one of the significant advantages of operation at mm-wave frequencies is the ability to implement arrays with a large number of elements in much less space than that required for operation at microwave frequencies. The net result from a link budget perspective is a higher antenna gain, which is necessary to offset the higher propagation losses incurred at mm-wave frequencies. This is not to preclude the use of 3.7 GHz or some other non-millimeter wave frequency for 5G, but rather to point out that operation at lower frequencies will require more careful transmitter design so as to minimize coupling loss at the closer element spacing. An example of a planar 8x8 phased array developed for operation at 3.5 and 5 GHz is described in [5], where the 2D dimensions were 287 x 367 mm. Note, although a square configuration has been assumed in the discussion above, a rectangular configuration is also quite viable, and may be a way to further exploit the vertical domain and/or keep the vertical beamwidth smaller if configured as a more conventional, base station antenna. In addition, there is also the possibility to "wrap" the square or rectangle around a structure so as to form a circular array.

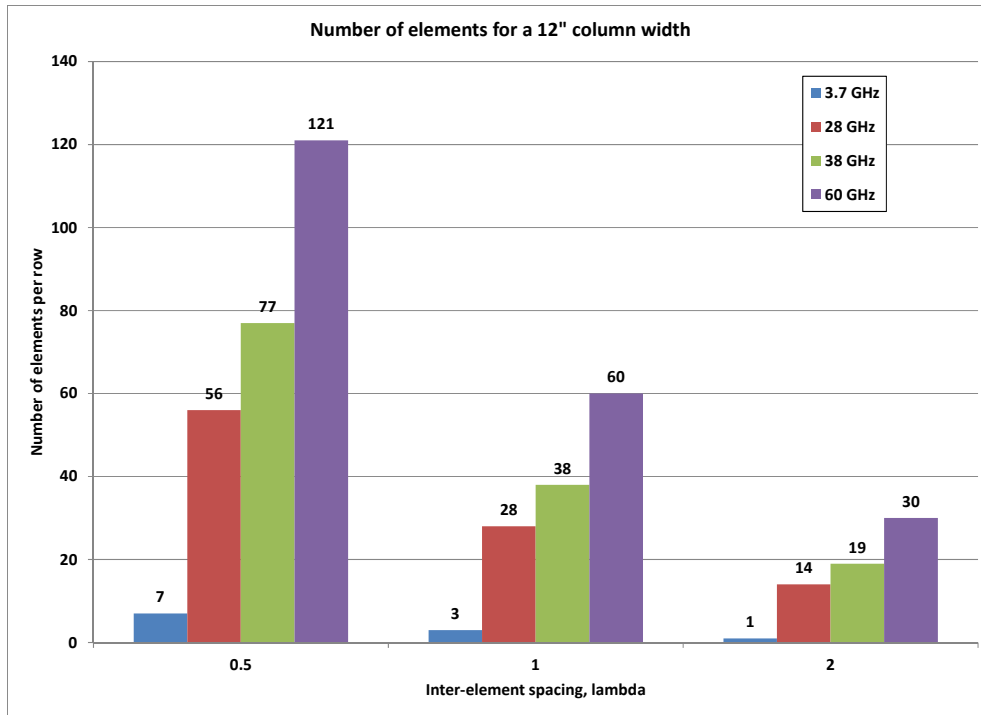


Figure 10-2. Number of antenna elements per row for frequencies of interest – 12" column width.

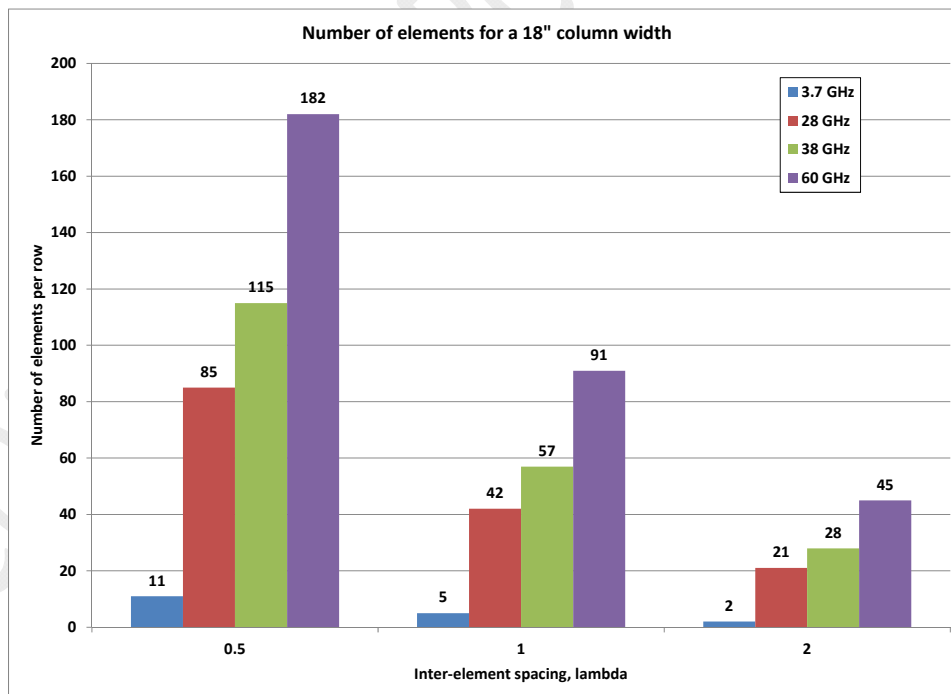


Figure 10-3. Number of antenna elements per row for frequencies of interest – 18" column width.

10.2 2D Phased Array Antenna Processing for 3 to 6 GHz Systems

As mentioned previously, 2D phased arrays designed for operation in the 3-6 GHz range can support what is sometimes referred to as a fully active antenna, which implies that each element can be connected to its own dedicated PA, LNA, and associated RF chain. This latter implementation is practical at microwave frequencies since the cost and complexity of multiple RF chains is not cost prohibitive. Currently, commercial LTE base stations use 2 and sometimes 4 transmit branches, and TDD LTE systems often use 8 transmit antennas.

Figure 10-4 shows a simplified block diagram of the main components that support each element. This block diagram is meant to be somewhat generic showing just the main functionality required, realizing that actual implementations could be quite varied. The transmit path, shown by the blocks in the upper portion of Figure 10-4, consists of a Digital-to-Analog Converter (DAC); analog phase control to support alignment and downlink beam pointing; an up-converter to convert the baseband (or IF) signal to RF; and the PA. The receive path, shown by the blocks in the lower portion of Figure 10-4, consists of an LNA; a down-converter to convert from RF to baseband (or IF); analog phase control to support alignment and uplink beam pointing; and an Analog-to-Digital Converter (ADC). The transmit and receive paths interface with the antenna through either a duplexer for FDD operation, or through an RF switch for TDD operation. The DAC and ADC are suitably interfaced to the baseband electronics. Although not shown, a synthesizer is required to provide the necessary “local oscillator” for the up-converter and down-converter, respectively. Also, not shown is any synchronization circuitry that will typically be required to ensure that all of the elements are phase and time aligned within acceptable limits.

The phase for both transmit and receive paths is shown to be controlled by baseband processing, but the synthesizer may also play a role. For the preferred, fully digital implementation, the analog phase for each element is statically set to ensure proper phase and timing between elements. This implies that it is not adaptive unlike in the case for the mm-wave implementation, which will be described in the next section. The above does not preclude a hybrid approach at 3-6 GHz, but the fully, unconstrained digital solution is typically preferred since it has been shown to offer optimal performance across a wider range of operating environments (78). Although not shown, the baseband processing consists of the appropriate precoding and combining for the TX and Rx paths, respectively. Precoding and combining consistent with a large 2D array communicating with multiple UEs, each with a single antenna, are described in (74) (79) (80).

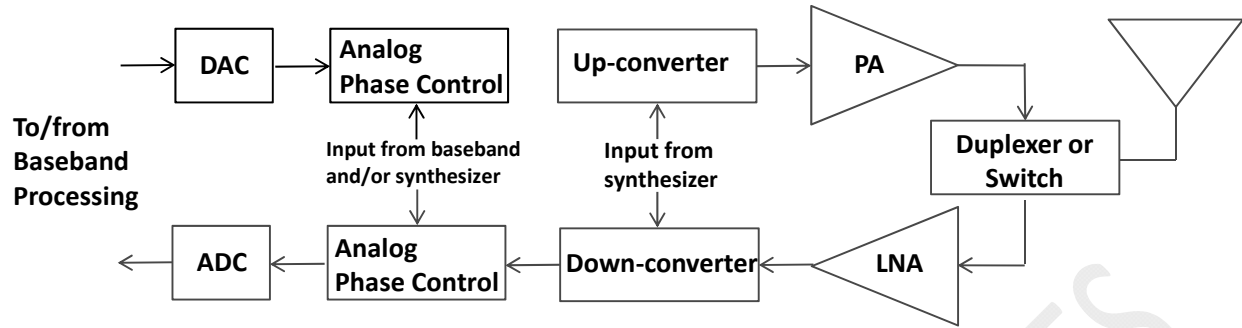


Figure 10-4. Simplified block diagram of components supporting each antenna element.

10.3 2D Phased Array Antenna Processing for mm-wave Systems

In this section the processing associated with 2D phase array antennas operating at mm-wave frequencies is described. As was mentioned earlier, the high cost and complexity of RF chains and mixed signal circuitry at mm-wave prohibits the use of a dedicated RF chain per antenna element as shown in Figure 10-4. Consequently, the signal processing for a typical mm-wave system is split between baseband and RF, which is shown generically in Figure 10-5. As shown in Figure 10-5, the transmitter consists of a baseband precoder, NtRF RF chains, and a transmit RF beamformer, while the receiver consists of a receiver RF beamformer, NrRF RF chains, and a baseband combiner.

The following describes the transmitter-receiver signal flow per the derivation developed in [9]. The baseband precoder accepts N_s data streams and develops outputs to each of the RF chains per the conversion described by the matrix FBB, which is of dimension $N_{tRF} \times N_s$. The Tx RF Beamformer then accepts the inputs from the RF chains and develop outputs to each of the N_t transmit paths (antenna elements) per the matrix FRF, which is of dimension $N_t \times N_{tRF}$. The resultant transmit signal is described by,

$$x = FRFFBBs \quad (4)$$

where s is the $N_s \times 1$ input signal vector, and x is the $N_t \times 1$ transmit signal vector. The transmit signal is input to the channel (not shown) which is described by an $N_r \times N_t$ channel response matrix, H , where N_r is the number of input receive paths at the receiver. The resultant received signal vector r of dimension $N_r \times 1$ is then given by

$$r = \sqrt{P}Hx + n = \sqrt{P}HFRFFBBs + n \quad (5)$$

where P is the average transmit power, and n is an $N_r \times 1$ Gaussian noise vector with zero mean and variance = σ^2 . The Rx RF beam former develops signals which are input to each of the N_{rRF} receive chains via the transformation described by the matrix WRF, which is of dimension $N_r \times N_{rRF}$. Finally, the baseband combiner develops an estimate of the transmitted data stream via the $N_s \times N_{rRF}$ matrix, WBB. The estimate of the data stream is given by

$$\tilde{s} = k\sqrt{P}W_{BB}^*W_{RF}^*H F_{RF}F_{BB}S + kW_{BB}^*W_{RF}^*n \quad (6)$$

where k accounts for any amplitude scaling required and $*$ means to take the conjugate transpose of the matrix.

In a typical design, $N_s \leq N_{tRF} \leq N_t$ and $N_s \leq N_{rRF} \leq N_r$. The transmitter-receiver pair described applies to both the downlink and uplink, where when channel reciprocity is assumed (a valid assumption for “well designed” TDD systems) the channel matrix for the UL is just the transpose of the channel response matrix for the DL.

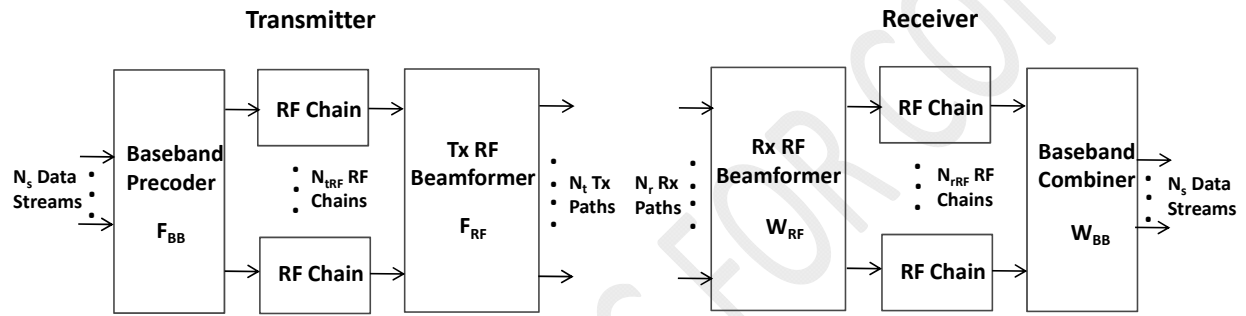


Figure 10-5. Simplified block diagram of mm-wave transmitter and receiver.

To provide some additional clarity, Figure 10-6 shows an implementation of a Tx RF beam former being fed by two RF chains. As shown in Figure 10-6, the outputs from each of the DACs within each RF chain are first up-converted to the carrier frequency, f_c via respective multipliers (mixers). Each up-converted signal is then input to its own set of analog phase shifters, with one phase shifter per antenna. It is important to note that only the phase is adjusted since amplitude control at mm-wave frequencies is complex to implement. The phase shifter outputs from each of the two RF chains intended for a given antenna are then summed and input to a PA, which then feeds its respective antenna. Some diagrams in the literature (75) depict a PA at the output of each phase shifter and there may very well be some pre-amplification required, but in the limit one final PA per antenna should lead to minimal complexity and cost. For clarity, only two of the N_t transmit antennas are shown in Figure 10-6, although many more are inferred by the arrangement of vertical dots, where N_t is typically much greater than the number of RF chains.

In like manner, Figure 10-7 shows an implementation of an Rx RF beam former which develops outputs for two RF chains. As shown in Figure 10-7 each of the N_r Rx antennas is input to a dedicated LNA, which in turn feeds two phase shifters, where each phase shifter is associated with a particular RF chain. The N_r phase shifter outputs that are intended for a respective RF chain are then summed, with the resultant signal down-converted before being input to the DAC of that respective RF chain. Similar to the Tx beam former, the number of antennas paths, N_r is typically much greater than the number of RF chains.

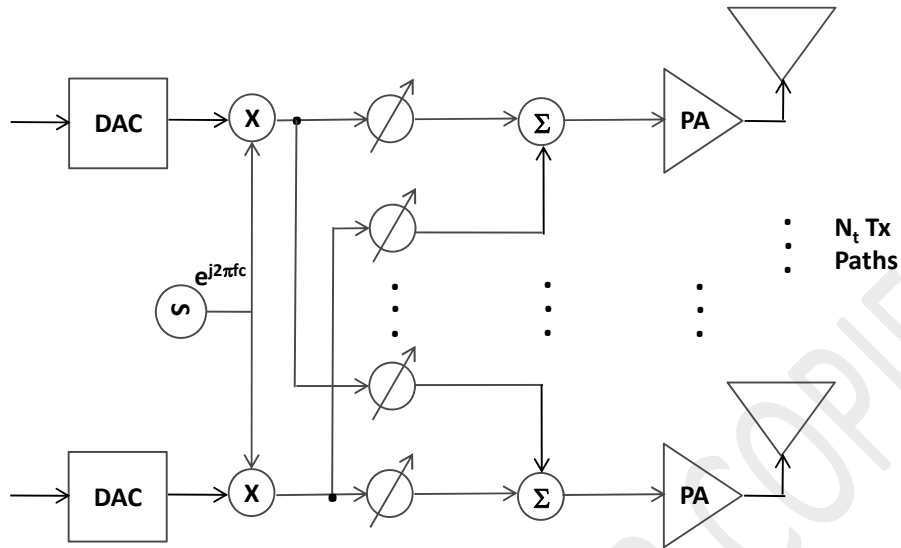


Figure 10-6. Tx RF Beam former with two RF chains

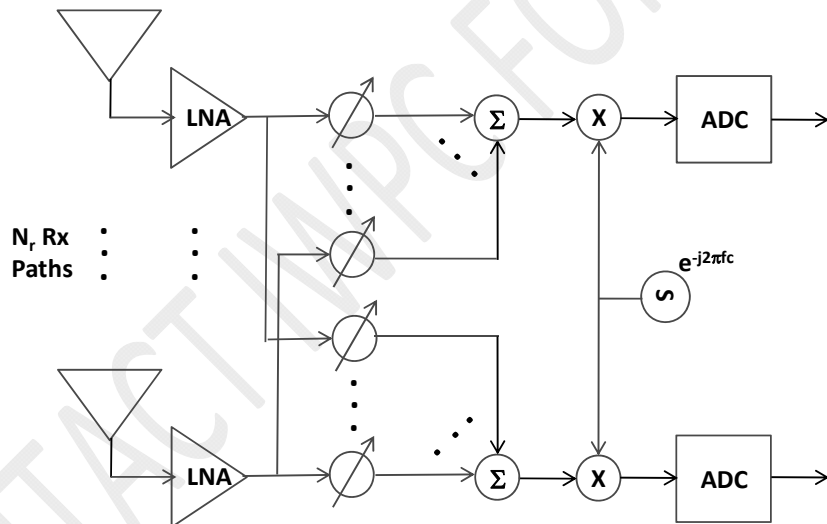


Figure 10-7. Rx RF Beam former with two RF chains.

A concern with the “hybrid” mix of baseband and RF processing required for mm-wave systems is that the resulting performance may be compromised compared to a fully digital implementation. However, a number of references have shown that practical implementations of this hybrid architecture can approach the performance of unconstrained digital beam forming solutions (75) (78) (81). For example, in (81) an iterative hybrid beam forming algorithm is described which accounts for the limitations of RF beam forming (phase control only) and assumes only partial channel knowledge at both the base station and UE in the form of local Angle of Arrival (AOA) information. The hybrid precoding strategy developed in (81) exploits the limited scattering (sparse) nature of the mm-wave channel (82) and uses a variant of matching pursuit to provide a practical solution to the hybrid beam forming problem. Simulation results

show that the proposed algorithm can support data rates that approach an unconstrained digital beam forming implementation. Further, analysis in (78) shows that for the sparse mm-wave channel, that the capacity achieved with unconstrained MIMO precoders based upon the channel's singular value decomposition (SVD), converges in the limit to what is achieved with large arrays using traditional beam steering via RF beam forming. Simulation results are provided in (78) which verify the optimality of the beam steering in large systems and for systems with realistic array sizes. Thus, the hybrid precoding approach required for mm-wave systems is shown to support system performance that closely approaches that of a much more complex (at mm-wave), fully digital solution.

10.4 UE Antennas for 3 to 6 GHz

In this section the device antenna requirements for operation in the 3-6 GHz range is described, where the associated wavelength typically limits the number of antennas to the single digits, with two being a typical value for feature and smart phones, while four is a possibility for tablets and laptops. Much work has been done in recent years in the development of antennas for devices, or what is typically referred to as User Equipments (UEs) in the 3GPP standards community, to accommodate MIMO and multi-band operation (83). In LTE, baseline performance as defined in Release 8 is based upon a minimum of two receive antennas at the UE. Device antenna vendors have been able to implement primary antennas with gains that approach -4 dBi at low frequency bands, e.g. lower 700 MHz, while the gain of the secondary or diversity antenna is typically within 3 dB of that value. In addition, envelope correlation values in the range of 0.5 to 0.6 have been achieved at these low frequencies to support MIMO and diversity operation. Assuming 5G at higher frequencies the resulting UE antenna performance characteristics should be significantly better with gains approaching 0 dBi and correlation values below 0.2. The shorter wavelengths associated with higher frequency operation are a significant advantage compared to the longer wavelengths at lower frequencies, when it comes to device antenna design where available space for implementation is typically quite limited.

The number of antennas required at the UE/device in 5G networks that operate in the 3-6 GHz range may well depend on the duplex mode employed. Numerous studies have been conducted of very large MIMO configurations employing Time Division Duplexing (TDD), which support Multi-User (MU) MIMO operation on both the DL and UL with just a single antenna at the UE for both receive and transmit (74) (79) (80). One of the significant advantages of TDD operation with large antenna arrays at the base station is that an estimate of the downlink channel can be inferred from the uplink channel. Thus, there is no need for pilot overhead on the downlink, as there is with Frequency Division Duplexing (FDD). This use of reciprocity in TDD systems is very helpful in beamforming to maximize the desired signal, but is less effective in an interference limited environment where one also desires to reduce interference to and from adjacent cells and users. The pilot overhead for TDD is limited to the uplink and increases linearly with the number of users, K . Each user is assigned a mutually orthogonal pilot sequence used by the base station to develop estimates of the uplink channel. In FDD, the pilot overhead increases with the number of antennas at the base station, N and thus, will typically limit the size of the array to a value less than what can be supported by TDD. To offset the resulting performance advantage afforded TDD

by virtue of a larger array may well require the UE to employ multiple antennas with all of the resulting complexities. With just one UE antenna for transmit and receive there are no correlation or coupling effects to consider, which are two of the main limiters in the performance achievable in MIMO networks. This implies further that UE antenna vendors can focus on implementing one very good antenna with high efficiency, and without any regard as to how it may interact with other antennas.

This is not to completely preclude the use of FDD in 5G; however the ability to support a larger value of N with TDD has other benefits including:

1. Improved PA power reduction on both DL and UL, where on the DL the power of each PA is typically $1/N$ of the total transmit power, and on the UL it has been shown that for perfect channel state information (CSI) the transmit power is proportional to $1/N$, while for imperfect CSI it is proportional to one over the square root of N (84); and
2. for $N \gg K$, optimal transmission can be achieved with simple linear precoders, i.e. maximum ratio transmission (MRT), and detectors, i.e. maximum ratio combining (MRC), while at the same time the effects of thermal noise, interference, and channel estimation errors are greatly reduced since the limit on performance now becomes pilot contamination due to reuse of pilot sequences in adjacent cells (79) (80). In addition, the use of slightly more complex precoding based upon Regularized Zero Forcing (RZF) on the DL, and Minimum Mean Squared Error (MMSE) detection on the UL, can lead to a reduction in the number of antennas required at the base station by almost an order of magnitude compared to that required for MRT precoding and MRC detection (79).

In summary, if the requirement for 5G operation in the 3-6 GHz frequency range is for just one antenna at the UE for both transmit and receive, which appears to be the case for TDD, then the design task is greatly simplified compared to what was required for LTE. However, if multiple antennas are required at the UE to support FDD operation then design techniques used for LTE and other technologies as described in (83) (85) are readily available, and should be easier to implement by virtue of the shorter wavelengths associated with 5G operation. For example, (85) describes a dual-antenna design at 930 MHz, where a folded monopole at one chassis edge excites the chassis' fundamental electric dipole mode and a coupled loop at the other chassis edge excites its own fundamental magnetic dipole mode. Since the two radiation modes are nearly orthogonal an isolation of over 30 dB was achieved. Further, by controlling the current on the folded monopole the two antennas can be co-located on the same chassis edge with over 20 dB of isolation.

10.5 IC Technology for mm-wave Systems

In this section the IC technology which might be best suited for mm-wave circuits and systems is discussed. There are three main IC technologies to consider:

1. Devices based upon III-V semiconductor compounds and processes, e.g. gallium arsenide (GaAs), which has been the traditional choice in the past for mm-wave RF circuits;
2. Standard complementary metal oxide semiconductor (CMOS) processes and

3. Silicon based CMOS processes.

Most of the early devices were based upon III-V semiconductor compounds, which are expensive and do not integrate well with digital circuitry. Thus, according to (86) “their design is not a viable solution for extremely cheap, ubiquitous, and highly integrated consumer products”. In recent years, silicon based CMOS has become a viable alternative as shrinking transistor gate sizes (<50 nm) allow for transit frequencies greater than 100 GHz. Another key figure of merit is the maximum frequency of operation, f_{\max} where CMOS and BiCMOS processes have been shown to support a value near 300 GHz, while silicon for high-resistivity silicon-on-insulator (SOI) processes can support a value near 325 GHz (86). Thus, lower cost standard CMOS and slightly more expensive, silicon based CMOS implementations are now considered a viable alternative to the more expensive III-V semiconductors. According to (87), “SOI CMOS processes are also attractive for high end applications as they allow for higher quality factors due to reduced values of parasitic capacitances and inductances for passive components.” However, as mentioned above, silicon based CMOS is more expensive than standard CMOS since in the former devices channels and substrates are engineered separately, while that is not the case for the latter. Thus, if cost is the ultimate driver, then standard CMOS would be the preferred IC technology.

The end result, whether it is based upon standard CMOS or silicon based CMOS, is the realization of a single chip mm-wave system, complete with a digital baseband and mm-wave analog front end.

10.6 On-chip and In-Package Antennas for mm-wave Systems

A possible implementation for antennas at mm-wave frequencies is what is referred to as on-chip antennas. As the name implies the antenna is literally fabricated directly on the chip as opposed to an in-package implementation where the antenna elements are placed in the package surrounding the chip. The on-chip approach has the advantage of removing all external connections between the antennas and the associated RF circuits thereby reducing cost and allowing for more flexibility in circuit design. The primary disadvantage of on-chip antennas is an extremely large radiation loss due to substrate absorption and conductive currents (86). For example, typical on-chip antennas on doped silicon substrates only have an efficiency of about 10%.

To improve performance a dielectric lens can be placed above or below the antenna, which has the effect of reducing the energy lost to the substrate modes. A dielectric lens above the antenna reduces the difference in the dielectric constants above and below the antenna, thereby increasing the radiation intensity away from the substrate. For proper operation this lens should have a dielectric constant greater than or equal to that of the substrate. A dielectric lens below the chip increases performance by releasing and radiating energy trapped as substrate modes in the silicon out the back of the chip. The problem however is that the inclusion of a dielectric lens located above or below the antenna substrate is nonstandard with regards to typical foundry production processes. Other possibilities for increasing performance include the use of frequency selective screens and meta materials, and the use of symmetric electromagnetic band gap structures (86).

A higher cost but better performing alternative to the on-chip antenna is the in-package antenna, which has much higher efficiencies by virtue of the antenna being located further from the lossy chip substrate. In general, the best gain-bandwidth products will be obtained using materials with low dielectric constants, ϵ_r . Representative package technologies include Teflon, low temperature co-fired ceramic (LTCC), fused silica, and liquid crystal polymer (LCP) with respective dielectric constants of 2.2, 5.9-7.7, 3.8, and 3.1 (86). There are a number of challenges associated with in-package antenna design including: detuning of antennas due to the presence of packaging materials; mechanical and electrical reliability; antenna interference from heat sinks; and the possible high cost of the packing process itself. Of the candidate package technologies, LCP is currently viewed as a practical low-cost method for implementing in-package antennas at mm-wave frequencies.

Another challenge of mm-wave antennas in portable devices is their highly directive properties which can create difficulties in obtaining the necessary gain and polarization in the direction of the base station, particularly if the antenna is compromised due to the proximity of obstructions such as a hand or head. Practical solutions may involve the placement of several antennas at different locations on the device.

Finally, advanced packaging technologies provide more flexibility in the integration of antennas and other mm-wave components than a single chip solution, and will most likely be required in the implementation of a 2D phased array. A critical component of this integrated solution is the type of interconnect used in the package. The two main interconnect technologies are flip chip connections, which facilitate stacked structures, and coupling connections that can reach higher frequencies than standard wire bonds (86). Coupling connections come in many forms, and are based upon capacitive connections between components in a package, and may prove to be especially useful for integrating multiple chips into a single package. For example, an antenna array could be fabricated in CMOS, which could then be capacitively coupled to a more advanced process chip, which contains active mm-wave components, e.g. a PA or LNA. The antenna would benefit from the lower doping concentration and higher resistivity of the CMOS process, which results in a less conductive, less lossy substrate compared to a newer process technology. To support an antenna array, simple low-speed active switches, i.e. diodes could be integrated onto the antenna chip with phased passive feed lines to perform element tuning, phase shifting, and beam steering. An illustration of such an integrated solution is provided in Figure 10-5 of (86).

10.7 User Equipment Power Consumption

Variations in network deployment strategies are expected to become larger than today. Small cell deployments are expected with an overall heterogeneous radio access technology combination handling dense traffic situations, combined with more macro cell type of deployments in other areas. In such heterogeneous network topology utilizing several combined network technologies in a multi-layered approach the user equipment power consumption can become an important traffic scheduling aspect. This is mainly due to power amplifier consumption in the user equipment which is heavily dependent on the output power levels while the increase in power consumption versus increased bandwidth

utilization is not as large. Several radio access technologies are also assumed to operate simultaneously in the same terminal to a larger extent than today. Hence it is expected that variations in power consumption per transferred bit will be large, and optimizing the user equipment battery life will be crucial.

Another power consumption aspect is the utilization of mesh topologies and device to device communication in general, where power consumption of involved terminals is relevant in the routing decisions. This can be relevant to consider both in terms of defining most power efficient mesh links, but also taking end user expectations of total terminal battery life into account.

10.8 Massive MIMO

Massive MIMO is defined as a system where all antenna configuration is made in the digital domain and hence, can simultaneously be configured for multi beams and array antenna is utilized at BS/AP side only. For the 0.5-6 GHz frequency band most of the literature assumes a single antenna on the UE side. Two antennas for MIMO are, however, already implemented in LTE UEs and methods to generate a dedicated beam for the second/diversity antenna have been proposed but needs to be evaluated from system throughput and complexity point of view. This could either be achieved by two UL RF chains or UL antenna selection. Additionally, SAR needs to be handled, either by power reduction or antenna reselection. It has also been mentioned that there might be areas not covered by the BS, due to shadowing or fading, and then a 2nd antenna might help, the size and frequency of such areas will probably need more study.

10.9 Device Integration for mm-Wave

Highly integrated RFIC solutions providing complete transmitter and receiver chains are clearly desirable to provide the size, cost and power consumption needed for future generations of mm-wave radio products. For >6GHz UE antennas are likely to be fully integrated modules with antenna arrays and RF FEM in the same component. Hence, array to mitigate the small aperture and the module approach due to high loss when routing the RF signals. Also here the user loading will be a problem and the module might be treated as a single antenna where a second module needs to be introduced for diversity and to overcome LOS blockage. Additionally, as discussed earlier, an array by nature has the potential of adding antenna gain by beam forming, this adds to the transceiver complexity and current consumption. As the coverage angle of an array might be more limited than that of a single antenna element and possibly arrays on each side of the UE will be needed in order to achieve a proper user experience. Also the network might need to (at least in LOS scenario) cover the same area from different angles, for the same reason. Hence, limited coverage angle. SAR might be an issue and can be mitigated by antenna reselection.

10.10 Mobility considerations for mm-wave antennas

Common for any system where an array is involved, mobility needs to be handled. The array configuration exists in a rich NLOS environment and is only valid in a very small range ($<\lambda/2$) and needs

to be updated as soon as one of the antennas has been moved. Most proposed system involves frames with a training sequence that needs to be sent in a rate which will define the limit of mobility; the maximum UE speed. For a mm-Wave system where both BS and UE utilize beam forming a significant amount of signal processing will be needed and hence potentially increase the power consumption in the UE.

11 Proposed Network Features for Future Cellular Systems (may be termed as 5G systems)

- Role of Self Organizing Network (SON)
- Cell Identity Management
- Load Balancing & Mobility Robustness
- Power Saving features

The deployment challenges for unplanned (semi-planned) small cells result primarily from the fact that unlike a macro network, the small cells are installed with limited, if any, network planning and site-specific system configuration settings. These devices are required to be plug-n-play with self-configuration capabilities. Another important challenge is to offer seamless mobility within this unplanned network to prevent any service interruption or degradation in user experience. Neighbor discovery and frequent handover mitigations are important to optimize handover performance and reduce signaling load. In addition, transmit power management of small cells is needed to optimize capacity offload while minimizing pilot pollution (i.e. regions with high interference) under dense small cell deployments. Furthermore, radio resource management techniques such as interference coordination and load balancing are important to optimize capacity and user experience. As the small cell backhaul may be shared by other devices, Tx power and radio resource management methods need to take into account backhaul constraints. In this section the scope/requirements on some SON techniques to address the challenges mentioned above is covered.

11.1 Mobility Management

Effective mobility management is essential for the viability of dense small cell approach to reach the massive capacity goal. The mobility management problem basically boils down to ensuring all mobiles, including legacy, are supported in idle and connected modes in the small cell network. Figure 11-1 shows all the various possible transitions a mobile has to traverse through in a small cell network in both idle and connected modes: Macro-to-Small Cell, Small Cell-to-Small Cell, and Small Cell-to-Macro.

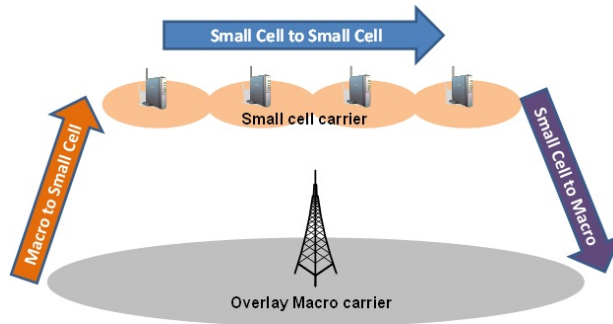


Figure 11-1: Scenarios for Mobility Management in a Neighborhood Small Cell Network

The following subsections describe various mobility management challenges specific to small cell deployment for the scenarios illustrated in Figure 11-1.

11.1.1 Idle Mobility

11.1.1.1 Discovery

For Small cell-to-Small cell and Small cell-to-Macro mobility, the discovery is not a challenge as it can happen naturally due to channel degradation of the serving cell (assuming in the latter case that the macro cell-ID can be provisioned by the network management on small cells).

For Macro-to-Small cell mobility, a mobile device needs to discover small cells when it is on the overlay macro network, even in good channel conditions since channel degradation may not happen due to the fact that the small cells are deployed on another frequency. This challenge can be addressed in multiple ways. One method is to configure a higher search threshold on the macrocells. This ensures that the UE searches the small cell frequency even under good macro signal quality. The downside of this approach is some impact on the UE's battery life as the UE will need to perform a search every time it wakes up irrespective of macro signal quality. An alternative approach is to prioritize the small cell frequency in case of dedicated carrier deployment for the small cell layer. UE autonomous search on the small cell frequency is another method for enabling small cell discovery. By changing the periodicity of these searches, a tradeoff between discovery time and UE battery life can be achieved. An alternative approach is to use cell reselection beacons to enable small cell discovery. In this approach, the small cell transmits narrow beacon bursts on the macro-only channels to temporarily reduce the macro signal quality and trigger a search when the UE is near the small cell. Proper beacon design can ensure fast discovery while minimizing impact on nearby voice/data users.

11.1.1.2 Paging Load Optimization

It may not be desirable to let a small cell handle the same paging load as that of a macrocell due to its lower processing power, capabilities and backhaul capacity. Hence, paging optimization schemes are needed to limit the size of the paging area and hence, paging load under the resource constrained small cells.

In order to limit the paging area of a small cell to a geographical area covered by one macrocell, all small cells can use the cell identity of their strongest neighboring macrocell to decide on their initial paging area code. Because multiple macrocells are typically associated with a single paging area code, say 'n' macrocells, then by adopting the above scheme, roughly, the paging area under small cells is reduced by the factor of '1/n'.

After this initial selection, if the paging load at any small cell turns out to be greater than what it can handle, the small cell can update its initial selection and select a different tracking area code.

If too many paging areas are created, it can lead to too many UE registrations at paging area boundaries, as whenever a UE enters a new paging area, it needs to perform a registration. To address this problem, the small cell can change its paging area code to be the same as the neighboring paging area, in case it experiences too many frequent registrations from the neighboring paging area. In LTE, the concept of UE-specific TAC list can also be used to address the issue of frequent registrations at the paging area boundaries. In this concept, if too many registrations from neighboring TACs are received from a UE, then those TACs can be added to the UE's TAC list by MME (Mobility Management Entity). For any of the TACs present in its TAC list, the UE does not perform registrations and is paged on all of them, i.e., the benefit needs to be contrasted with the increase in paging load.

11.1.2 Connected-Mode Mobility

11.1.2.1 Selection of Physical Layer Identifier

Available physical layer identifiers are limited and hence have to be re-used among the cells. In LTE for instance, there are 504 unique Physical Cell Identities (PCIs). While re-using these PCIs, there are two main issues to avoid: a) Collision and b) Confusion. PCI collision occurs when two neighboring cells with overlapping coverage area share the same PCI. This is a serious problem as mobile devices in that overlapping area cannot distinguish between the signals coming from the two cells, causing loss of processing gain, synchronization issues, and high decoding errors.

PCI confusion occurs when PCI reuse happens among the neighboring cells of the same cell. This leads to cell identification problem, where the serving cell is unable to uniquely identify its neighbors from their PCI. Consequently, when a connected mode UE moves towards one of these cells, the serving cell is unable to initiate a handover to the correct cell. Figure 11-2 illustrates PCI confusion problem.

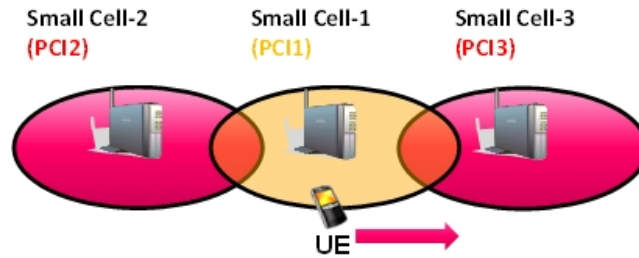


Figure 11-2 Case of PCI Confusion. Small Cell 1 cannot uniquely identify Small Cell 2 and Small Cell 3 from their PCI

In a macrocell deployment, careful RF planning ensures that PCI collision or confusion does not happen. However, in a dense unplanned small cell deployment, PCI collision/confusion may occur and hence need to be handled.

To avoid PCI collision/confusion, a small cell can use a UE-like receiver/sniffer, a.k.a. a Network Listening Module (NLM) to detect physical layer identifiers of the neighboring cells and hence, avoid selecting the ones that are already being used in its neighborhood. In addition, to address hidden node problems where the small cells cannot detect each other but a UE in the middle can detect both, UE reports and backhaul message exchange (e.g. over X2 in LTE) can be used to detect and resolve PCI collision/confusion. For example, the small cell can ask the UE to report cell identity of the neighboring cells, in addition to their PCIs. Since cell identity of each cell is unique, two neighboring cells with different cell identities but same PCI can indicate collision/confusion.

11.1.2.2 Neighbor Discovery

When a mobile device served by a small cell leaves the small cell coverage area, it needs to be handed out to a neighboring small cell or macrocell. For handover to take place, accurate information of the neighboring cells is required at the small cell (i.e., for LTE that would be the PCI to Cell ID mapping). Absence or incompleteness of this information can cause the mobile devices to have call drops.

For neighbor discovery, a small cell can use the NLM to detect its neighboring cells. This mechanism allows the small cell to construct its Neighbor Relation Table (NRT) at boot-up without any assistance. However, NLM at the small cell location may not be able to detect all neighboring cells that the small cell users within the coverage area can detect. This may cause handout failures. To resolve this problem, the small cell can utilize UE reports and backhaul messages exchanges in addition to its NLM functionality to generate a complete NRT.

In 3GPP, the Automatic Neighbor Relation (ANR) framework is defined to discover neighboring cells via UE reports. Small cells can request the UEs to report the PCI and Cell ID of neighboring small cells. With this information, each small cell can establish an X2 connection with its neighbors and exchange neighbor relation information with them. This allows each small to enhance their NRT based on the UE reports and X2 messages received from the neighbors.

11.2 Frequent Handover Mitigation

In a neighborhood small cell deployment, due to small coverage area of small cells, an active high speed UE may go through frequent handovers between small cells. Stationary or slow moving UEs can also experience frequent handovers due to shadowing and/or channel fading when they are located in areas where pilots from different small cells are about the same strength (i.e., pilot pollution). Figure 11-3 illustrates these scenarios.

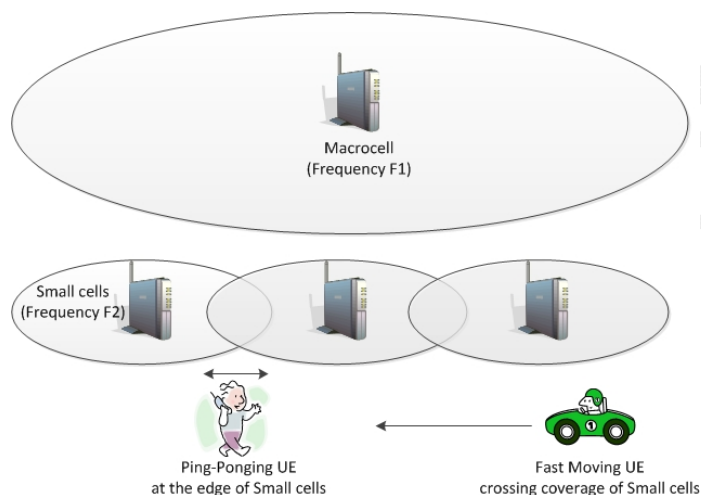


Figure 11-3: Scenarios of frequent handovers in neighborhood small cell deployment

Frequent handovers between small cells are undesirable as they can cause packet losses and/or packet delays leading to voice artifacts and/or poor user experience. They also can lead to large signaling load at the small cell gateway and/or core network. Thus, it is desirable to take appropriate action to avoid such frequent UE handovers in small cell deployment. There is a general rule that high mobility users are better served by lower frequency cells which tend to have larger coverage areas leaving smaller high frequency cells for lower mobility users. A three-step approach can then further mitigate frequent handovers:

1. Determine if a UE is experiencing frequent handovers
2. Classify frequent handovers based on cause (high speed UE or ping-ponging UE).
3. Determine actions based on the number of frequent handovers and their classification.

To determine frequent UE handovers, UE handover information needs to be obtained. In LTE, this information can be obtained from “UE History Information”, which is passed during the handovers from one cell to the other. This contains information for the cells (up to 16) that a UE has been served by in active state prior to the target cell. For each of these cells, it contains cell identity, cell type (i.e., macro, small cell, etc.) and the time UE stayed in that cell. By checking the average time UE stayed on each cell for a few of the past cells, a small cell can determine if frequent handovers are happening.

To understand if frequent handovers are ‘Ping-Pong’ handovers, the small cell can check the last few handovers in UE history information to see if a cell identity is getting repeated. If that is the case, then it can classify them as ‘Ping-Pong handovers’, otherwise, they can be assumed to be ‘fast moving handovers’.

If handovers are ‘frequent handovers’ and are classified as ‘fast moving handovers’, then the small cell can initiate inter-frequency handover to a macrocell on the other carrier. The idea here is to send the fast moving UE to a clean macrocell carrier where the number of handovers would be reduced due to large coverage of macrocells.

If handovers are ‘frequent handovers’ and are classified as ‘Ping-Pong handovers’, then the small cell can make it more difficult for this UE to handover to the ping-ponging (or neighboring) cells through the adjustment of UE specific handover parameters. If delaying handovers to the ping-ponging cells does not work (i.e., frequent handovers continue), inter-frequency handover to the macrocell may be initiated by the small cell, as a fallback option.

Additional improvements to handover performance can be obtained by monitoring handover failure scenarios and adjusting handover policy to reduce handover failures. For instance, in LTE, the Mobility Robustness Optimization (MRO) feature of the 3GPP standard defines several techniques for handover failure monitoring, including message exchange between source and target cells to monitor failures that the source cell would otherwise not be aware of. The standard leaves the handover policy adjustments to implementation.

11.3 Transmit Power Management

A dense deployment of small cells in a neighborhood while providing improved capacity via spatial reuse results in two main challenges which affect user mobility:

Islands where multiple small cells are at nearly equal strength resulting in users, stationary or mobile, experiencing very frequent handovers between small cells. Smaller coverage footprints: Since the density of small cells in a geographical area is very large, the coverage area per small cell ends up being much smaller than the coverage area of a macrocell. As a result, pedestrian or vehicular users moving within the network experience much more frequent handovers between small cells.

These mobility related challenges can be mitigated, in addition to the schemes described above, by correctly calibrating the small cell downlink transmit power level. Each small cell can monitor the surrounding RF using the NLM and UE measurements. Each small cell performs RF measurements of other small cells’ pilot channel and determines its own transmit power level. NLM measurements can be done at the power-up and repeated periodically to monitor any changes in the neighborhood. Furthermore, UE measurements can be used to enhance the NLM measurements and address RF mismatch issues.

Figure 11-4 and Figure 11-5 illustrates the need for power calibration from the mobility point of view for an LTE system. It shows a dense urban neighborhood with 18% small cell penetration. In Figure 11-4 each small cell transmits with a fixed power of 20 dBm. As an example and to illustrate the benefits of Tx power calibration, in Figure 11-5 each small cell calibrates its transmit power level and transmits at 20 dBm or 0 dBm depending on the RF signal strength observed from other small cells. The contour plots depict difference in received pilot power from the strongest RSRP and second strongest RSRP.

Without power calibration a significant portion of the neighborhood sees another small cell within 3 dB from the strongest. Furthermore, channel fading can cause stationary or mobile users to experience frequent handovers. This simple power calibration schemes can minimize the creation of such regions.

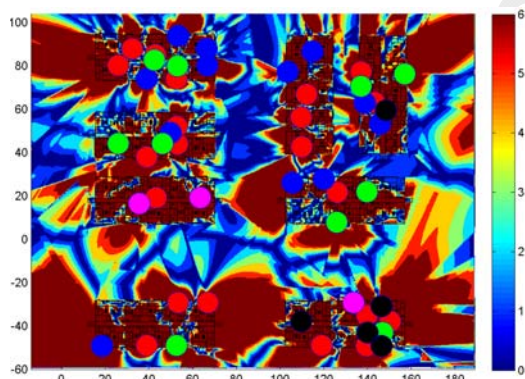


Figure 11-4 Pilot pollution regions: shows pilot pollution without power calibration

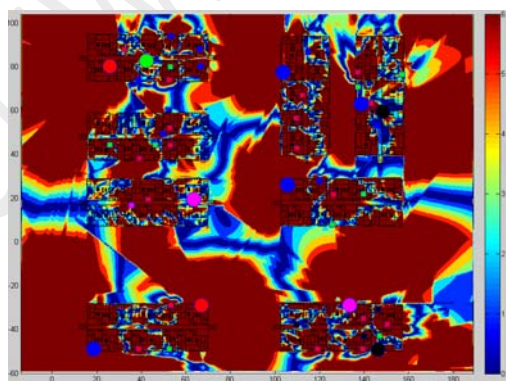


Figure 11-5: Pilot pollution regions: shows pilot pollution with power calibration

Figure 11-6 and Figure 11-7 shows the coverage footprint of small cells. In Figure 11-6 each small cell transmits at the same 20 dBm power level. In Figure 11-7 each small cell calibrates its transmit power level and transmits at 20 dBm or 0 dBm depending on the RF signal strength from other small cells. The mobility benefits of power calibration can be quantified by the number of handovers experienced by users. A mobile user traveling along the white route experiences about six handovers when small cells transmit at a fixed power. With power calibration the number of handover experienced is about one along the route.

Reducing the Tx power of some of the small cells reduces pilot pollution but on the other hand can impact the capacity offload to small cells. Hence, intelligent Tx power management algorithms are needed to optimize the capacity offload while minimizing pilot pollution. Furthermore, joint Tx power management, scheduling and resource coordination among multiple small cells can further optimize the system capacity. For example, soft Fractional Frequency Reuse can be used where a cell site user is served at a lower Tx power in the same resource block as a cell edge user in a neighboring small cell at a higher Tx power. This can result in better frequency reuse and improvement in the overall system capacity.

Transmit power management should also take into account backhaul limitations. For example, a small cell with lower backhaul capacity should in general transmit at a lower power to avoid attracting many users and hence causing congestion due to limited backhaul.

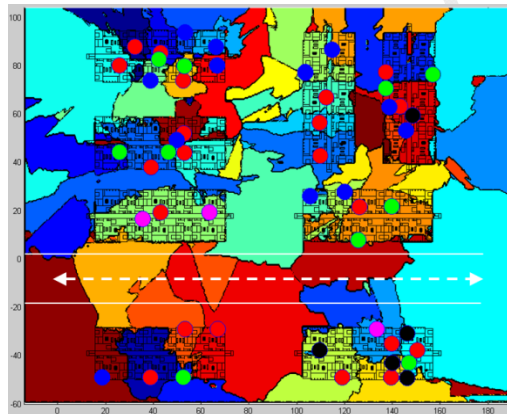


Figure 11-6: Small cell coverage footprints: shows coverage footprints without power calibration

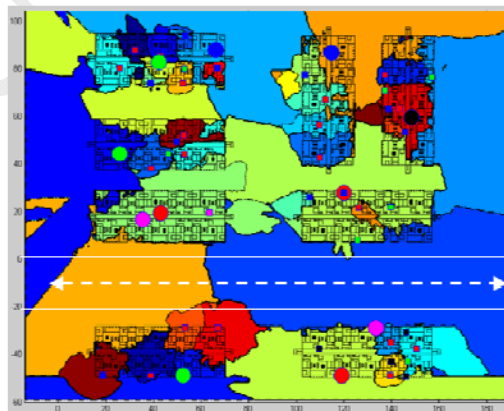


Figure 11-7: cell coverage footprints: shows coverage footprints with power calibration

11.4 Radio Resource and Interference Management

In conjunction with Tx power management, radio resource and interference management is needed to further optimize system capacity and user experience. In particular, time and frequency resource

partitioning and coordination can be used to mitigate the co-channel and adjacent-channel interference between small cells and macro cells as well as between small cells. In LTE, the Inter-Cell Interference Coordination (ICIC) framework was established that serves as prime technique for co-channel Hetnet deployments.

Small cells may become channel element (CE) limited due to their extended coverage area and open/hybrid access mode of operation. Resource limitations need to be handled properly to ensure a certain level of QoS for the small cell owner. This is particularly important to convince the users to allow public use of their small cell device and backhaul.

When a small cell runs into channel element limitations, the small cell owner needs to be prioritized. This prioritization can be achieved by handing over other users to the macro network. small cell coverage can also be adjusted based on long-term CE usage statistics.

User experience on neighborhood small cells depends on the signal quality as well as the small cell loading. One other important aspect of resource management is to maximize the user throughput via intelligent load balancing between small cells and macro cells. The small cell can estimate the macro load by monitoring the macro transmission or get load information through the X2 interface if available. Load balancing can be performed over the long term by adjusting the handover/reselection parameters for small cells or by adjusting their Tx power. In addition, short term load balancing can be achieved via handover between small cells or between small cells and macro cells.

11.5 Backhaul Management

Small cells are likely to utilize different qualities of backhaul starting from consumer-grade all the way to fiber optics. In addition, provisioning of customer's backhaul open to all users presents interesting opportunities and challenges for the operators. For instance, when a small cell runs into backhaul limitations, the small cell owner needs to be prioritized by handing over other users to the macro network or limiting the backhaul usage of other users via radio resource management and scheduling. Small cell coverage can also be adjusted based on long-term backhaul usage statistics. The small cell may need to estimate the backhaul availability and limit its backhaul traffic in order to prevent any impact. Estimating backhaul is a challenging problem by itself. One way is to monitor traffic on the backhaul in a passive sense. Another is to actively probe the backhaul bandwidth/latency maybe through pinging some server on the core network.

11.6 Power Saving

One basic element to reach massive increase in capacity (e.g. 5000x) is the spatial reuse through deploying more cells. In fact, it is reasonable to believe that a major portion of capacity will come through spatial reuse. With the increase in the number of cells comes increase in power consumption. One viable solution to limit power consumption is to opportunistically light up cells depending on network loading. That brings up a number of challenges including user's discovery, idle camping,

interference burstiness due to cells suddenly appearing/disappearing, and others. The 5G networks design should include viable solutions to allow opportunistic support of small cells for power saving.

11.7 Centralized versus Distributed RAN

Clearly solving the problems mentioned above, which in general fall under the class of self-organizing network (SON), is a significant challenge to be addressed by the wireless community if massive increase in capacity (e.g. 5000x) is to be realized. One can envision a solution where a centralized entity on top of small cells solves the problems mentioned above and more (this is along the lines of the already proposed in 3GPP cloud-RAN approach). For instance, solving a very complicated optimization problem maximizing network capacity (e.g. to achieve 5000x), subject to a minimum link quality (to aid mobility) and backhaul constraints (like cells with poor backhaul serve limited number of users). The outcome would be what transmit power distribution to be used across cells, what mobility parameter configuration to be used and how to distribute the load across cells. In addition, this central server can configure small cells to avoid problems like cell ambiguity and enable cells with neighbor lists to aid mobility.

A different approach would be to solve the same problem but in a distributed manner where cells take local decisions that converge to the optimal solution globally. In addition, cells can be self-configured in efficient way to avoid cell ambiguity and automatically finds their neighbor lists to aid mobility.

A third, and more realistic approach would be a hybrid centralized-distributed solution where tasks that are global in nature and/or don't require high backhaul bandwidth can be addressed in a centralized way, while tasks that are local in nature (such as mobility) and/or have the tendency to stress the backhaul bandwidth can be left to individual cells to tackle.

Splitting SON features between centralized and distributed architecture is not an easy problem and does depend on many factors; the two most important ones may be cells density and type of deployment (Hotspots, Enterprise, residential, etc.).

12 List of Contributors

Company	Contact
Agilent Technologies	Moray Rumney
Agilent Technologies	Bob Cutler
Alcatel-Lucent	Stephen A. Wilkus
Blackberry	Daniel Badiere
Blackberry	Dr. Yan Xin
Blackberry	Dongsheng Yu
Broadcom	Nick Ilyadis
China Mobile	Clark (Kuilin) Chen
CommScope, Inc.	Ray Butler
CommScope, Inc.	Phillip Sorrells
DragonWave, Inc.	Erik Boch
Ericsson	Erik Dahlman
Ericsson	Hossam Hmimy, PhD
Fraunhofer Heinrich Hertz Institute	Dr. Wilhelm Keusgen
Huawei Technologies Co., Ltd	Chin Chiu
InterDigital Communications, LLC	Douglas Castor
InterDigital Communications, LLC	Philip Pietraski, PhD
InterDigital Communications, LLC	Tao Deng
IWPC	Graham Carter
IWPC – retired	Don Brown
New York University	Prof. Theodore S. Rappaport
Nokia Solutions and Networks	Amitava Ghosh, PhD
Nokia Solutions and Networks	Harri Holma
Northrop Grumman	Stephen J. Sarkozy, PhD
Qualcomm, Inc.	Jean Au
Qualcomm, Inc.	Tamer Kadous
Samsung Telecommunications America	Rakesh Taori
Siklu Communications	Izik Kirshenbaum
Sony Mobile	Dr. Peter Karlsson
TriQuint Semiconductor	Brian P. Balut
TriQuint Semiconductor	John Bellantoni
TriQuint Semiconductor	Elias Reese
TriQuint Semiconductor	Sumit Tomar

13 List of acronyms

ADC	Analog-to-Digital Converter
ANR	Automatic Neighbor Relation
AOA	Angle of Arrival
AP	Access Point
AOD	Angle of Departure
CAGR	Compound Annual Growth Rate
CDN	Content Delivery Network
CE	Channel Element
CoMP	Co-Ordinated Multipoint
CMOS	Complementary Metal Oxide Semiconductor
CP	Cyclic Prefix
CPE	Customer Premises Equipment
CP-SC	Cyclic Prefixed Single Carrier
CRC	Cyclic Redundancy Check
CSI	Channel State Information
CSG	Closed Subscriber Group
DAC	Digital-to-Analog Converter
DL	Downlink
EIRP	Effective Isotropic Radiated Power
EPC	Evolved Packet Core
eNB	Evolved Node B
E-UTRAN	Evolved Universal Terrestrial Radio Access Network
FDD	Frequency Division Duplex
HARQ	Hybrid Automatic Request
ICIC	Inter-Cell Interference Coordination
IF	Intermediate Frequency
ISD	Inter-Site Distance
ITU-R	International Telecommunications Union Radiocommunication Sector
LCP	Liquid Crystal Polymer
LIPA	Local IP Access
LOS	Line of Sight
LPWA	Low Power Wide Area
LTCC	Low Temperature Co-fired Ceramic
LTE	Long Term Evolution (of UMTS)
LSA	Licensed Shared Access
MAC	Medium Access Control
mB	mm-wave Basestation
mBA	mm-wave Basestation Aggregation
MC-CDMA	Multi-carrier Code Division Multiple Access
METIS	Mobile and wireless communications Enablers for the Twenty-twenty Information Society
MME	Mobility Management Entity
MMSR	Minimum Mean Squared Error
MOU	Minutes of Use
MRO	Mobility Robustness Optimization

MRT	Maximum Ratio Transmission
MU	Multi User
NCP-SC	Null CP-SC
NLM	Network Listening Module
NLOS	Non-Line-of-Sight
NRT	Neighbor Relation Table
OFDM`	Orthogonal Frequency Division Multiplexing
OFDMA	Orthogonal Frequency Division Multiple Access
OLOS	Obstructed Line-of-Sight
OTT	Over the Top
PAPR	Peak to Average Power Ratio
PBCH	Physical Broadcast Channel
PCFICH	Physical Control Format Indicator Channel
PCI	Physical Cell Identity
PDCCH	Physical Downlink Control Channel
PDCP	Packet Data Convergence Protocol
PDP	Power Delay Profile
PDSCH	Physical Downlink Shared Channel
P-GW	Packet Data Network Gateway
PHICH	Physical Hybrid ARQ Indicator Channel
PHY	Physical Layer
PMCH	Physical Multicast Channel
PN	Pseudorandom Number
PRACH	Physical Random Access Channel
PSC	Primary Scrambling Code
PMP	Point to Multipoint
PTP	Point to Point
PUCCH	Physical Uplink Control Channel
PUSCH	Physical Uplink Shared Channel
RAN	Radio Access Network
RZF	Regularized Zero Forcing
SAS	Spectrum Authorization Systems
SC-FDMA	Single-Carrier Frequency Division Multiple Access
SCM	Spatial Channel Model
SC-OFDM	Single Carrier OFDM
S-GW	Serving Gateway
SIPTO	Selective IP Traffic Offload
SON	Self Organizing Network
SVD	Singular Value Decomposition
TDD	Time Division Duplex
TTI	Transmission Time Interval
UE	User Equipment
UL	Uplink
ZT-OFDM	Zero Tailed OFDM

14 References

1. **METIS**. Deliverable D1.1: ICT-317669 METIS project, “Scenarios, requirements and KPIs for 5G mobile and wireless system”. *METIS Project*. [Online] May 29, 2013. [Cited: 10 29, 2013.] amazingly fast, great service in a crowd, ubiquitous things communicating, best experience follows you, super real time and reliable connections . https://www.metis2020.com/wp-content/uploads/2013/05/METIS_D1.1_v1.pdf. Deliverable D1.1.
2. **Gordon Mansfield**. Mobile data traffic on AT&T’s network has increased more than 30,000% (2007 – 2012). . *AT&T Connecting your World, AT&T Small Cells*. [Online] AT&T, May 8, 2013. [Cited: Oct 1, 2013.] <http://www.att.com/gen/press-room?pid=23971>.
3. *Traffic types and growth in backbone networks*. **A. Gerber, R. Doverspike**. Los Angeles, CA : NFOEC, 2011. Optical Fiber Communication Conference and Exposition (OFC/NFOEC) 2011 and the National Fiber Optic Engineers Conference. Vols. March 6-10, 2011, pp. 1,3. ISBN: 978-1-4577-0213-6.
4. **CISCO VNI**. Cisco VNI Mobile Forecast, 2013. *CISCO VNI Mobile Forecast*. [Online] August 2013, CISCO, August 2013. [Cited: October 1, 2013.] http://www.cisco.com/en/US/solutions/collateral/ns341/ns525/ns537/ns705/ns827/white_paper_c11-520862.html.
5. **Ericsson**. Ericsson Mobility Report, On the pulse of the networked society, August 2013, last accessed Sept. 2013:. *Ericsson Mobility Report*. [Online] August 2013. [Cited: September 18, 2013.] www.ericsson.com/ericsson-mobility-report .
6. Ericsson Traffic Explorer. *Traffic Exploration*. [Online] Ericsson, August 2013. <http://www.ericsson.com/TET/trafficView/loadBasicEditor.ericsson>.
7. **Moore, Geoffrey A**. *Crossing the Chasm: Marketing and Selling High-Tech Products to Mainstream Customers*. s.l. : Harper Business Essentials., 1998. ISBN: 0-06-051712-3.
8. *Future Wireless Opportunities for Millimeter Wave Systems*. **Castor, Doug**. Guilford : s.n., 2013.
9. **3GPP**. *Scenarios and requirements for small cell enhancements*. March 2013. TR 36.932.
10. **3GPP**. *Small cell enhancements for E-UTRA and E-UTRAN*. Dec 2013. TS 36.872.
11. **3GPP**. *Study on Small Cell enhancements for E-UTRA and E-UTRAN*; Dec 2013. TR 36.842.
12. *Millimeter Wave Mobile Communications for 5G Cellular: It Will Work!* **Rappaport, T.S., et al., et al.** 1, s.l. : IEEE Access Journal, May 2013, Vol. 1.
13. *Opportunistic Third-Party Backhaul for Cellular Wireless Networks*. **Ford, R., Kim, C. and Rangan, S.** s.l. : arXiv preprint arXiv:1305.0958, May 4, 2013.

14. **ITU-R. WORKING DOCUMENT TOWARDS A PRELIMINARY DRAFT NEW REPORT ITU-R M.[IMT.ABOVE 6 GHz].** Feb 2014.
15. *Millimeter Wave Picocellular System Evaluation for Urban Deployments.* **Akdeniz, M.R., et al., et al.** s.l. : arXiv preprint arXiv:1304.3963, April 15, 2013.
16. **Rappaport, T.S.** *Wireless Communications: Principles and Practice (2nd Edition).* Upper Saddle River, NJ : Prentice Hall, 2002.
17. *State of the art in 60 GHz Integrated Circuits and Systems for Wireless Communications.* **Rappaport, T.S., Murdock, J. and Gutierrez, F.** s.l. : Proceedings of the IEEE, August 2011. Vol. 99, pp. 1390-1436. 8.
18. **Rappaport, T.S.** *Wireless Communications: Principles and Practice.* Prentice Hall, NJ : Pearson, 2002.
19. **IST-WINNER II.** WINNER II Channel Models. *WINNER II - Public Deliverables.* [Online] 9 30, 2007. [Cited: 10 8, 2013.] <http://www.ist-winner.org/deliverables.html>. D1.1.2.
20. **WINNER+.** WINNER+ Final Channel Models . *CELTIC-Initiative.* [Online] 6 30, 2010. [Cited: 10 8, 2013.] http://projects.celtic-initiative.org/winner+/WINNER+%20Deliverables/D5.3_v1.0.pdf. D5.3.
21. *Crosscorrelation between the envelopes of 900 MHz signals received at a mobile radio base station site.* **F. Adachi, M.T. Feeney, A.G. Williamson and J.D. Parsons.** s.l. : IEE, October, 1986. Vol. 133, p. F(6). IEE Proceedings.
22. *Further advancements for E-UTRA physical layer aspects,.* **3rd Generation Partnership Project.** s.l. : 3GPP, 2010. TR 36.814 V9.0.0 (2010-03).
23. *28 GHz Propagation Measurements for Outdoor Cellular Communications Using Steerable Beam Antennas in New York City.* **Azar, Y., et al., et al.** s.l. : IEEE International Conference on Communications (ICC), June 9-13, 2013.
24. *Rain Attenuation in Millimeter Wave Ranges.* **Li, Q. Zhao and J. Guilin,** China : International Symposium on Antennas, Propagation and EM Theory, 2006.
25. *State of the Art in 60-GHz Integrated Circuits and Systems for Wireless Communications.* **T. S. Rappaport, J. N. Murdock, and F. Gutierrez.** No. 8, pp. 1390–1436, s.l. : Proceedings of the IEEE, August 2011, Vol. 99.
26. *On-chip integrated antenna structures in CMOS for 60 GHz WPAN systems.* **Gutierrez, F., et al., et al.** 8, s.l. : IEEE J. Sel. Areas Communications, October 2009, Vol. 27, pp. 1367-1378.
27. *Consumption Factor and Power-Efficiency Factor: A Theory for Evaluating the Energy Efficiency of Cascaded Communication Systems.* **Murdock, J. and Rappaport, T.** 12, s.l. : Selected Areas in Communications, IEEE Journal, December 2014, Vol. 32.

28. *A note on a simple transmission formula.* **Friis, H.** s.l. : Proceedings of the IRE, 1946. Vol. 5, pp. 254-256.
29. *The indoor radio propagation channel.* **Hashemi, H.** s.l. : Proceedings of the IEEE, 1993. Vol. 7, pp. 943-968.
30. *MPM – an atmospheric millimeter wave propagation model.* **Liebe, H. J.** s.l. : Infrared and Millimeter Waves, International Journal on, 1989, Vol. 10, pp. 631-650.
31. *Measurements and models for 38-GHz point-to-multipoint radiowave propagation.* **Xu, H., et al., et al.** s.l. : IEEE J. Sel. Areas Comm., 2000, Vol. 18, pp. 310-321.
32. *Transmission and isolation of signals in buildings at 60 GHz.* **Correia, L. M. and Frances, P.O.** s.l. : Sixth IEEE International Symposium, 1995. Vol. 3, pp. 1031-1034.
33. *Measurement of the complex refractive index of concrete at 57.5 GHz.* **Sato, K., et al., et al.** s.l. : Antennas and Propagation, IEEE Transactions on, 1996. Vol. 44, pp. 35-40.
34. *Millimeter Wave Cellular Communication Measurements for Reflection and Penetration Loss in and Around Buildings in New York City.* **Zhao, Hang et al.** Budapest : IEEE International Conference on Communications, June 2013.
35. *Measurements and models for radio path loss and penetration loss in and around homes and trees at 5.85 GHz.* **Durgin, G., Rappaport, T. and Xu, H.** s.l. : Communications, IEEE Transactions on, 1998. Vol. 11, pp. 1484-1496.
36. *Radio-wave propagation for emerging wireless personal-communication systems.* **Sandhu, S. and Rappaport, T.S.** s.l. : IEEE Antennas and Propagation Magazine, 1994, Vol. 36, pp. 14-24.
37. *Review of constitutive parameters of building materials.* **Stavrou, S. and Saunders, S.** s.l. : Antennas and Propagation, 12th International Conference on (Conf. Publ. No. 491), 2003. Vol. 1, pp. 211-215.
38. *Reflection and transmission behaviour of building materials at 60 GHz.* **Langen, B., Lober, G. and Herzig, W.** s.l. : Personal, Indoor and Mobile Radio Communications - Wireless Networks, Catching the Mobile Future, 1994, Vol. 2, pp. 505-509.
39. *Propagation Measurements and Models for Wireless Communication Channels.* **Andersen, J., Rappaport, T. and Yoshida, S.** s.l. : Communications Magazine, 1995, Vol. 33, pp. 42-49.
40. **Nie, S., et al., et al.** London : 24th Annual IEEE International Symposium on Personal, Indoor and Mobile Radio Communications (PIMRC), 2013.
41. *Propagation prediction models for wireless communication systems.* **Iskander, M.F. and Yun, Z.** s.l. : Microwave Theory and Techniques, IEEE Transactions on, 2002. Vol. 3, pp. 662-673.

42. **Parsons, J.D.** [ed.] John Wiley & Sons Ltd. 2. s.l. : The Mobile Radio Propagation Channel, 2000.
43. *A comparison of theoretical and empirical reflection coefficients for typical exterior wall surfaces in a mobile radio environment.* **Landron, O., Feuerstein, M. and Rappaport, T.** s.l. : Antennas and Propagation, IEEE Transactions on, 1996, Vol. 44, pp. 341-351.
44. *Broadband Millimeter-Wave Propagation Measurements and Models Using Adaptive-Beam Antennas for Outdoor Urban Cellular Communications.* **Rappaport, T.S., et al., et al.** s.l. : IEEE Trans. Antennas and Propagation, 2013. Vol. 61, pp. 1850, 1859.
45. *Millimeterwave 60 GHz Outdoor and Vehicle AOA Propagation Measurements Using a Broadband Channel Sounder.* **Ben-Dor, E., et al., et al.** s.l. : Global Telecommunications Conference (GLOBECOM 2011), 2011. pp. 1-6.
46. *Cellular and Peer-to-Peer Broadband Millimeter Wave Outdoor propagation measurements and Angle of Arrival characteristics using adaptive beam steering.* **Rappaport, T.S., et al., et al.** Santa Clara, CA : IEEE Radio and Wireless Symposium (RWS), 2012.
47. **Al-Nuaimi, M. and Hammoudeh, A.** *Measurements and Predictions of Attenuation and Scatter of Microwave Signals by Trees.* 1994. pp. 70-76. Vol. 141.
48. *Millimeter-wave propagation in vegetation: experiments and theory.* **Schwering, F., Violette, E. and Espeland, R.** s.l. : Geoscience and Remote Sensing, IEEE Transactions on, 1988. Vol. 26, pp. 355-367.
49. *Fading characteristics of RF signals due to foliage in frequency bands from 2 to 60 GHz.* **Perras, S. and Bouchard, L.** s.l. : Wireless Personal Multimedia Communications, The 5th International Symposium on, 2002. pp. 267-271.
50. *Vegetation attenuation: modelling and measurements at millimetric frequencies.* **Seville, A.** s.l. : Antennas and Propagation, Tenth International Conference on (Conf. Publ. No. 436), 1997. Vol. 2, pp. 5-8.
51. *28 GHz Angle of Arrival and Angle of Departure Analysis for Outdoor Cellular Communications using Steerable Beam Antennas in New York City.* **Samimi, M., et al., et al.** s.l. : IEEE Vehicular Technology Conference (VTC), 2013.
52. *72 GHz millimeter wave indoor measurements for wireless and backhaul communications.* **S. Nie, et al.** s.l. : Personal Indoor and Mobile Radio Communications (PIMRC) IEEE 24th International Symposium , September 2013.
53. *38 GHz and 60 GHz angle-dependent propagation for cellular & peer-to-peer wireless communications.* **Rappaport, T., et al., et al.** s.l. : Communications (ICC), IEEE International Conference on, 2012. pp. 4568-4573.

54. *Multi-beam Antenna Combining for 28 GHz Cellular Link Improvement in Urban Environments*. **Sun, S. and Rappaport, T.S.** Atlanta, GA : IEEE Global Communications Conference (GLOBECOM), 2013.
55. *Path loss, delay spread, and outage models as functions of antenna height for microcellular system design*. **Feuerstein, M., et al., et al.** s.l. : Vehicular Technology, IEEE Transactions on, 1994. Vol. 3, pp. 497-498.
56. *Path loss and multipath delay statistics in four European cities for 900 MHz cellular and microcellular communications*. **Seidel, S., Rappaport, T. and Singh, R.** s.l. : Electronics Letters, 1990, Vol. 26, pp. 1713-1715.
57. *Characterisation of propagation in 60 GHz radio channels*. **Smulders, P.F.M. and Correia, L.M.** s.l. : Electronics & Communication Engineering Journal, 1997, Vol. 9, pp. 73-80.
58. *Wideband characterisation of the propagation channel for outdoors at 60 GHz*. **Correia, L. and Reis, J.** s.l. : Personal, Indoor and Mobile Radio Communications, Seventh IEEE International Symposium, 1996. Vol. 2, pp. 752-755.
59. **Bischl, H. and Schafer, W.** *The 60 GHz mobile-to-mobile radio channel fading statistics and estimated packet error rates*. s.l. : Vehicular Technology Conference, IEEE 44th, 1994. pp. 910-913. Vol. 2.
60. *Indoor and outdoor frequency measurements for mm-waves in the range of 60 GHz*. **Matic, D., Harada, H. and Prasad, R.** s.l. : Vehicular Technology Conference - VTC98, 48th IEEE, 1998. Vol. 1, pp. 567-571.
61. *Channel feasibility for outdoor non-line-of-sight mmwave mobile communication*. **Rajagopal, S., Abu-Surra, S. and MalmirChegini, M.** s.l. : Vehicular Technology Conference, VTC Fall, 2012. pp. 1-6.
62. *Cellular broadband millimeter wave propagation and angle of arrival for adaptive beam steering systems (invited paper)*. **Rappaport, T., et al., et al.** s.l. : Radio and Wireless Symposium (RWS), IEEE, 2012. pp. 151-154.
63. *Propagation characteristics at 60 GHz for ITS inter-vehicle communications*. **Kato, A., Sato, K. and Fujise, M.** s.l. : IEICE transactions on communications, 2000. Vols. E84-B.
64. *Indoor and outdoor propagation measurements at 5 and 60 GHz for radio LAN application*. **Plattner, A., Prediger, N. and Herzig, W.** s.l. : Microwave Symposium Digest, IEEE MTT-S International, 1993, Vol. 2, pp. 853-856.
65. *Experimental propagation channel characterization of mm-wave radio links in urban scenarios*. **Kyro, M., Kolmonen, V. and Vainikainen, P.** s.l. : Antennas and Wireless Propagation Letters, IEEE, 2012, Vol. 11, pp. 865-868.

66. *Impact of antenna configuration and shadowing on the characteristics of the 60 GHz indoor wideband radio channel.* **Peter, M and Keusgen, W.** s.l. : XXIXth General Assembly of the International Union of Radio Science, URSI GA, 2008.
67. *Measurement and analysis of the 60 GHz in-vehicular broadband radio channel.* **Peter, M., Keusgen, W. and Schirmacher, M.** s.l. : Vehicular Technology Conference, VTC 2007 - Fall, 2007.
68. *IST-4-027756 WINNER II D1.1.2, WINNER II channel models, ver. 1.1.* **Kyösti, P., et al., et al.** s.l. : Tech. Rep., 2007.
69. *A street canyon approximation model for the 60 ghz propagation channel in an urban environment with rough surfaces.* **Rasekh, M., Farzaneh, F. and Shishegar, A.** s.l. : Telecommunications (IST), 5th International Symposium on, 2010. pp. 132-137.
70. **Parker, T.** OFDM non-line of sight to dominate small cell backhaul in 2017. *FierceBroadbandWireless*. [Online] September 12, 2012. http://www.fiercebroadbandwireless.com/story/abi-ofdm-non-line-sight-dominate-small-cell-backhaul-2017/2012-09-12?utm_medium=nl&utm_source=internal.
71. *Air-Interface Design and Ray-Tracing Study for 5G Millimeter Wave Communications.* **S. Larew, T. Thomas, M. Cudak and A. Ghosh.** s.l. : Proc. IEEE Globecom, December 2013.
72. *Zero-tail DFT-spread-OFDM signals.* **Gilberto Berardinell, Fernando M. L. Tavares, Troels B. Sørensen, Preben Mogensen, and Kari Pajukoski,.** s.l. : Proc. IEEE Globecom, December 2013.
73. **NGMN Alliance.** Small Cell Backhaul Requirements. [Online] http://www.ngmn.org/fileadmin/user_upload/Downloads/Technical/NGMN_Whitepaper_Small_Cell_Backhaul_Requirements.pdf.
74. *Scaling Up MIMO.* **Rusek, F., et al.** s.l. : IEEE Signal Processing Magazine, 2013.
75. *Low Complexity Precoding for Large Millimeter Wave MIMO Systems.* **Ayach, O.E., Heath, R., et al.** s.l. : Proc. of IEEE International Conference on Communications, 2012.
76. *MIMO Systems with Mutual Coupling: How Many Antennas to Pack into Fixed-Length Arrays?* **Shen, S., et al.** Taichung, Taiwan : ISITA2010, 2010.
77. *Performance and Feasibility of mmWave Beamforming Prototype for 5G Cellular Communications.* **Samsung.** s.l. : IEEE ICC, 2013.
78. *The Capacity Optimality of Beam Steering in Large Millimeter Wave MIMO Systems.* **Ayach, O.E., Heath, R., et al.** s.l. : IEEE 12th International Workshop on Signal Processing Advances in Wireless Communications, 2012.
79. *Massive MIMO in the UL/DL of Cellular Networks: How Many Antennas Do We Need?* **Hoydis, J., et al.** s.l. : IEEE Journal on Selected Areas in Communications, 2013, Vol. 31.

80. *Pilot Contamination and Precoding in Multi-Cell TDD Systems*. **Jose, J., et al.** s.l. : IEEE Transactions on Wireless Communications, 2011. Vol. 8.
81. *Hybrid Precoding for Millimeter Wave Cellular Systems with Partial Channel Knowledge*. **Alkahateeb, A., et al.** s.l. : Information Theory and Application Workshop, 2013.
82. **Xu, H., Kukshya, V., Rappaport, T.** *Spatial and temporal characteristics of 60 GHz indoor channels*. s.l. : IEEE Journal on Selected Areas in Communications, 2002. pp. 620-630. Vol. 3.
83. *Antennas in Cellular Phones for Mobile Communications*. **Ying, Z.** s.l. : Proceedings of the IEEE, 2012. Vol. 100.
84. *The Multicell Multiuser MIMO Uplink with Very Large Antenna Arrays and a Finite-Dimensional Channel*. **Ngo, H.Q., et al.** s.l. : IEEE Transactions on Communications, 2013.
85. *Decoupling of Multiple Antennas in Terminals with Chassis Excitation Using Polarization Diversity, Angle Diversity and Current Control*. **Li, H., et al.** s.l. : IEEE Transactions on Antennas and Propagation, 2012, Vol. 60.
86. **Rappaport, T., et al.** *State of the Art in 60-GHz Integrated Circuits and Systems for Wireless Communications*. s.l. : Proceedings of the IEEE, 2011. Vol. 99.
87. *60 GHz Wireless: Up Close and Personal*. **Daniels, R.C., et al.** s.l. : IEEE Microwave Magazine, 2010.